ETH
Eidgenössische Technische Hochschule Zürich
Swiss Federal Institute of Technology Zurich

Power Electronic Systems Laboratory

APEC 2012

Optimal Design of Inductive Components Based on Accurate Loss and Thermal Models

Jonas Mühlethaler and Johann W. Kolar

Power Electronic Systems Laboratory, ETH Zurich

Introduction

System Layer

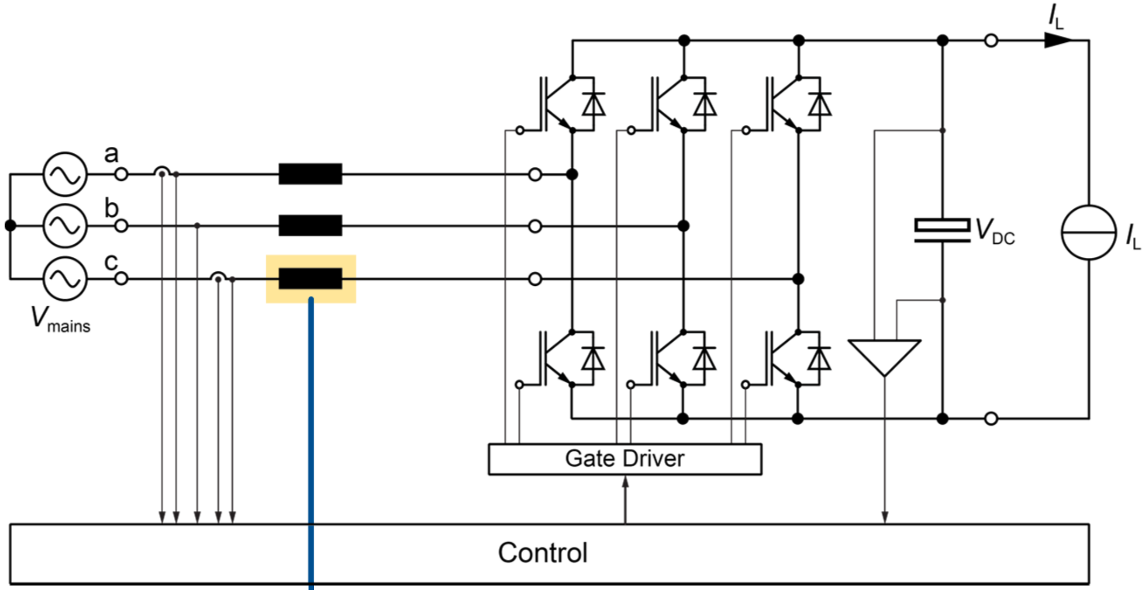

Component Layer

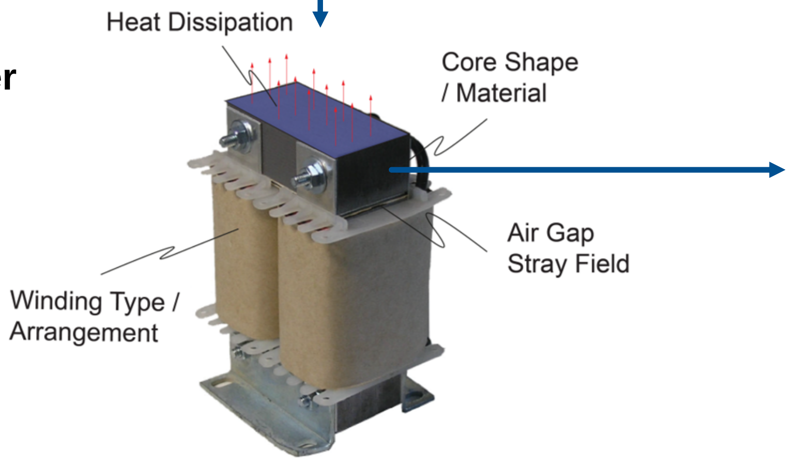

Material Layer

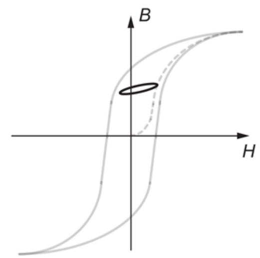

Introduction

Application of Inductive Components (1) : Buck Converter

(DC Current + HF Ripple)

Schematic

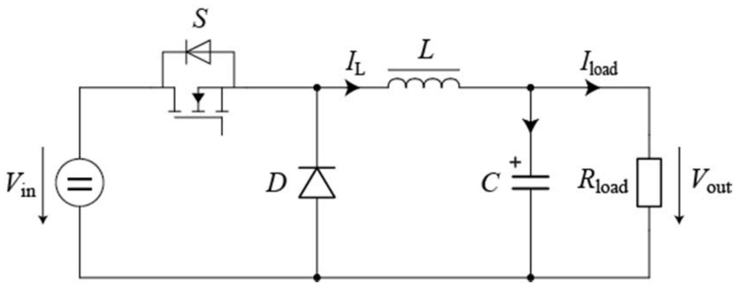

Current / Flux Waveform

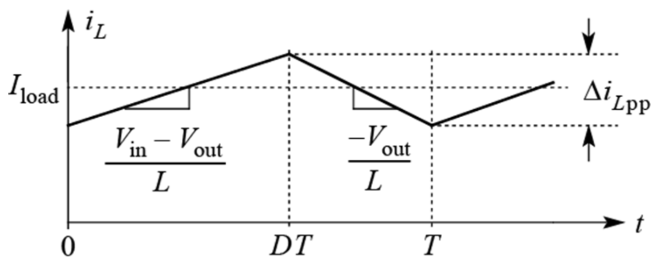

Modeling Difficulties

- Non-sinusoidal current / flux waveform
- Current / flux is DC biased

Solutions

- FFT of current waveform for the calculation of winding losses
- Determine core loss energy for each segment and for each corner point in the piecewise-linear flux waveform
- Loss Map enables to consider a DC bias

Introduction

Application of Inductive Components (2) : Inductor of DAB Converter

(Non-Sinusoidal AC Current)

Schematic

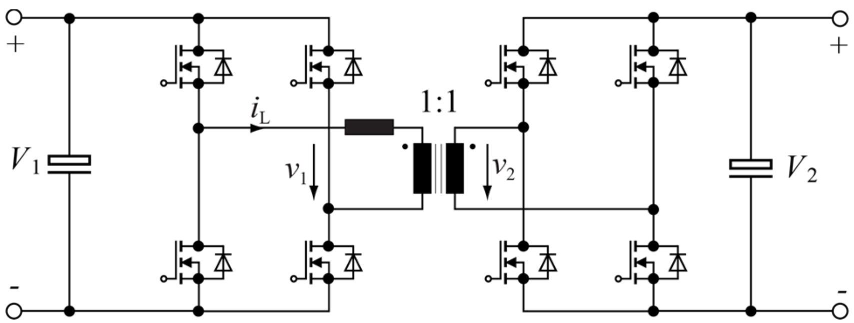

Current / Flux Waveform

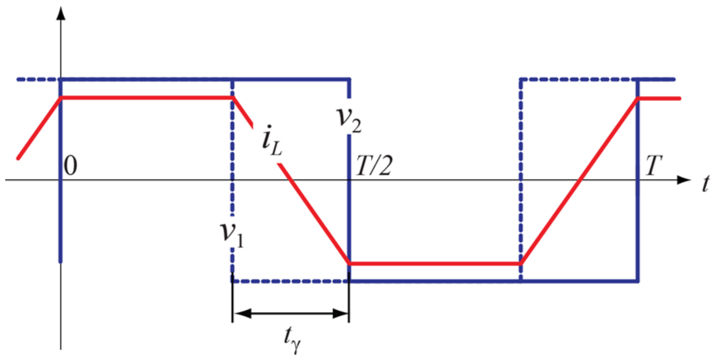

Modeling Difficulties

- Non-sinusoidal current / flux waveform
- Core losses occur in the interval of constant flux

Solutions

- FFT of current waveform for the calculation of winding losses
- Improved core loss equation that considers relaxation effects

Introduction

Application of Inductive Components (3) : Three-Phase PFC
(Sinusoidal Current + HF Ripple)

Schematic

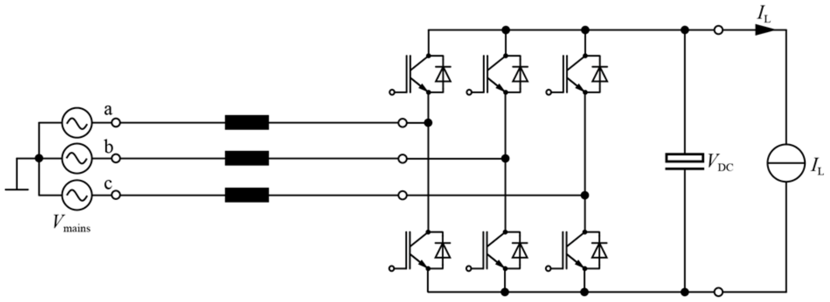

Current / Flux Waveform

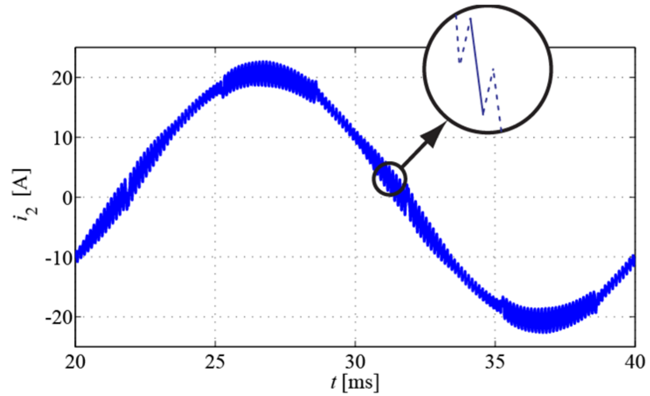

Modeling Difficulties

- Non-sinusoidal current / flux waveform
- Major loop and many (DC biased) minor loops

Solutions

- FFT of current waveform for the calculation of winding losses
- Determine core loss energy for each segment and for each corner point in the piecewise-linear flux waveform (-> minor loop losses)
- Add major loop losses

Introduction
Overview About Different Flux Waveforms

Sinusoidal

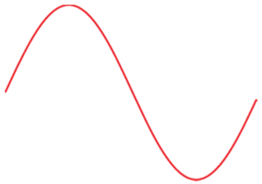

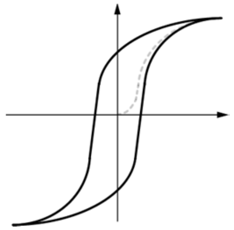

DC Current +
HF Ripple

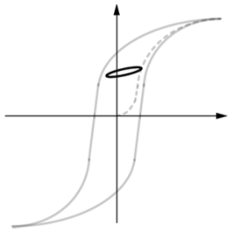

Non-Sinusoidal AC
Current

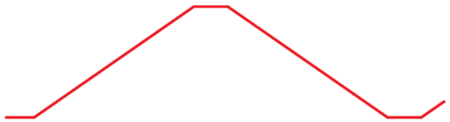

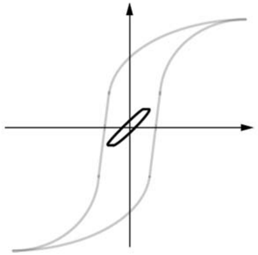

Sinusoidal Current
+ HF Ripple

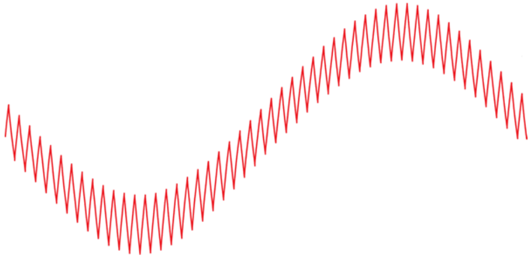

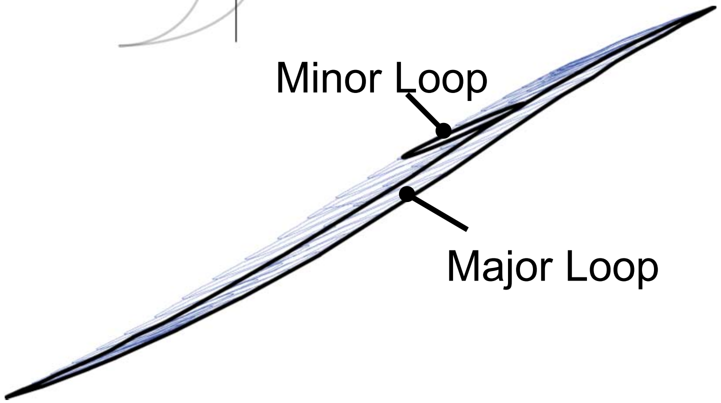

Introduction

System Layer

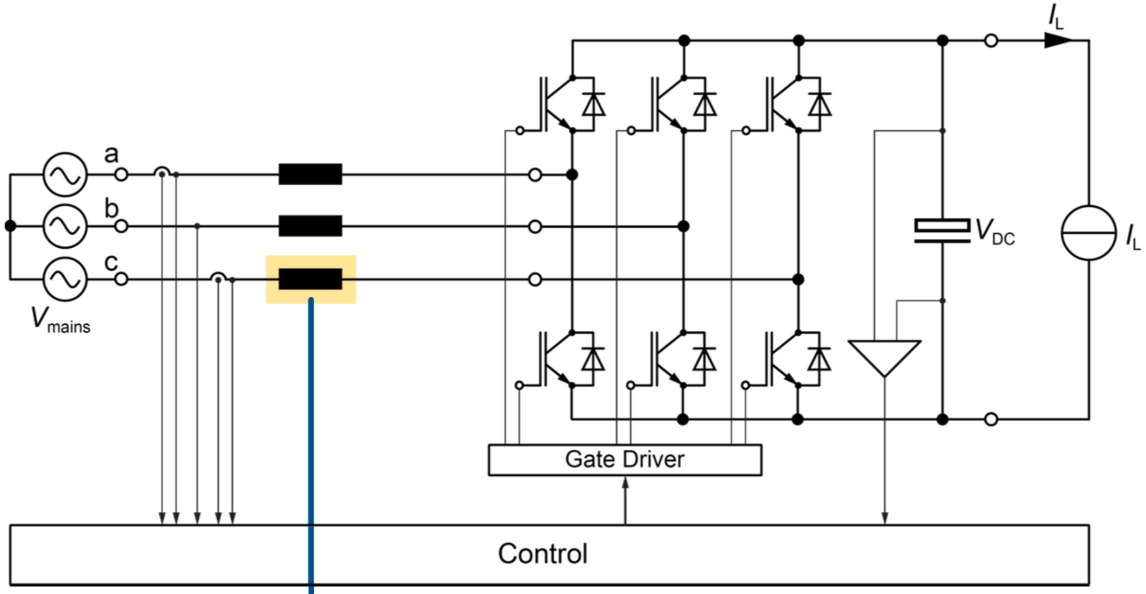

Component Layer

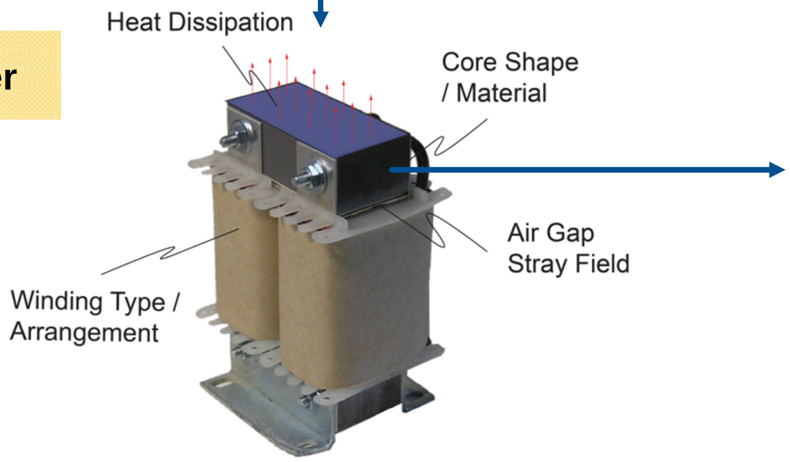

Material Layer

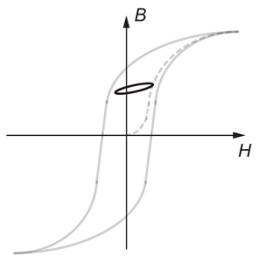

Introduction

Overview About Other Modeling Issues

Heat Dissipation

Core Type

Winding Type / Arrangement

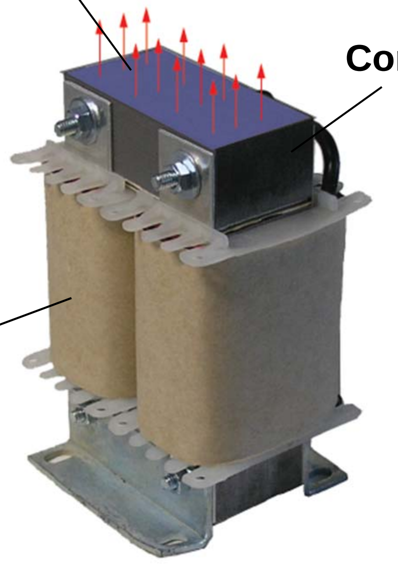

Flux Density Distribution

Air Gap Stray Field

Current Distribution

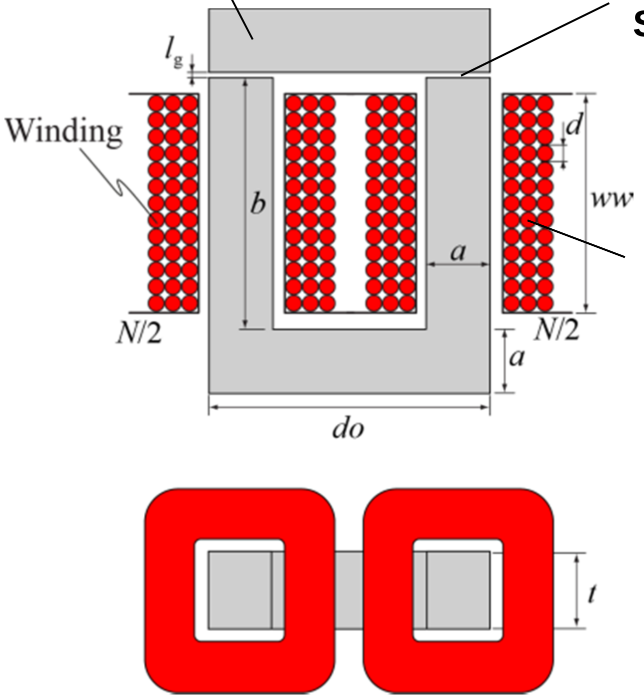

Introduction
Wide Range of Realization Options

Inductors / Transformers

www.wagnergrimm.ch, www.ferroxcube.com

Core Shapes

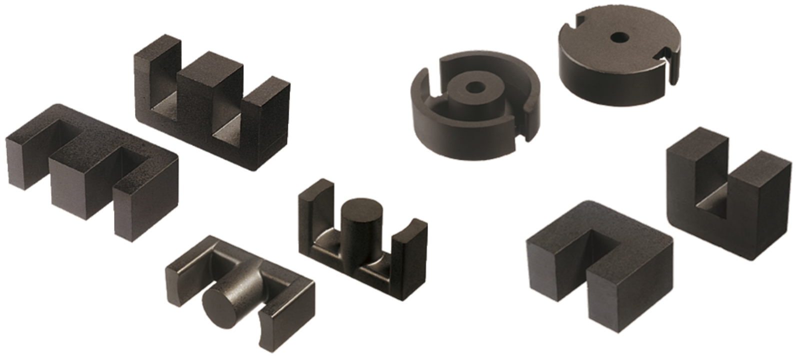

www.ferroxcube.com

Conductor Shapes

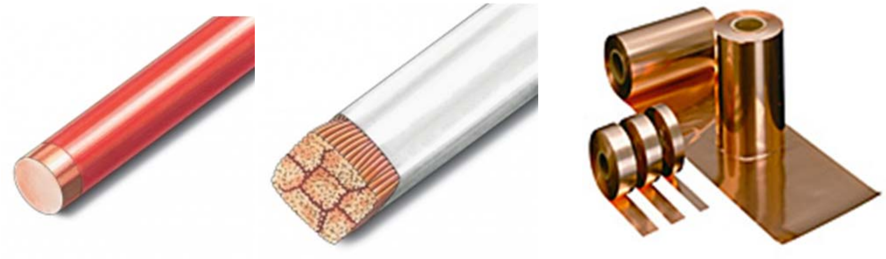

www.pack-feindraehte.de, www.jiricek.de

Introduction
Modeling Inductive Components (1)

Procedure

1) A reluctance model is introduced to describe the electric / magnetic interface, i.e. $L = f(i)$.

2) Core losses are calculated.

3) Winding losses are calculated.

4) Inductor temperature is calculated.

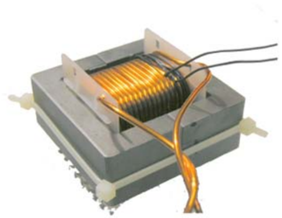

Reluctance Model

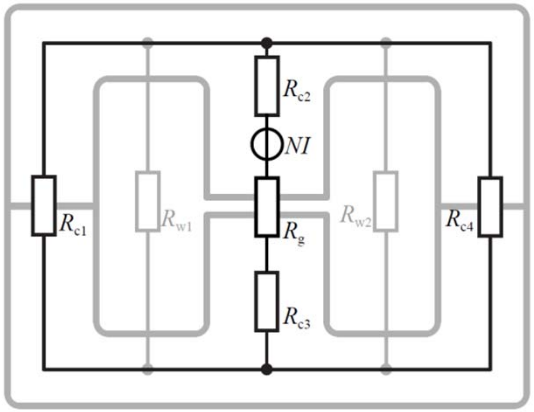

Introduction
Modeling Inductive Components (2)

The following effects will be taken into consideration:

Magnetic Circuit Model (e.g. for Inductance Calculation):

- Air gap stray field
- Non-linearity of core material

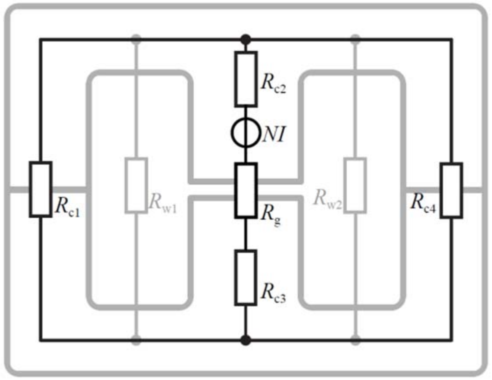

Core Losses:

- DC Bias
- Different flux waveforms (link to circuit simulator)
- Wide range of flux densities and frequencies
- Different core shapes

Winding Losses:

- Skin and proximity effect
- Stray field proximity effect
- Effect of core on magnetic field distribution
- Litz, solid, and foil conductors

Introduction

System Layer

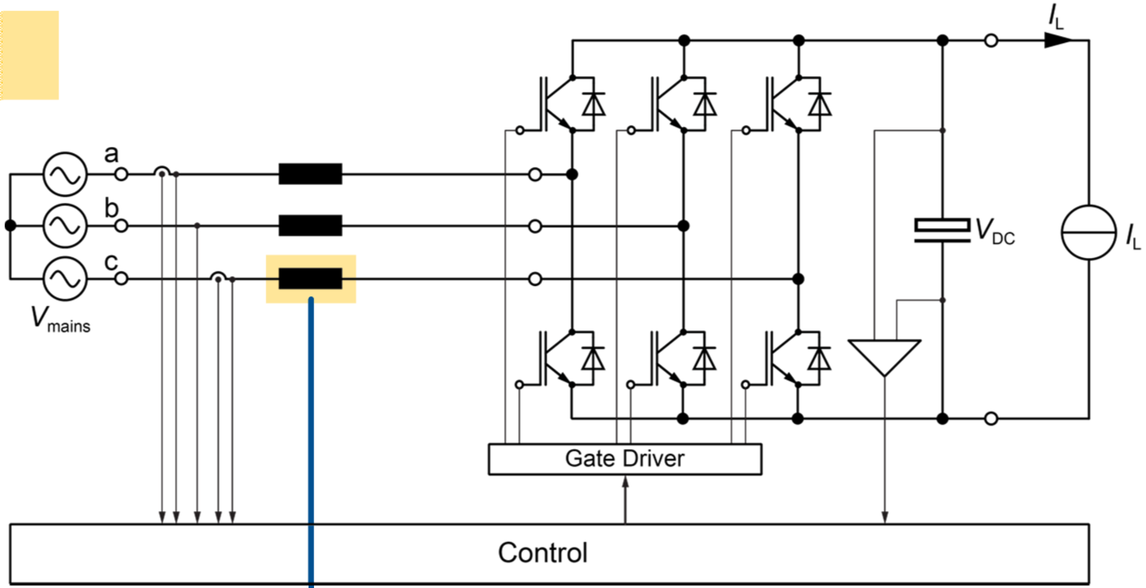

Component Layer

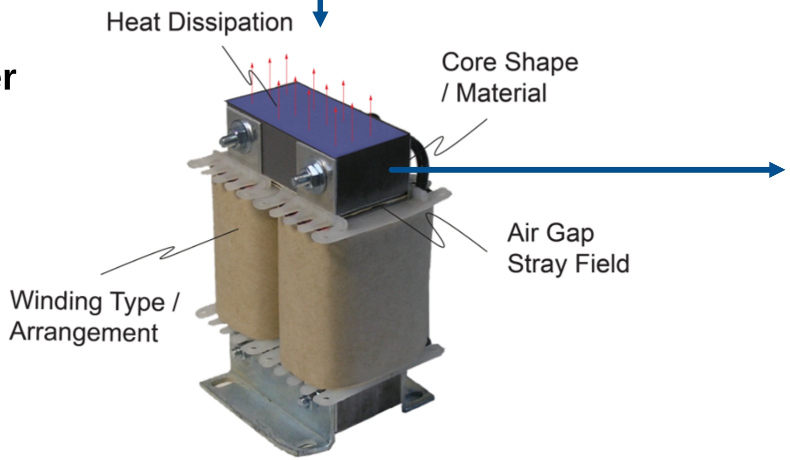

Material Layer

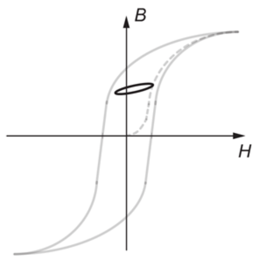

Introduction
Motivation for an Accurate Loss Modeling : Multi-Objective Optimization (1)

PFC Rectifier with Input LCL filter

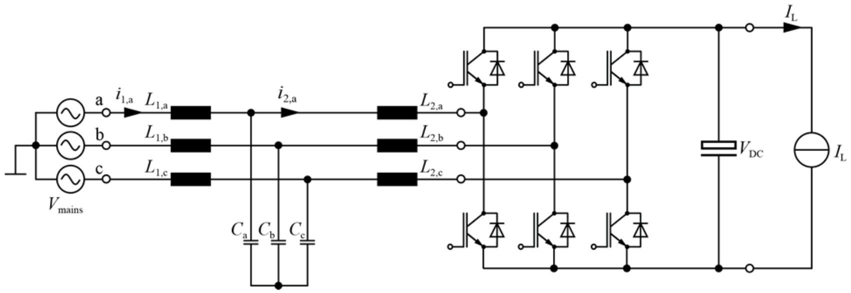

Filter Losses vs. Filter Volume

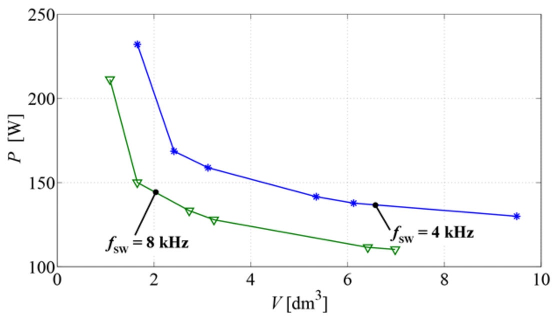

Converter Losses vs. Converter Volume

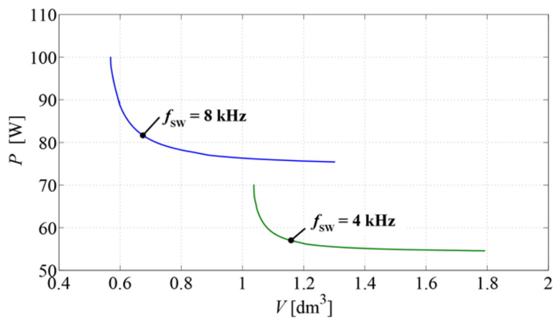

Converter =
Cooling System
+ Switches

→ Sometime there are parameters that bring advantages for one subsystem while deteriorating another subsystem (e.g. frequency in above example).

Introduction

Motivation for an Accurate Loss Modeling : Multi-Objective Optimization (2)

Losses of a Loss-Optimized Design

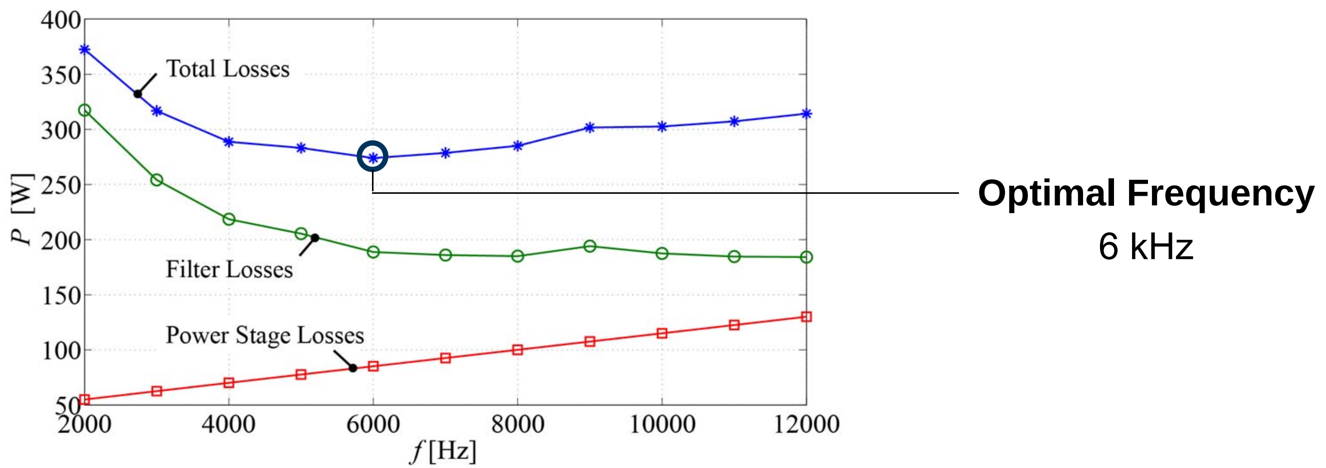

→ In order to get an optimal system design, an overall system optimization has to be performed.

→ It is (often) not enough to optimize subsystems independent of each other.

Introduction

Motivation for an Accurate Loss Modeling : Multi-Objective Optimization (3)

PFC Rectifier with Input LCL filter

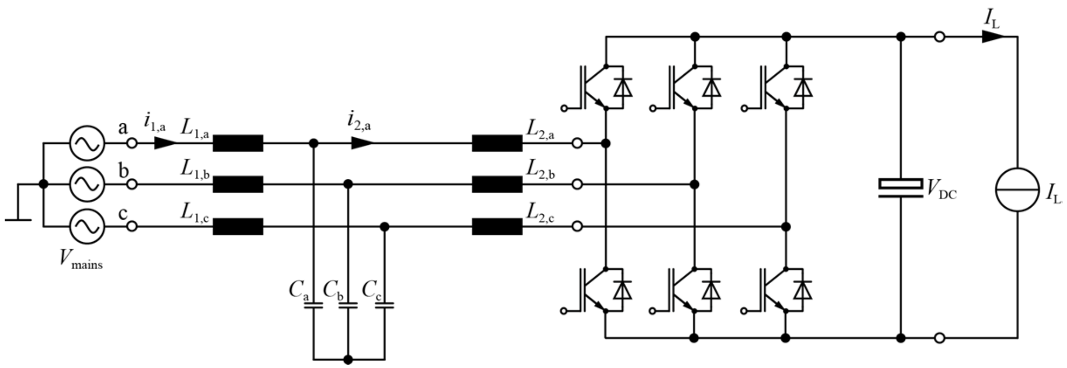

Limits concerning mains

- Tolerable mains harmonics.
- Max. admissible VAr consumption.

Limits concerning rectifier

- Max. admissible $T_{j,max}$
- Max. cooling system vol. $V_{CS,max}$

Limits concerning filter structure

- Max. admissible volume
- Max. admissible losses

Optimize for

- Overall PFC rectifier volume
- Overall PFC rectifier losses
- (PFC system cost)

Outline

- **Magnetic Circuit Modeling**
- **Core Loss Modeling**
- **Winding Loss Modeling**
- **Thermal Modeling**
- **Multi-Objective Optimization**
- **Summary & Conclusion**

Magnetic Circuit Modeling
Reluctance Model

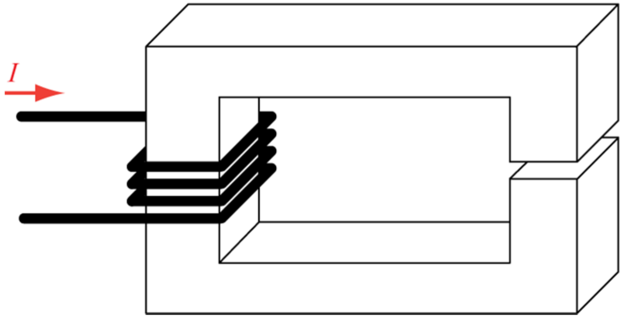

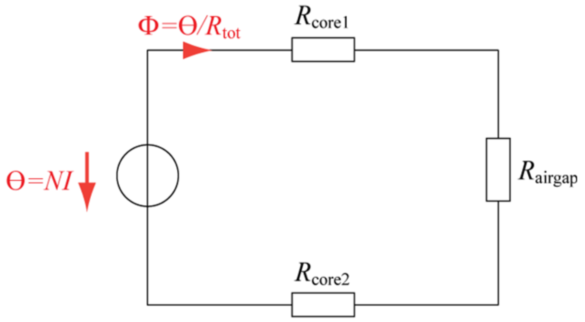

	Electric Network	**Magnetic Network**
Conductivity / Permeability	κ	μ
Resistance / Reluctance	$R = l \,/\, (\kappa A)$	$R_\mathrm{m} = l \,/\, (\mu A)$
Voltage / MMF	$V = \int_{P_1}^{P_2} \vec{E}\,\mathrm{d}\vec{s}$	$V_\mathrm{m} = \int_{P_1}^{P_2} \vec{H}\,\mathrm{d}\vec{s}$
Current / Flux	$I = \iint_A \vec{J}\,\mathrm{d}\vec{A}$	$\Phi = \iint_A \vec{B}\,\mathrm{d}\vec{A}$

Magnetic Circuit Modeling

Why a Reluctance Model is Needed

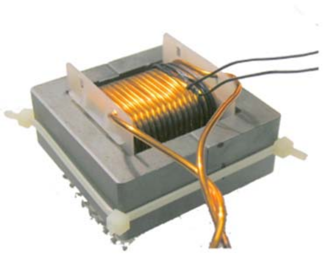

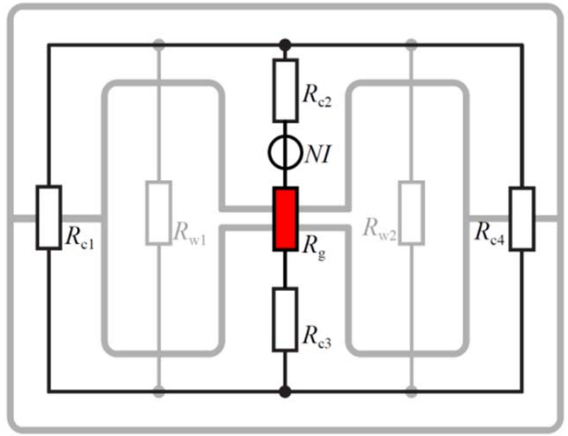

A reluctance model is needed in order to

calculate the inductance ($L = N^2/R_{tot}$)
calculation the saturation current
calculate the air gap stray field
calculate the core flux density

Magnetic Circuit Modeling
Core Reluctance

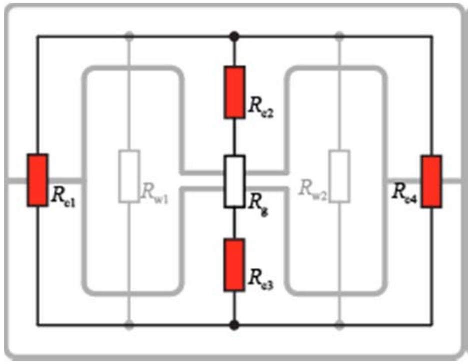

Reluctance Calculation

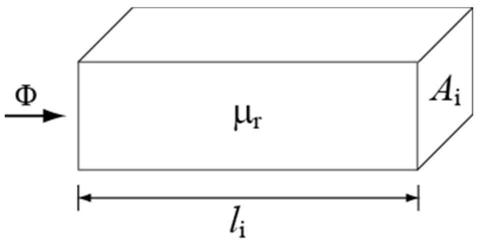

$$R_m = \frac{l_i}{\mu_0 \mu_r A_i}$$

Core Reluctance Dimensions

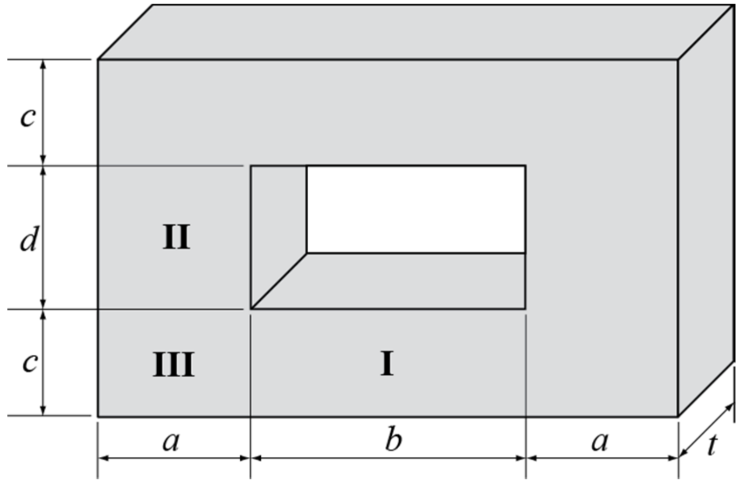

Section	l_i	A_i
I	b	$c \cdot t$
II	d	$a \cdot t$
III	$\frac{2\pi}{4} \cdot \frac{(a+c)}{4} = \frac{\pi}{8}(a+c)$	$\frac{t(a+c)}{2}$

Mean magnetic length

Mean magnetic cross-sectional area

Magnetic Circuit Modeling

Air Gap Reluctance : Different Approaches (1)

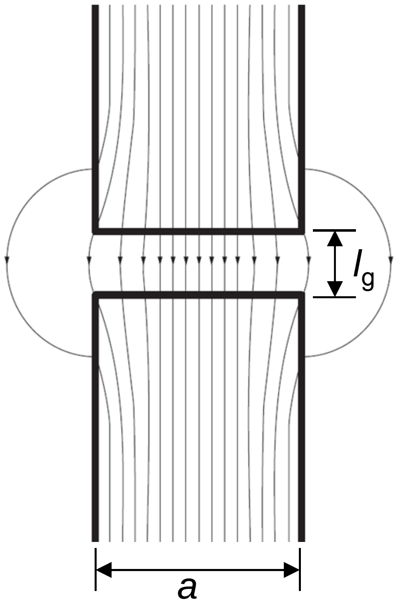

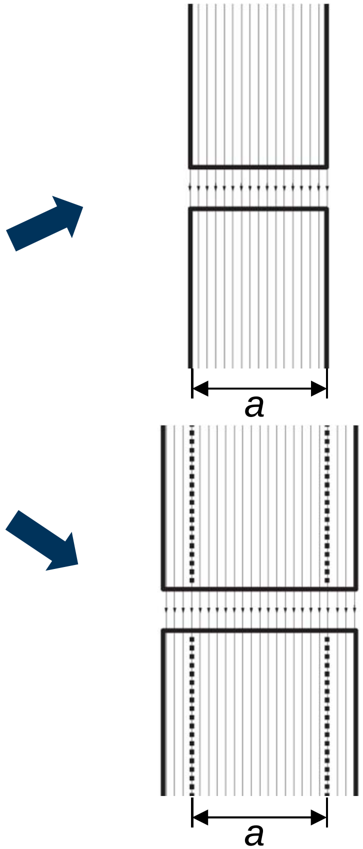

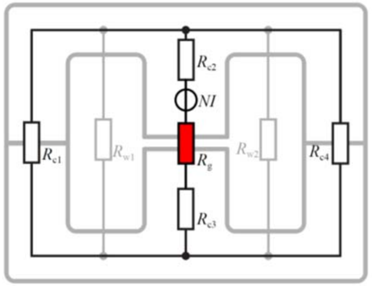

Assumption of Homogeneous Field Distribution

$$R_m = \frac{l_g}{\mu_0 A_g}$$

l_g Air gap length
A_g Air gap cross-sectional area

Increase of the Air Gap Cross-Sectional Area

e.g. [1] (for a cross section with dimension *a* x *t*):

$$R_m = \frac{l_g}{\mu_0 (a + l_g)(t + l_g)}$$

[1] N. Mohan, T. M. Undeland, and W. P. Robbins - "Power Electronics – Converter, Applications, and Design", John Wiley & Sons, Inc., 2003

Magnetic Circuit Modeling

Air Gap Reluctance : Different Approaches (2)

Schwarz-Christoffel Transformation

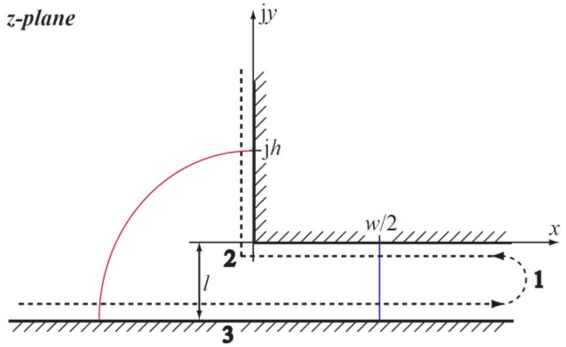

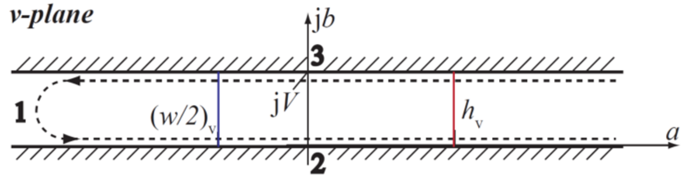

Transformation Equation *z*(*t*)

$$z(t) = \frac{l}{\pi}\left(2\ln\left(1+\sqrt{1-t}\right) - \ln t - 2\sqrt{1-t}\right)$$

(*z* and *t* are complex numbers)

Transformation Equation *v*(*t*)

$$v(t) = \frac{V}{\pi}\ln t$$

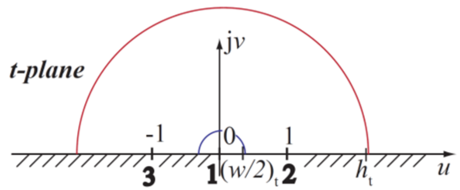

[2] K. J. Binns, P. J. Lawrenson, and C. W. Trowbridge, «The Analytical and Numerical Solution of Electric and Magnetic Fields», John Wiley & Sons, Inc., 1992

Magnetic Circuit Modeling

Air Gap Reluctance : Different Approaches (3)

Solution to 2-D problems found in literature, e.g. in [3]

Can’t be directly applied to 3-D problems.

Some 3-D solution to problem found in literature; however, they are complex [4] and/or limited to one air gape shape [5]

More simple and universal model desired.

[3] A. Balakrishnan, W. T. Joines, and T. G. Wilson - “Air-gap reluctance and inductance calculations for magnetic circuits using a Schwarz-Christoffel transformation”, IEEE Transaction on Power Electronics, vol. 12, pp. 654—663, July 1997.

[4] P. Wallmeier, “Automatisierte Optimierung von induktiven Bauelementen für Stromrichteranwendungen”, PhD Thesis, Universität – Gesamthochschule Paderborn, 2001.

[5] E. C. Snelling, “Soft Ferrites - Properties and Applications”, 2nd edition, Butterworths, 1988

Magnetic Circuit Modeling
Aim of New Model

Air gap reluctance calculation that

- considers the three dimensionality,
- is reasonable easy-to-handle,
- is capable of modeling different shapes of air gaps,
- while still achieving a high accuracy.

Illustration of Different Air Gap Shapes:

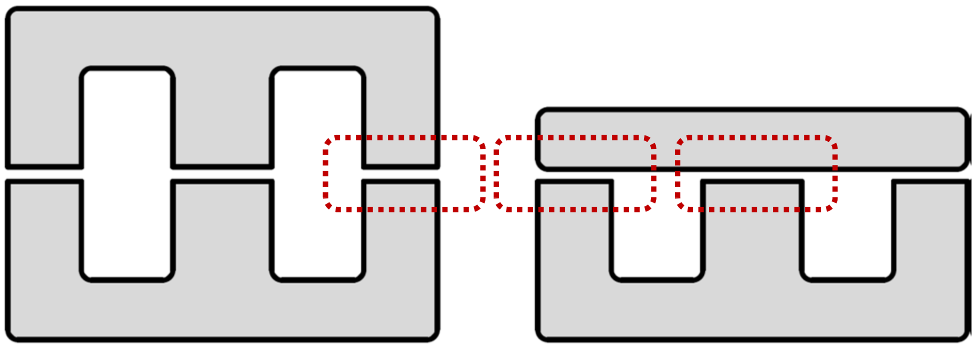

Magnetic Circuit Modeling

New Model (1)

Basic Structure for the Air Gap Calculation (2-D) [3]

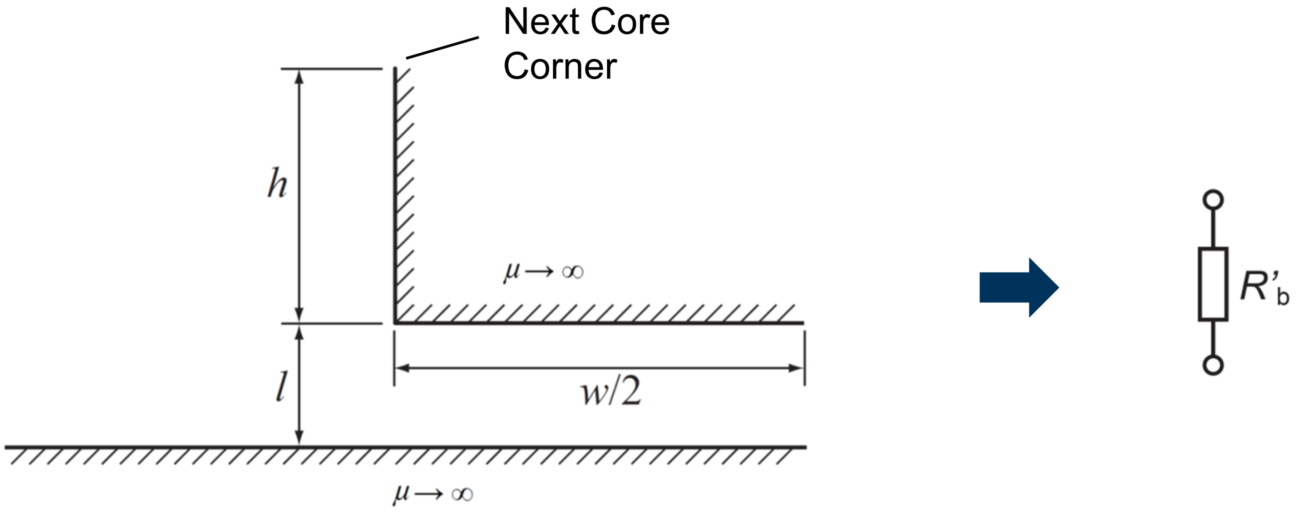

$$R'_{\text{basic}} = \frac{1}{\mu_0 \left[\frac{w}{2l} + \frac{2}{\pi} \left(1 + \ln \frac{\pi h}{4l} \right) \right]}$$

Magnetic Circuit Modeling

New Model (2)

2-D (1)

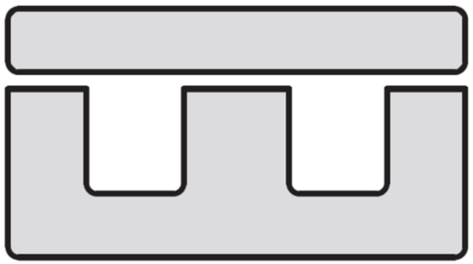

Basic Structure for the Air Gap Calculation

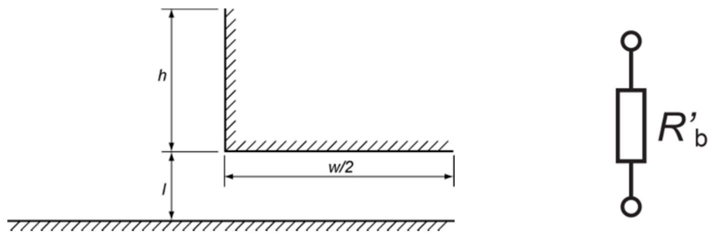

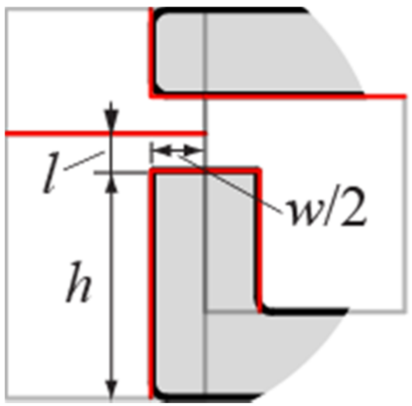

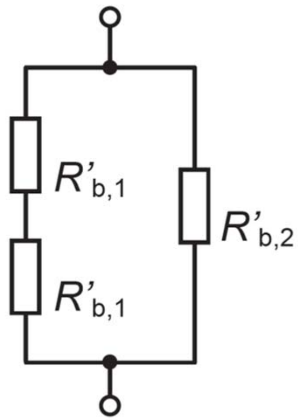

Magnetic Circuit Modeling

New Model (3)

2-D (2)

Air Gap Type 1

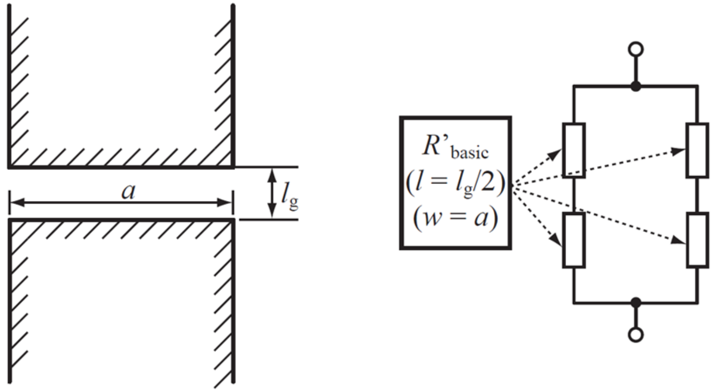

Basic Structure for the Air Gap Calculation

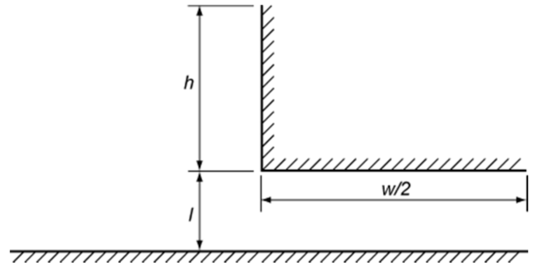

$$R'_{basic} = \frac{1}{\mu_0 \left[\frac{w}{2l} + \frac{2}{\pi}\left(1 + \ln\frac{\pi h}{4l}\right)\right]}$$

Air Gap Type 2

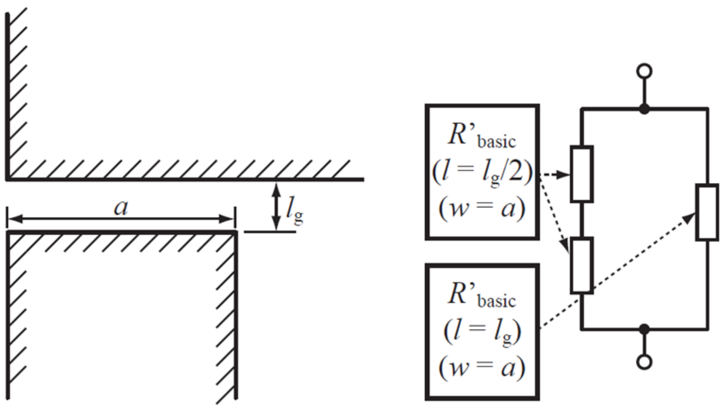

Air Gap Type 3

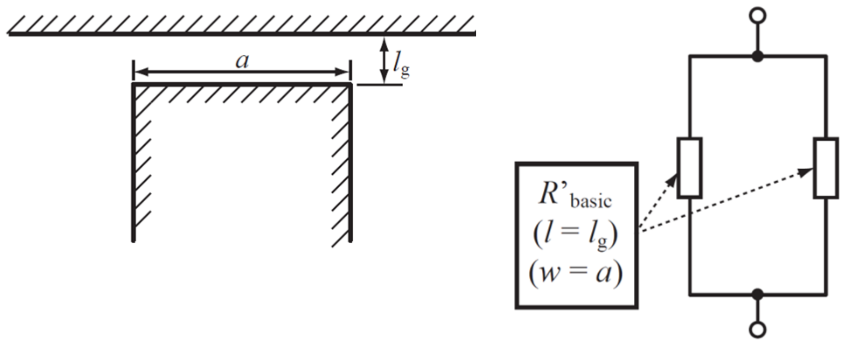

Magnetic Circuit Modeling

New Model (4)

2D → 3D : Fringing Factor (1)

Illustrative Example

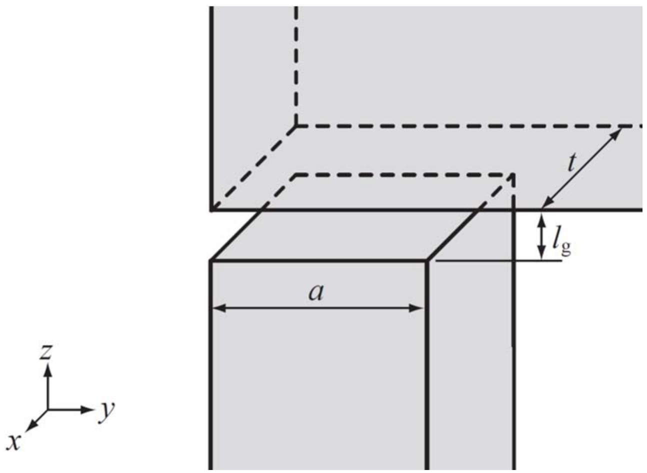

***zy*-plane**

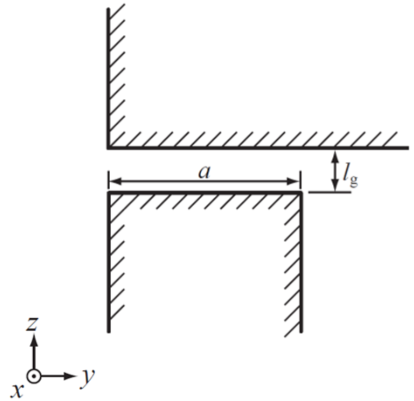

Air gap per unit length

$$\Rightarrow R'_{zy} \Rightarrow \sigma_y = \frac{R'_{zy}}{\dfrac{l_g}{\mu_0 a}}$$

“Idealized” air gap (no fringing flux)

***zx*-plane**

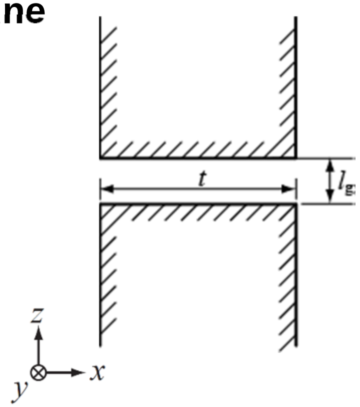

$$\Rightarrow R'_{zx} \Rightarrow \sigma_x = \frac{R'_{zx}}{\dfrac{l_g}{\mu_0 t}}$$

Magnetic Circuit Modeling
New Model (5)

2D → 3D : Fringing Factor (2)

Illustrative Example

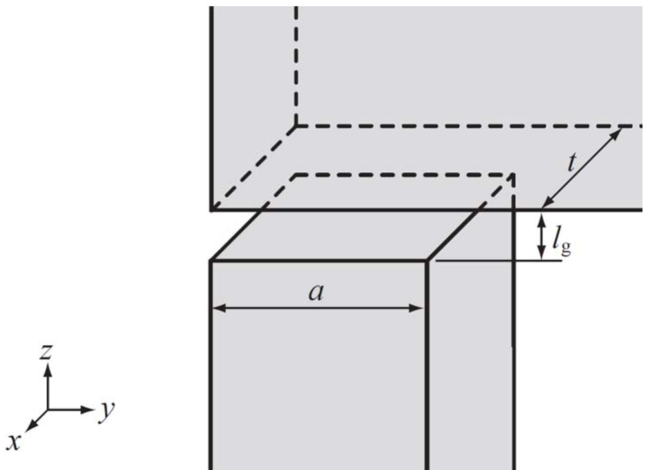

3-D Fringing Factor:

$$\sigma = \sigma_x \sigma_y$$

$$R_g = \sigma \frac{l_g}{\mu_0 a t}$$

"Idealized" air gap
(no fringing flux)

Alternative Interpretation:

Increase of air gap cross sectional area

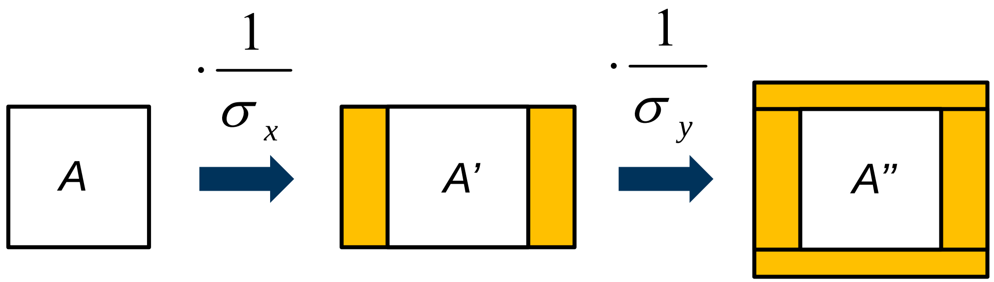

[6] J. Mühlethaler, J.W. Kolar, and A. Ecklebe, "A Novel Approach for 3D Air Gap Reluctance Calculations", in Proc. of the ICPE - ECCE Asia, Jeju, Korea, 2011

Magnetic Circuit Modeling
FEM Results

3-D FEM Simulation

Modeled Example

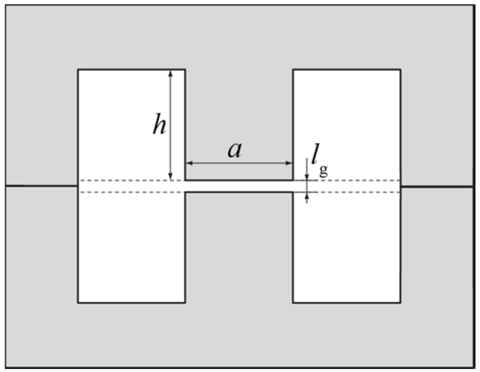

a = 40 mm; h = 40 mm

Results

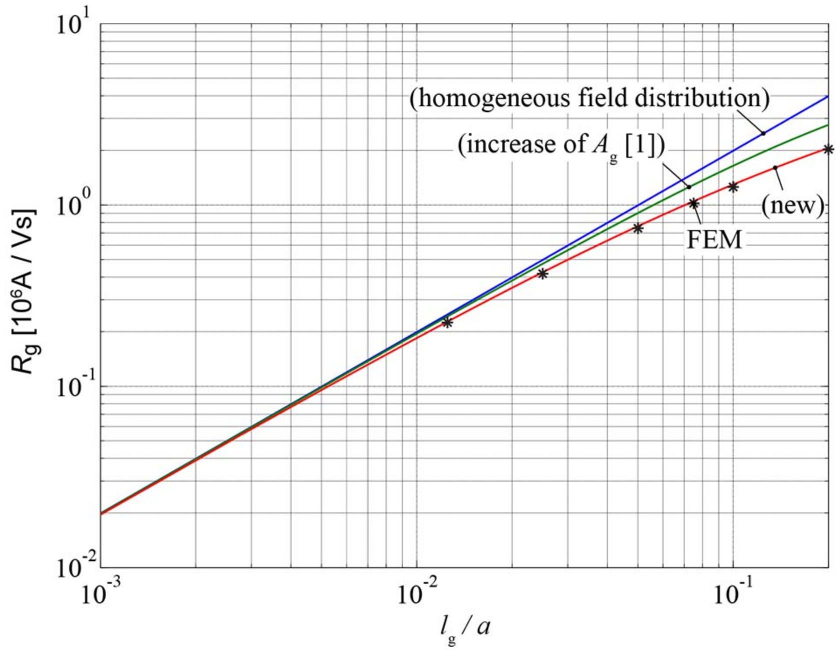

Magnetic Circuit Modeling
Experimental Results

Inductance Calculation
EPCOS E55/28/21, N = 80

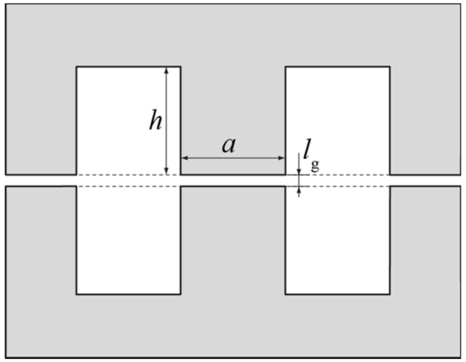

TABLE I
MEASUREMENT RESULTS OF E-CORE

Air Gap Length l_g	Calculated classically (3)	Calculated with new approach (12)	Measured
1.0 mm	1.42 mH	1.97 mH	2.07 mH
1.5 mm	0.96 mH	1.47 mH	1.58 mH
2.0 mm	0.72 mH	1.22 mH	1.26 mH

Saturation Calculation
EPCOS E55/28/21, N = 80,
l_g = 1 mm, B_{sat} = 0.45 T

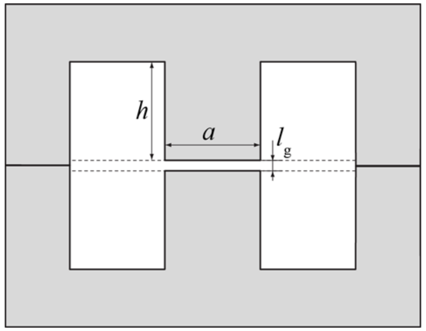

TABLE II
MEASUREMENT RESULTS OF E-CORE

	Calculated classically (3)	Calculated with new approach (12)
L	2.75 mH	3.55 mH
I_{sat}	4.6 A	3.6 A

Measurement

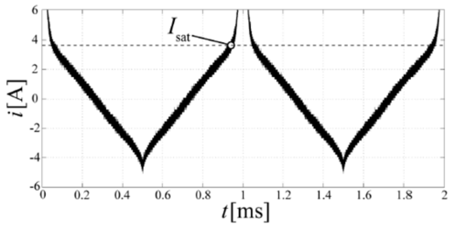

I_{sat} = 3.7 A

Magnetic Circuit Modeling

Non-Linearity of the Core Material

Flux and Reluctance Calculation

$$\emptyset = f(R_\mathrm{m}(\emptyset), I)$$

This equation must be solved iteratively by using a numerical solving method, e.g. the Newton's method.

Reluctance Model

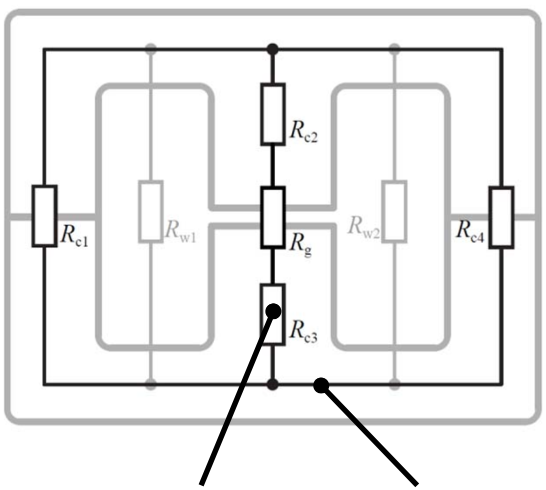

$$R_\mathrm{m} = f(\emptyset) \qquad \emptyset = f(R_\mathrm{m}(\emptyset), I) = f(\emptyset, I)$$

Inductance Calculation

$$L = \frac{N^2}{R_\mathrm{tot}(I)}$$

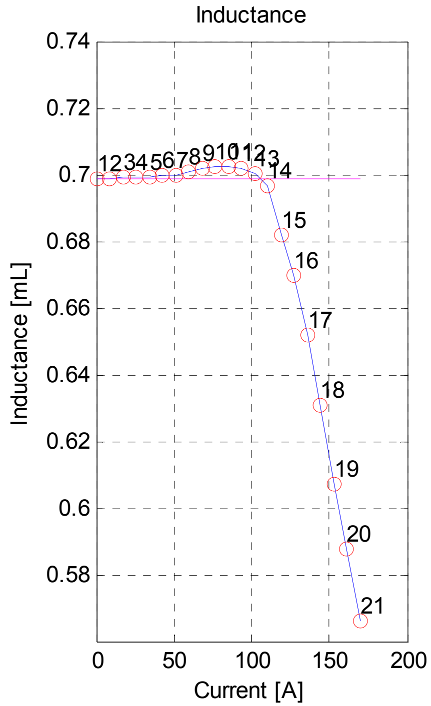

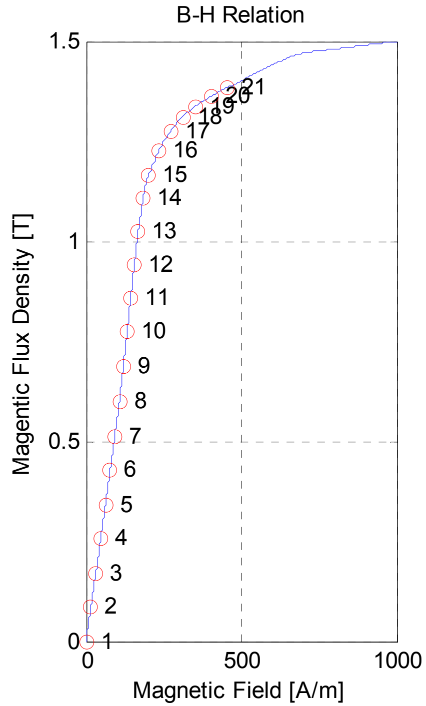

Example
Introduction

Schematic

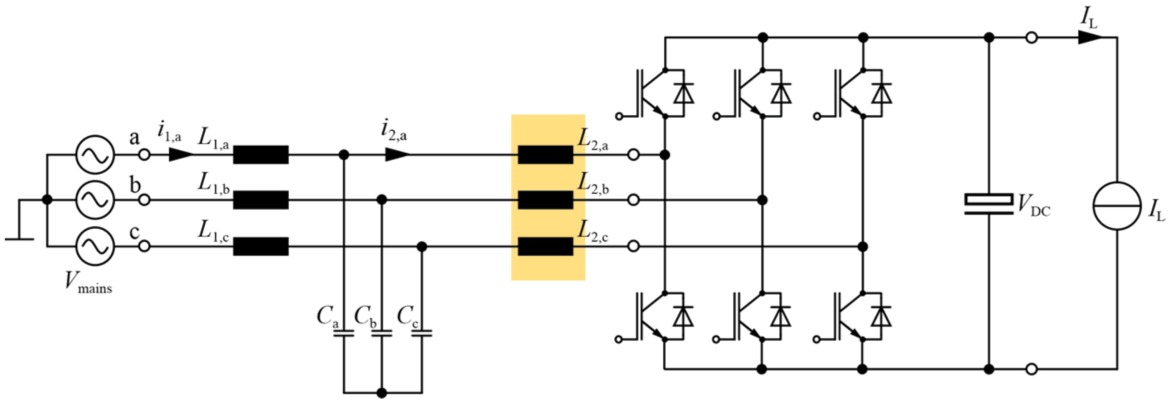

Aim

Design PFC rectifier system.

Show trade-off between losses and volume.

Illustrative example.

Modeling of boost inductors (three individual inductors $L_{2a} = L_{2b} = L_{2c}$) will be step-by-step illustrated in the course of this presentation.

Example
Reluctance Model (1)

Photo & Dimensions

Dimensions

l_g	1.95 mm
do	60 mm
b	60 mm
a	20 mm
t	28 mm
ww	56.9 mm
d	2.24 mm

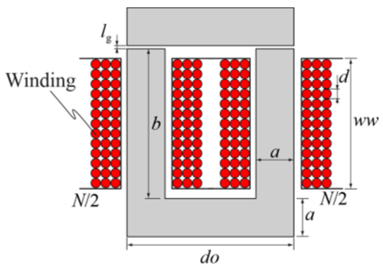

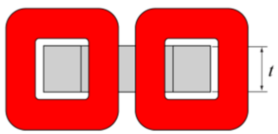

Material

Grain-oriented steel (M165-35S)

Reluctance Model

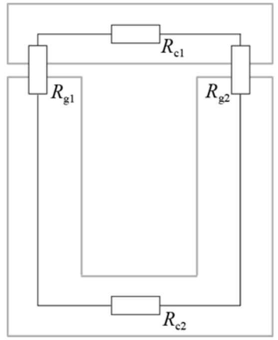

Calculation of Core Reluctances

$$R_{c1} = \frac{do - 2a}{\mu_0 \mu_r a t} + 2\frac{\frac{\pi}{8}(2a)}{\mu_0 \mu_r t \frac{(2a)}{2}}$$

$$= \frac{60\text{mm} - 2\cdot 20\text{mm}}{\mu_0 \cdot 20'000 \cdot 20\text{mm} \cdot 28\text{mm}} + 2\frac{\frac{\pi}{8}(2\cdot 20\text{mm})}{\mu_0 \cdot 20'000 \cdot 28\text{mm}\frac{(2\cdot 20\text{mm})}{2}} = 3654\,\frac{\text{A}}{\text{Vs}}$$

$$R_{c2} = \frac{do - 2a + 2b}{\mu_0 \mu_r a t} + 2\frac{\frac{\pi}{8}(2a)}{\mu_0 \mu_r t \frac{(2a)}{2}}$$

$$= \frac{60\text{mm} - 2\cdot 20\text{mm} + 2\cdot \text{h}}{\mu_0 \cdot 20'000 \cdot 20\text{mm} \cdot 28\text{mm}} + 2\frac{\frac{\pi}{8}(2\cdot 20\text{mm})}{\mu_0 \cdot 20'000 \cdot 28\text{mm}\frac{(2\cdot 20\text{mm})}{2}} = 12184\,\frac{\text{A}}{\text{Vs}}$$

Example
Reluctance Model (2)

Photo & Dimensions

Dimensions

l_g	1.95 mm
do	60 mm
b	60 mm
a	20 mm
t	28 mm
ww	56.9 mm
d	2.24 mm

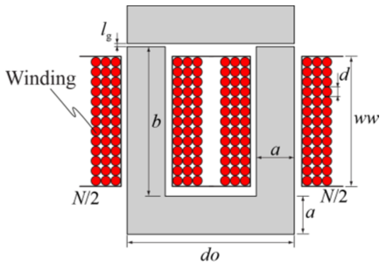

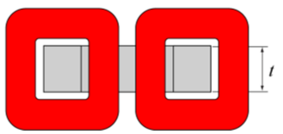

Material
Grain-oriented steel (M165-35S)

Calculation Air Gap Reluctances

***zy*-plane**

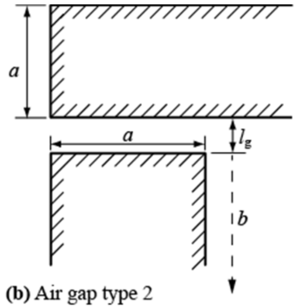

(b) Air gap type 2

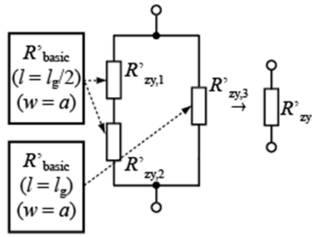

$$\Rightarrow R'_{zy,1} = \frac{1}{\mu_0\left[\frac{a}{2\frac{l_g}{2}} + \frac{2}{\pi}\left(1 + \ln\frac{\pi a}{4\frac{l_g}{2}}\right)\right]} \quad R'_{zy,2} = \frac{1}{\mu_0\left[\frac{a}{2\frac{l_g}{2}} + \frac{2}{\pi}\left(1 + \ln\frac{\pi(b+a)}{4\frac{l_g}{2}}\right)\right]}$$

$$R'_{zy,3} = \frac{1}{\mu_0\left[\frac{a}{2l_g} + \frac{2}{\pi}\left(1 + \ln\frac{\pi b}{4l_g}\right)\right]} \quad \Rightarrow R'_{zy} = \frac{\left(R'_{zy,1} + R'_{zy,2}\right)R'_{zy,3}}{R'_{zy,1} + R'_{zy,2} + R'_{zy,3}}$$

$$\Rightarrow \sigma_y = \frac{R'_{zy}}{\frac{l_g}{\mu_0 a}} = 0.72$$

***zx*-plane**

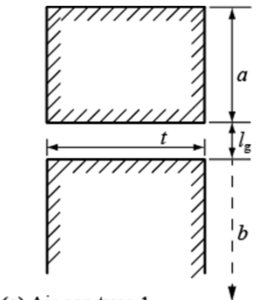

(a) Air gap type 1

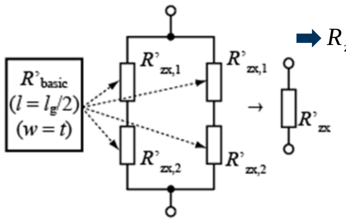

$$\Rightarrow R'_{zx,1} = \frac{1}{\mu_0\left[\frac{t}{2\frac{l_g}{2}} + \frac{2}{\pi}\left(1 + \ln\frac{\pi a}{4\frac{l_g}{2}}\right)\right]} \quad R'_{zx,2} = \frac{1}{\mu_0\left[\frac{t}{2\frac{l_g}{2}} + \frac{2}{\pi}\left(1 + \ln\frac{\pi(b+a)}{4\frac{l_g}{2}}\right)\right]}$$

$$\Rightarrow R'_{zx} = \frac{R'_{zx,1} + R'_{zx,2}}{2} \qquad \Rightarrow \sigma_x = \frac{R'_{zx}}{\frac{l_g}{\mu_0 t}} = 0.84$$

$$R_g = \sigma_x \sigma_y \frac{l_g}{\mu_0 a t} = 1.66\,\frac{\text{MA}}{\text{Wb}}$$

Basic Reluctance

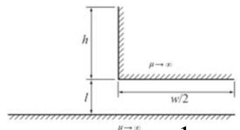

$$R'_{basic} = \frac{1}{\mu_0\left[\frac{w}{2l} + \frac{2}{\pi}\left(1 + \ln\frac{\pi h}{4l}\right)\right]}$$

Inductance

$$L = \frac{N^2}{R_{c1} + R_{c2} + R_{g1} + R_{g2}} = 2.66\,\text{mH}$$

meas.
2.69 mH

Outline

- Magnetic Circuit Modeling
- Core Loss Modeling
- Winding Loss Modeling
- Thermal Modeling
- Multi-Objective Optimization
- Summary & Conclusion

Core Loss Modeling

Overview of Different Core Materials (1)

- Magnetic Materials
  - Soft Magnetic Materials
    - Iron Based Alloys
      - ferromagnetics -
      Alloys with some amount of Si, Ni, Cr or Co.
      Low electric resistivity.
      High saturation flux density.
      - Laminated Cores
        Laminations are electrically isolated to reduce eddy currents.
      - Powder Iron Cores
        Consist of small iron particles, which are electrically isolated to each other.
      - Amorphous Alloys
        Made of alloys without crystallyine order (cf. glasses, liquids).
      - Nanocrystalline Materials
        Ultra fine grain FeSi, which are embedded in an amorphous minority phase.
    - Ferrites
      - ferrimagnetics -
      Ceramic materials, oxide mixtures of iron and Mn, Zn, Ni or Co.
      High electric resistivity.
      Small saturation flux density compared to ferromagnetics.
  - Hard Magnetic Materials

Core Loss Modeling
Overview of Different Core Materials (2)

Selection Criteria

Saturation Flux Density
Power Loss Density
(Frequency Range)
Price
etc.

Ferrite

Low Sat. Flux Density (0.45 T)
Low Losses
Low Price
Many Different Shapes
Very Brittle

Powder Iron Core

High Sat. Flux Density (1.5 T)
Moderate Losses
Low Price
Many Different Shapes
Distributed Air Gap (low rel. permeability)

Laminated Steel Cores

Very High Sat. Flux Density (2.2T)
High Losses
Low Price
Many Different Shapes

Amorphous Alloys

High Sat. Flux Density (1.5T)
Low Losses
High Price
Limited Available Shapes

Nanocrystalline Materials

High Sat. Flux Density (1.1T)
Very Low Losses
Very High Price
Limited Available Shapes

LF: $B_{\mathrm{SAT}} = B_{\mathrm{max}}$.
HF: B_{max} is limited by core losses.

Core Loss Modeling

Overview of Different Core Materials (3)

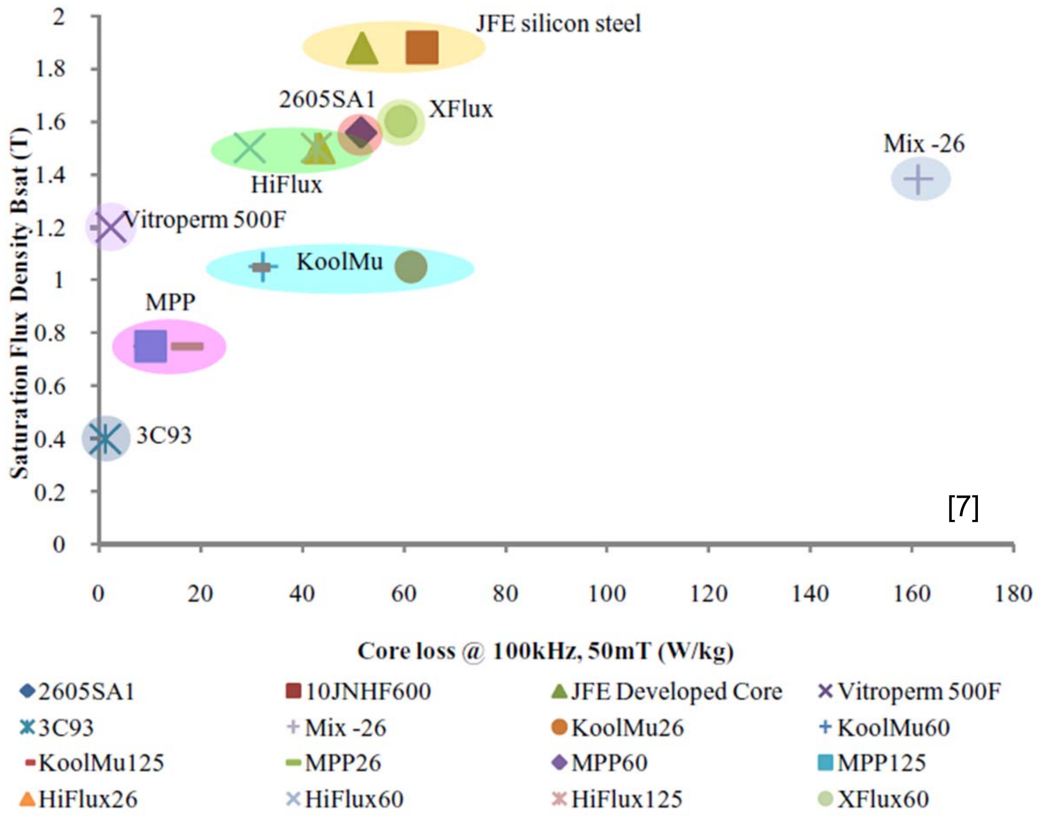

[7] M. S. Rylko, K. J. Hartnett, J. G. Hayes, M.G. Egan, "Magnetic Material Selection for High Power High Frequency Inductors in DC-DC Converters", in Proc. of the APEC 2009.

Core Loss Modeling

Physical Origin of Core Losses (1)

Weiss Domains / Domain Walls

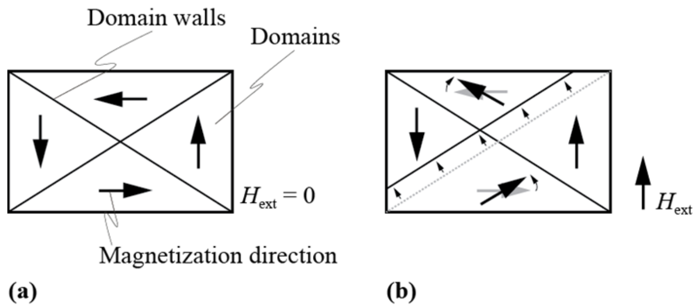

- Spontaneous magnetization.
- Material is divided to saturated domains (Weiss domains).
- In case an external field is applied, the domain walls are shifted or the magnetic moments within the domains change their direction. → The net magnetization becomes greater than zero.

B-*H*-Loop

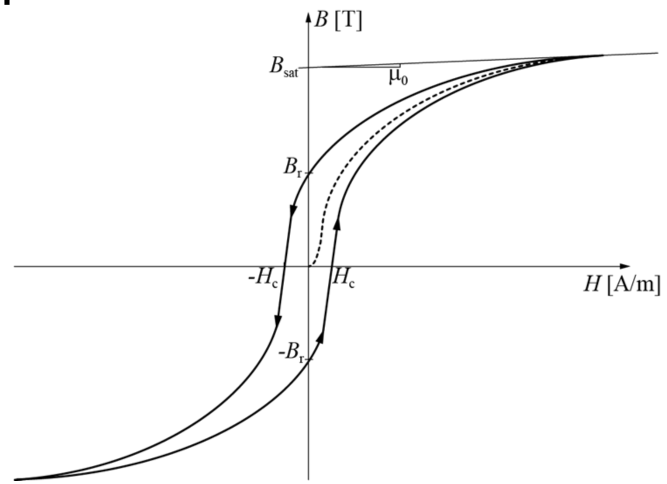

- The flux change is partly irreversible, i.e. energy is dissipated as heat.
- The reason for this are the so called Barkhausen jumps, that lead to local eddy current losses.
- In case the loop is traversed very slowly, these Barkhausen jumps lead to the *static hysteresis losses*.

Core Loss Modeling

Physical Origin of Core Losses (2)

***B*-*H*-Loop**

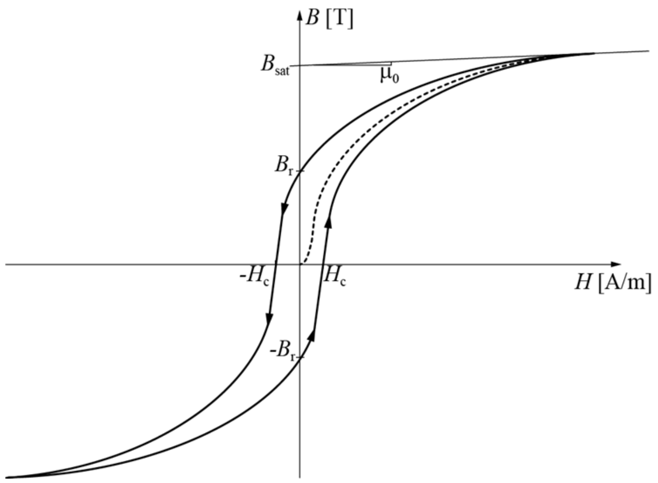

- If the process would be fully reversible, going from B_1 to B_2 would store potential energy in the magnetic material that is later released (i.e. the area of the closed loop would be zero).

- Since the process is partly irreversible, the area of the closed loop represents the energy loss per cycle

$$W = \oint H \mathrm{d}B$$

Core Loss Modeling
Classification of Losses (1)

- **(Static) hysteresis loss**
  - Rate-independent *BH* Loop.
  - Loss energy per cycle is constant.
  - Irreversible changes each within a small region of the lattice (Barkhausen jumps).
  - These rapid, irreversible changes are produced by relatively strong local fields within the material.

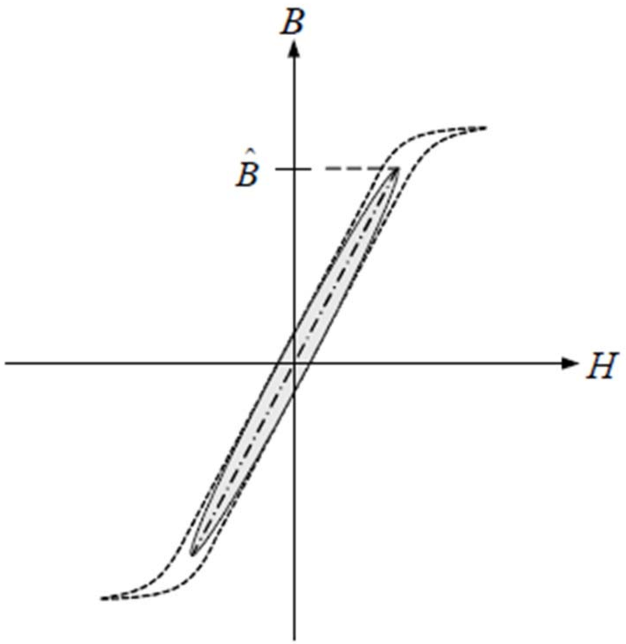

- **Eddy current losses**
- **Residual Losses – Relaxation losses**

Core Loss Modeling
Classification of Losses (2)

- **(Static) hysteresis loss**
- **Eddy current losses**
  - Depend on material conductivity and core shape.
  - Affect *BH* loop.
- **Residual Losses – Relaxation losses**

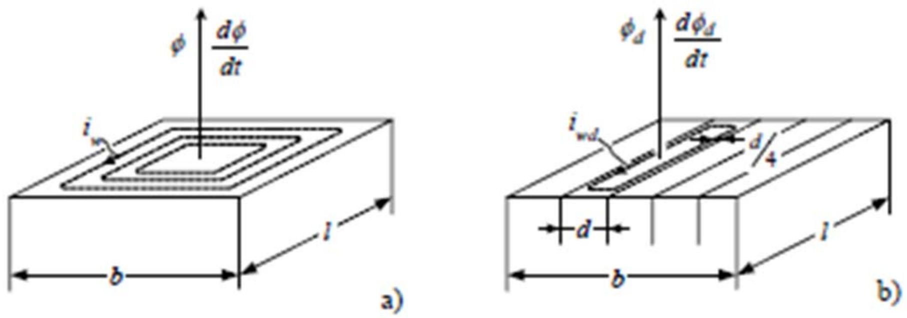

Measurements

VITROPERM 500F

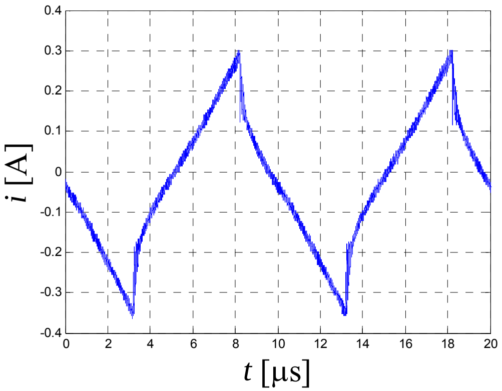

Core Loss Modeling

Classification of Losses (3)

- **(Static) hysteresis loss**
- **Eddy current losses**
- **Residual losses – Relaxation losses**
    - Rate-dependent *BH* Loop.
    - Reestablishment of a thermal equilibrium is governed by relaxation processes.
    - Restricted domain wall motion.

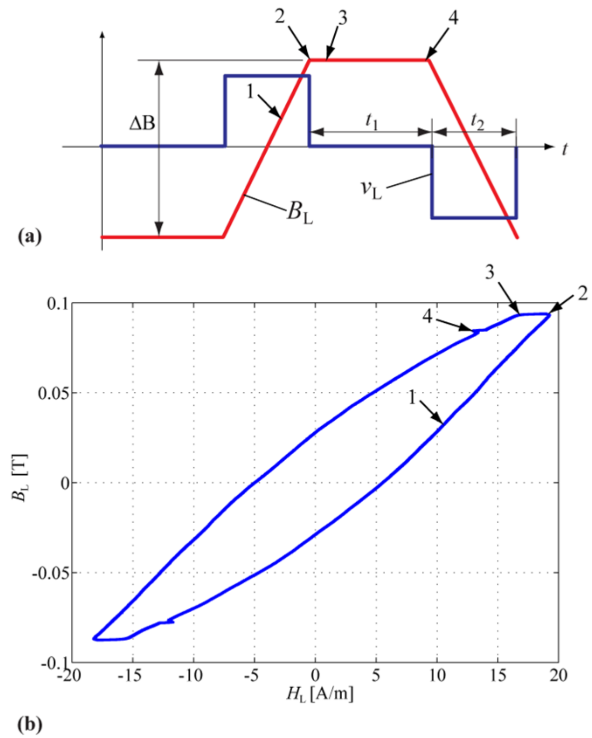

Core Loss Modeling

Typical Flux Waveforms

Sinusoidal

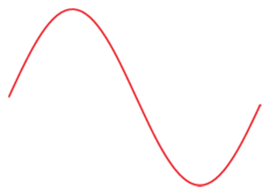

e.g. 50/60 Hz isolation transformer

Triangular

e.g. Buck / Boost converter

Trapezoidal

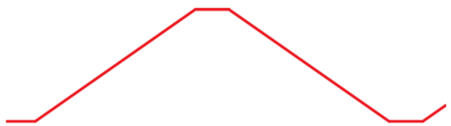

e.g. boost inductor of Dual Active Bridge

Combination

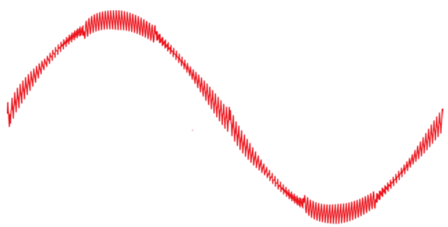

e.g. Boost inductor in PFC

Core Loss Modeling

Outline of Different Modeling Approaches

Steinmetz Approach

$$P = k\, f^{\alpha} B^{\beta}$$

- Simple
- Steinmetz parameter are valid only in a limited flux density and frequency range
- DC Bias not considered
- (Only for sinusoidal flux waveforms)

Relative core losses versus frequency (measured on R16 toroids)

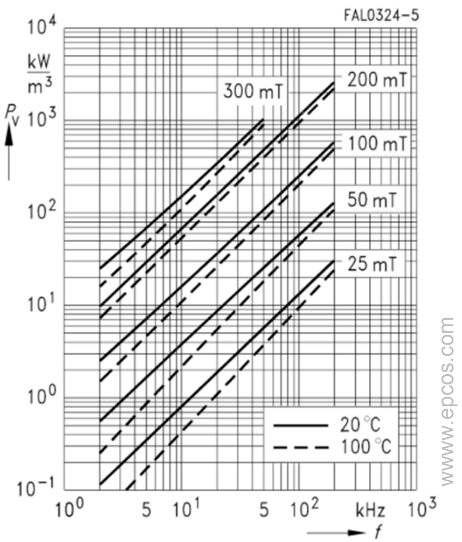

Loss Map Approach

(Loss Database)

- Measuring core losses is indispensable to overcome limits of Steinmetz approach

Loss Separation

$$P = P_{\text{hyst}} + P_{\text{eddy}} + P_{\text{residual}}$$

- Needed parameters often unknown
- Model is widely applicable
- Increases physical understanding of loss mechanisms

Hysteresis Model

(e.g. Preisach Model, Jiles-Atherton Model)

- Difficult to parameterize
- Increases physical understanding of loss mechanisms

Core Loss Modeling

Overview of Hybrid Modeling Approach

"The best of both worlds" (Steinmetz & Loss Map approach)

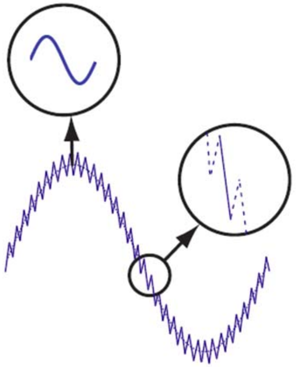

Loss Map
(Loss Material Database) **(2)/(3)**

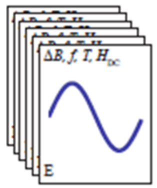

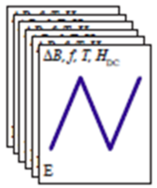

$$k, k_i, \alpha, \beta, \alpha_r, \beta_r, q_r, \tau$$

$$P_v = \frac{1}{T}\int_0^T k_i \left|\frac{dB}{dt}\right|^{\alpha} (\Delta B)^{\beta-\alpha}\,dt + \sum_{l=1}^{n} Q_{rl} P_{rl} \quad \textbf{(1)}$$

$$\frac{P}{V} \quad \textbf{(4)}$$

Outline of Discussion

- Derivation of the i²GSE. **(1)**
- How to measure core losses in order to build loss map. **(2)**
- Use of loss map. **(3)**
- How to calculate core losses for cores of different shapes? **(4)**

Core Loss Modeling

Derivation of the i²GSE – Motivation (1)

Steinmetz Equation SE

$$P_v = k\, f^{\alpha}\, \hat{B}^{\beta}$$

- Only sinusoidal waveforms (→ iGSE).

P_v : time-average power loss per unit volume

iGSE

$$P_v = \frac{1}{T}\int_0^T k_i \left|\frac{\mathrm{d}B}{\mathrm{d}t}\right|^{\alpha} (\Delta B)^{\beta-\alpha}\, \mathrm{d}t$$

$$k_i = \frac{k}{(2\pi)^{\alpha-1}\int_0^{2\pi} |\cos\theta|^{\alpha}\, 2^{\beta-\alpha}\, \mathrm{d}\theta}$$

- DC bias not considered
- Relaxation effect not considered (→ i²GSE)
- Steinmetz parameter are valid only for a limited flux density and frequency range

Core Loss Modeling

Derivation of the i²GSE – Motivation (2)

iGSE [8]

$$P_{\mathrm{v}} = \frac{1}{T}\int_0^T k_i \left|\frac{\mathrm{d}B}{\mathrm{d}t}\right|^{\alpha} (\Delta B)^{\beta-\alpha}\,\mathrm{d}t$$

$$k_i = \frac{k}{(2\pi)^{\alpha-1}\int_0^{2\pi} |\cos\theta|^{\alpha}\, 2^{\beta-\alpha}\,\mathrm{d}\theta}$$

How to apply the formula?

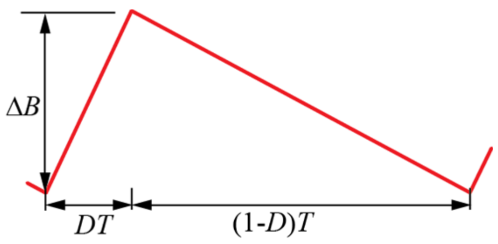

$$P_{\mathrm{v}} = \frac{k_i}{T}\left[DT\left(\frac{\Delta B}{DT}\right)^{\alpha}(\Delta B)^{\beta-\alpha} + (1-D)T\left(\frac{\Delta B}{(1-D)T}\right)^{\alpha}(\Delta B)^{\beta-\alpha}\right] = \ldots$$

Idea

- Generalized formula that is applicable for different flux waveforms
- Losses depend on dB/dt

For Sinusoidal Waveforms

$$P_{\mathrm{v}} = \frac{1}{T}\int_0^T k_i \left|\frac{\mathrm{d}B}{\mathrm{d}t}\right|^{\alpha} (\Delta B)^{\beta-\alpha}\,\mathrm{d}t = kf^{\alpha}\left(\frac{\Delta B}{2}\right)^{\beta}$$

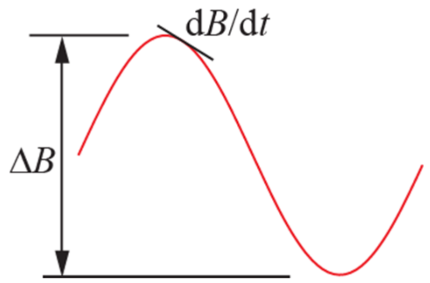

[8] K. Venkatachalam, C. R. Sullivan, T. Abdallah, and H. Tacca, “Accurate prediction of ferrite core loss with nonsinusoidal waveforms using only Steinmetz parameters”, in Proc. of IEEE Workshop on Computers in Power Electronics, pp. 36-41, 2002.

Core Loss Modeling

Derivation of the i²GSE – Motivation (3)

Waveform

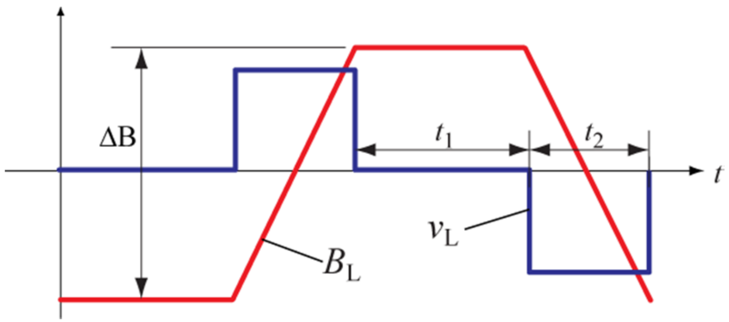

Results

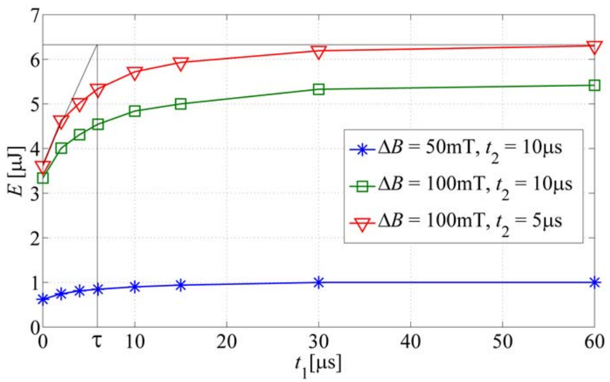

iGSE

$$P_v = \frac{1}{T}\int_0^T k_i \left|\frac{\mathrm{d}B}{\mathrm{d}t}\right|^{\alpha} (\Delta B)^{\beta-\alpha}\,\mathrm{d}t$$

Conclusion

Losses in the phase of constant flux!

Core Loss Modeling

Derivation of the i²GSE – *B*-*H*-Loop

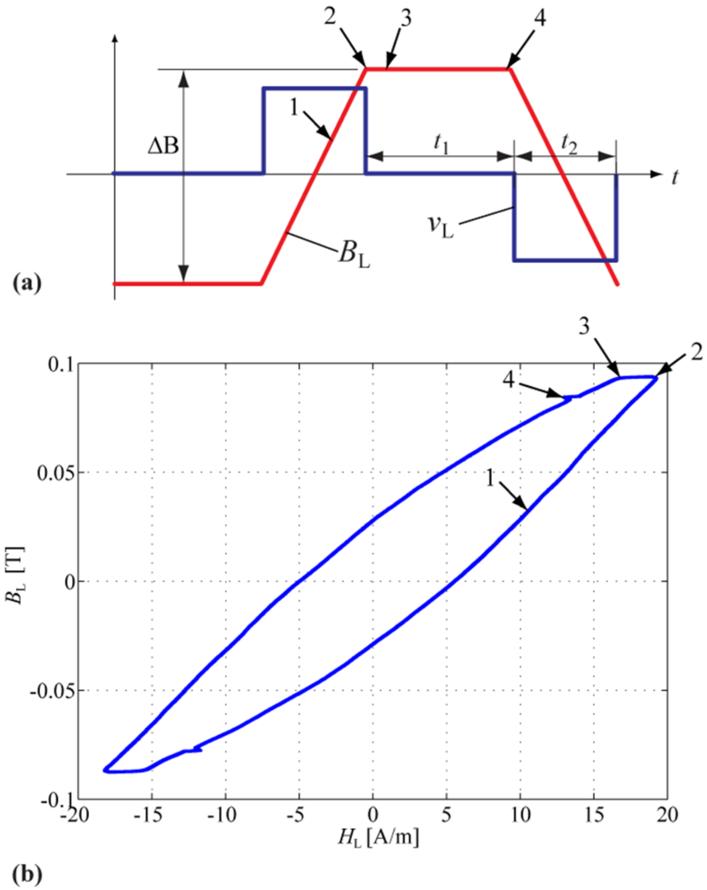

Relaxation Losses

- Rate-dependent *BH* Loop.
- Reestablishment of a thermal equilibrium is governed by relaxation processes.
- Restricted domain wall motion.

Current Waveform

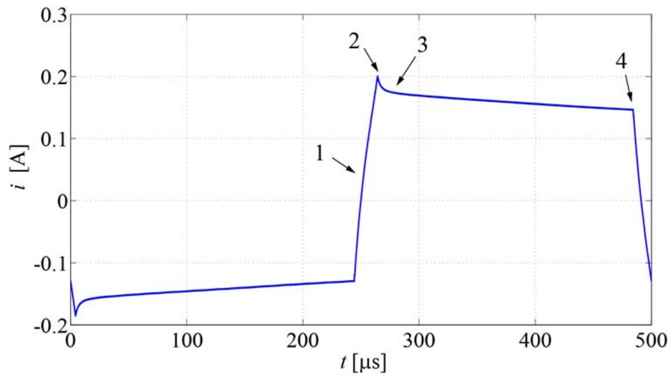

Core Loss Modeling

Derivation of the i²GSE – Model Derivation 1 (1)

Waveform

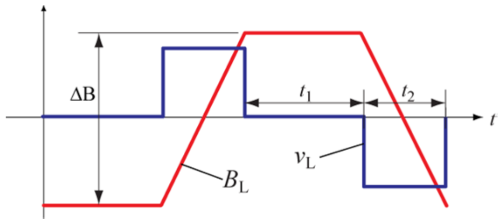

Loss Energy per Cycle

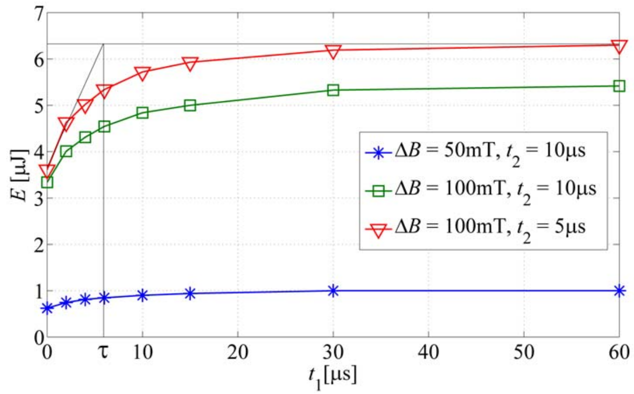

Derivation (1)

Relaxation loss energy can be described with

$$E = \Delta E\left(1 - e^{-\frac{t_1}{\tau}}\right)$$

τ is independent of operating point.

How to determine ΔE?

Core Loss Modeling

Derivation of the i²GSE – Model Derivation 1 (2)

ΔE – Measurements

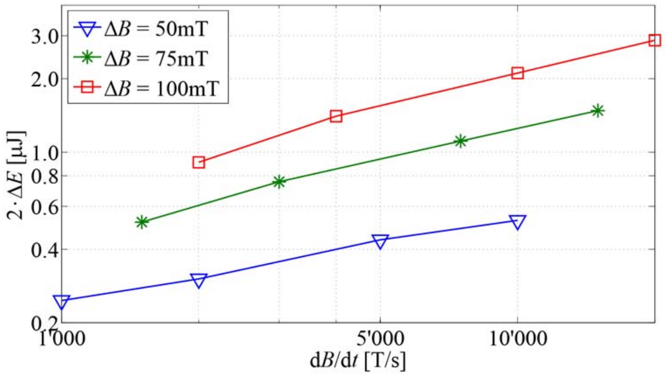

(a)

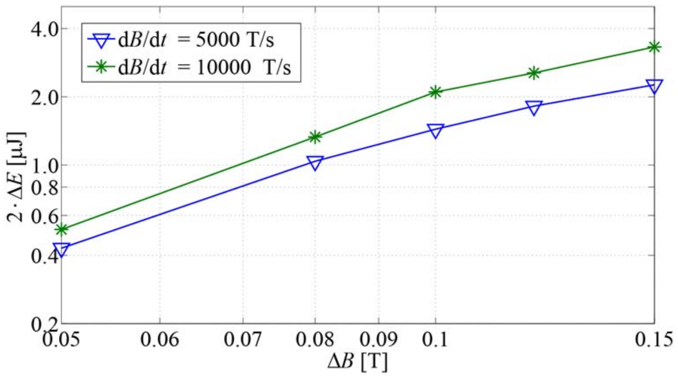

(b)

Waveform

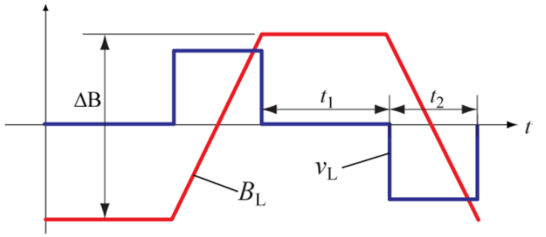

Conclusion

→ ΔE follows a power function!

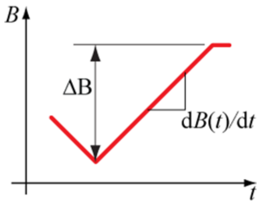

$$\Delta E = k_\mathrm{r} \left| \frac{\mathrm{d}}{\mathrm{d}t} B(t) \right|^{\alpha_\mathrm{r}} (\Delta B)^{\beta_\mathrm{r}}$$

Core Loss Modeling

Derivation of the i²GSE – Model Derivation 1 (3)

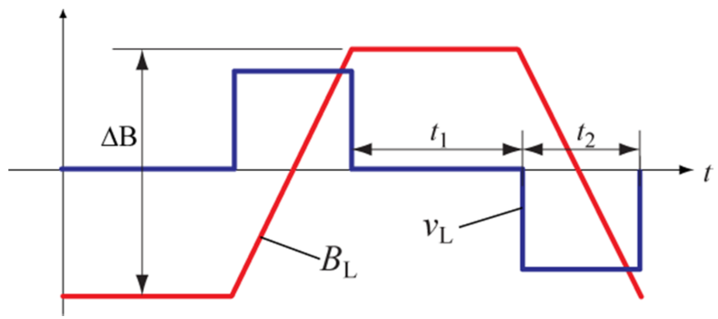

Model Part 1

$$P_v = \frac{1}{T}\int_0^T k_i \left|\frac{dB}{dt}\right|^{\alpha} (\Delta B)^{\beta-\alpha}\, dt + \sum_{l=1}^{n} P_{rl}$$

$$P_{rl} = \frac{1}{T} k_r \left|\frac{d}{dt}B(t)\right|^{\alpha_r} (\Delta B)^{\beta_r} \left(1 - e^{-\frac{t_1}{\tau}}\right)$$

Core Loss Modeling

Derivation of the i²GSE – Model Derivation 2 (1)

Waveform

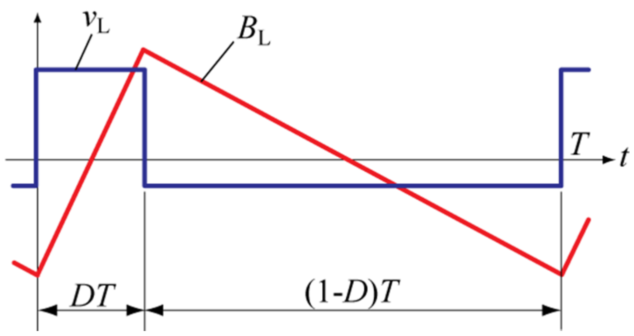

Power Loss

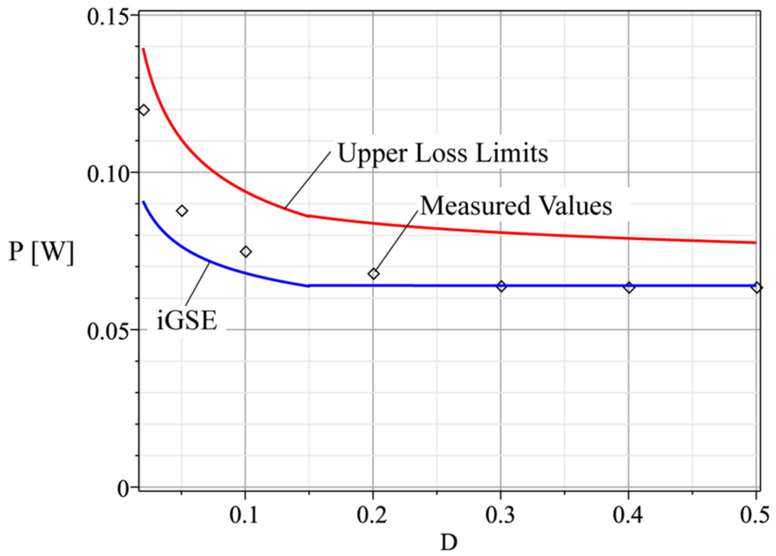

Explanation

1) For values of *D* close to 0 or close to 1 a loss underestimation is expected when calculating losses with iGSE (no relaxation losses included).
2) For values of *D* close to 0.5 the iGSE is expected to be accurate.
3) Adding the relaxation term leads to the upper loss limit, while the iGSE represents the lower loss limit.
4) Losses are expected to be in between the two limits, as has been confirmed with measurements.

Core Loss Modeling

Derivation of the i²GSE – Model Derivation 2 (2)

Waveform

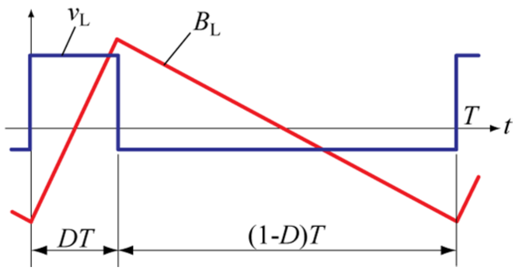

Power Loss

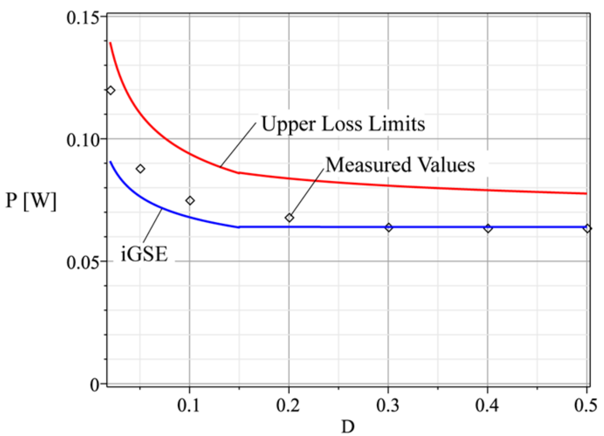

Model Adaption

$$P_v = \frac{1}{T}\int_0^T k_i \left|\frac{dB}{dt}\right|^{\alpha} (\Delta B)^{\beta-\alpha} dt + \sum_{l=1}^{n} Q_{rl} P_{rl}$$

Q_{rl} should be 1 for $D = 0$

Q_{rl} should be 0 for $D = 0.5$

Q_{rl} should be such that calculation fits a triangular waveform measurement.

$$Q_{rl} = e^{-q_r \left|\frac{dB(t+)/dt}{dB(t-)/dt}\right|} \left(= e^{-q_r \frac{D}{1-D}} \right)$$

Core Loss Modeling

Derivation of the i²GSE – Model Derivation 2 (3)

Waveform

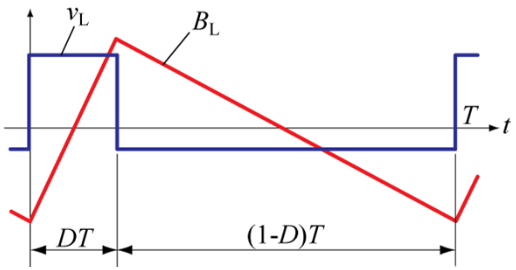

Power Loss

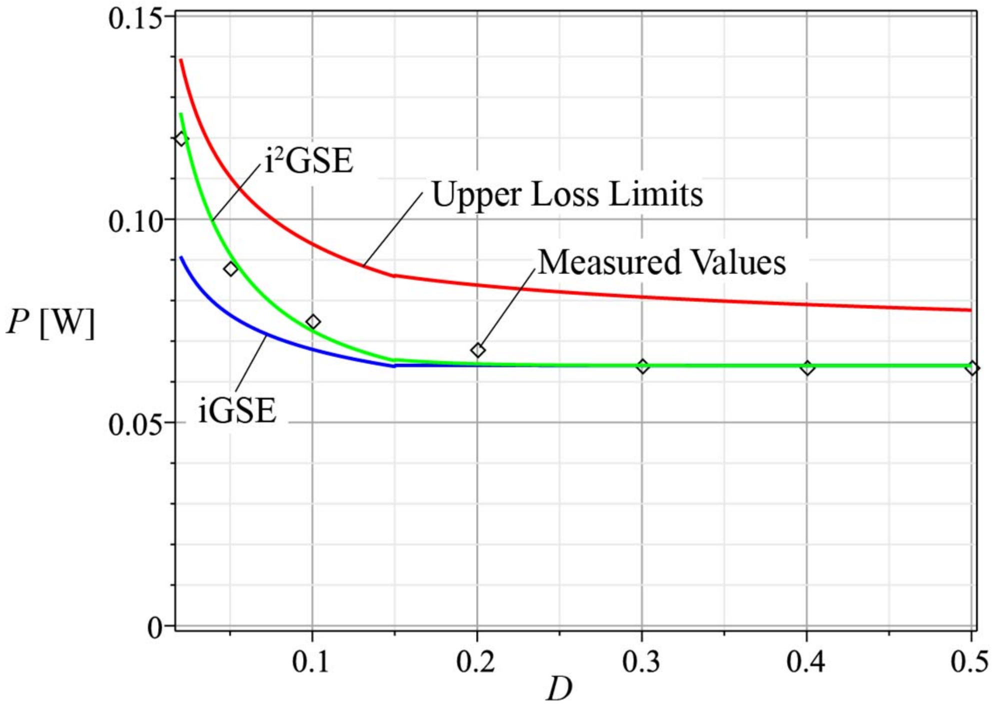

Core Loss Modeling

Derivation of the i²GSE – Summary

The improved-improved Generalized Steinmetz Equation (i²GSE) [9]

$$P_{\mathrm{v}} = \frac{1}{T}\int_0^T k_i \left|\frac{\mathrm{d}B}{\mathrm{d}t}\right|^{\alpha} (\Delta B)^{\beta-\alpha}\,\mathrm{d}t + \sum_{l=1}^{n} Q_{\mathrm{r}l} P_{\mathrm{r}l}$$

with

$$P_{\mathrm{r}l} = \frac{1}{T} k_{\mathrm{r}} \left|\frac{\mathrm{d}}{\mathrm{d}t} B(t)\right|^{\alpha_{\mathrm{r}}} (\Delta B)^{\beta_{\mathrm{r}}} \left(1 - \mathrm{e}^{-\frac{t_1}{\tau}}\right)$$

and

$$Q_{\mathrm{r}l} = \mathrm{e}^{-q_{\mathrm{r}} \left|\frac{\mathrm{d}B(t+)/\mathrm{d}t}{\mathrm{d}B(t-)/\mathrm{d}t}\right|}$$

[9] J. Mühlethaler, J. Biela, J.W. Kolar, and A. Ecklebe, “Improved Core Loss Calculation for Magnetic Components Employed in Power Electronic Systems”, in Proc. of the APEC, Ft. Worth, TX, USA, 2011.

Core Loss Modeling

Derivation of the i²GSE – Example

i²GSE

Evaluated for each piecewise-linear flux segment

Evaluated for each voltage step, i.e. for each corner point in a piecewise-linear flux waveform.

$$P_\mathrm{v} = \underbrace{\frac{1}{T}\int_0^T k_i \left|\frac{\mathrm{d}B}{\mathrm{d}t}\right|^\alpha (\Delta B)^{\beta-\alpha}\,\mathrm{d}t}_{} + \underbrace{\sum_{l=1}^{n} Q_{\mathrm{r}l} P_{\mathrm{r}l}}_{}$$

Example

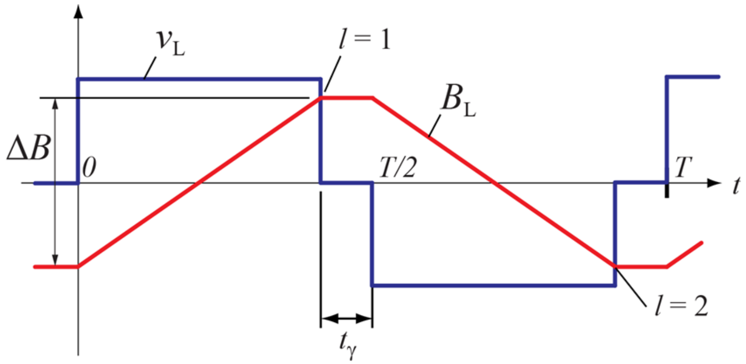

$$\frac{\mathrm{d}B}{\mathrm{d}t} = \begin{cases} \dfrac{\Delta B}{T/2-t_\gamma} & \text{for } t \geq 0 \text{ and } t < T/2-t_\gamma \\ 0 & \text{for } t \geq T/2-t_\gamma \text{ and } t < T/2 \\ -\dfrac{\Delta B}{T/2-t_\gamma} & \text{for } t \geq T/2 \text{ and } t < T-t_\gamma \\ 0 & \text{for } t \geq T-t_\gamma \text{ and } t < T \end{cases}$$

$$P_\mathrm{v} = \frac{T-2t_\gamma}{T} k_i \left|\frac{\Delta B}{T/2-t_\gamma}\right|^\alpha (\Delta B)^{\beta-\alpha} + \sum_{l=1}^{2} Q_{\mathrm{r}l} P_{\mathrm{r}l}$$

with $Q_{\mathrm{r}1} = Q_{\mathrm{r}2} = 0$

$$P_{\mathrm{r}1} = P_{\mathrm{r}2} = \frac{1}{T} k_\mathrm{r} \left|\frac{\Delta B}{T/2-t_\gamma}\right|^{\alpha_\mathrm{r}} (\Delta B)^{\beta_\mathrm{r}} \left(1-\mathrm{e}^{-\frac{t_\gamma}{\tau}}\right)$$

Core Loss Modeling

Derivation of the i²GSE – Conclusion

i²GSE

$$P_{\mathrm{v}} = \underbrace{\frac{1}{T}\int_0^T k_i \left|\frac{\mathrm{d}B}{\mathrm{d}t}\right|^{\alpha} (\Delta B)^{\beta-\alpha}\,\mathrm{d}t}_{\text{Evaluated for each piecewise-linear flux segment}} + \underbrace{\sum_{l=1}^{n} Q_{\mathrm{r}l} P_{\mathrm{r}l}}_{\text{Evaluated for each voltage step, i.e. for each corner point in a piecewise-linear flux waveform.}}$$

Remaining Problems

Steinmetz parameter are valid only in a limited flux density and frequency range.

Core Losses vary under DC bias condition.

Modeling relaxation and DC bias effects need parameters that are not given by core material manufacturers.

➡ **Measuring core losses is indispensable!**

Core Loss Modeling

Overview of Hybrid Modeling Approach

"The best of both worlds" (Steinmetz & Loss Map approach)

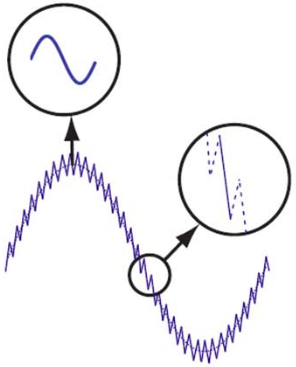

Loss Map
(Loss Material Database) **(2)/(3)**

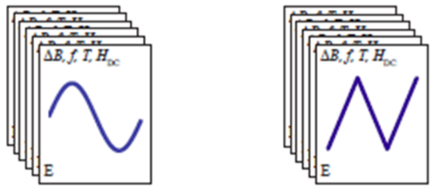

$$k, k_i, \alpha, \beta, \alpha_r, \beta_r, q_r, \tau$$

$$P_v = \frac{1}{T}\int_0^T k_i \left|\frac{dB}{dt}\right|^{\alpha} (\Delta B)^{\beta-\alpha} dt + \sum_{l=1}^{n} Q_{rl} P_{rl}$$ **(1)**

$$\frac{P}{V}$$ **(4)**

Outline of Discussion

- Derivation of the i²GSE. **(1)**
- How to measure core losses in order to build loss map. **(2)**
- Use of loss map. **(3)**
- How to calculate core losses for cores of different shapes? **(4)**

Core Loss Modeling

Core Loss Measurement – Measurement Principle

Waveforms

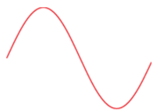

Sinusoidal

Triangular

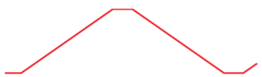

Trapezoidal

Excitation System

Voltage	0 … 450 V
Current	0 … 25 A
Frequency	0 … 200 kHz

Schematic

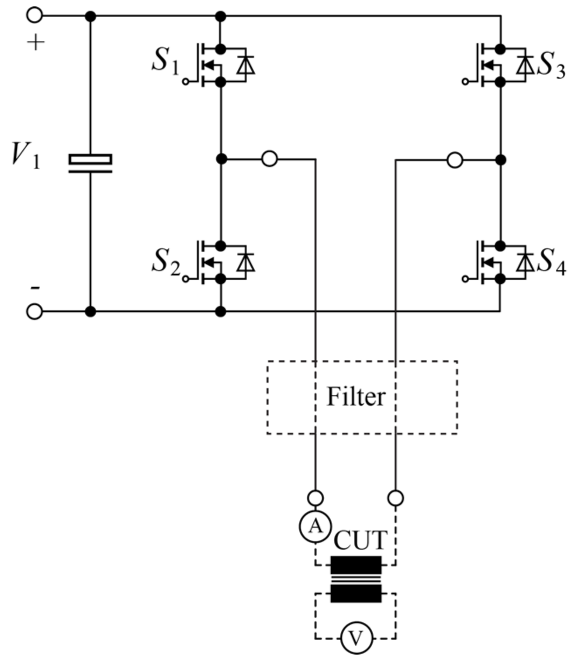

Loss Extraction

$$\left.\begin{aligned} B(t) &= \frac{1}{N_2 \cdot A_e} \int_0^t u(\tau)\, \mathrm{d}\tau \\ H(t) &= \frac{N_1 \cdot i(t)}{l_e} \end{aligned}\right\}$$

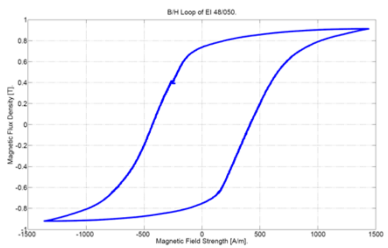

$$\frac{P[W]}{V[m^3]} = f \oint H \, \mathrm{d}B$$

Core Loss Modeling
Core Loss Measurement - Overview

System Overview

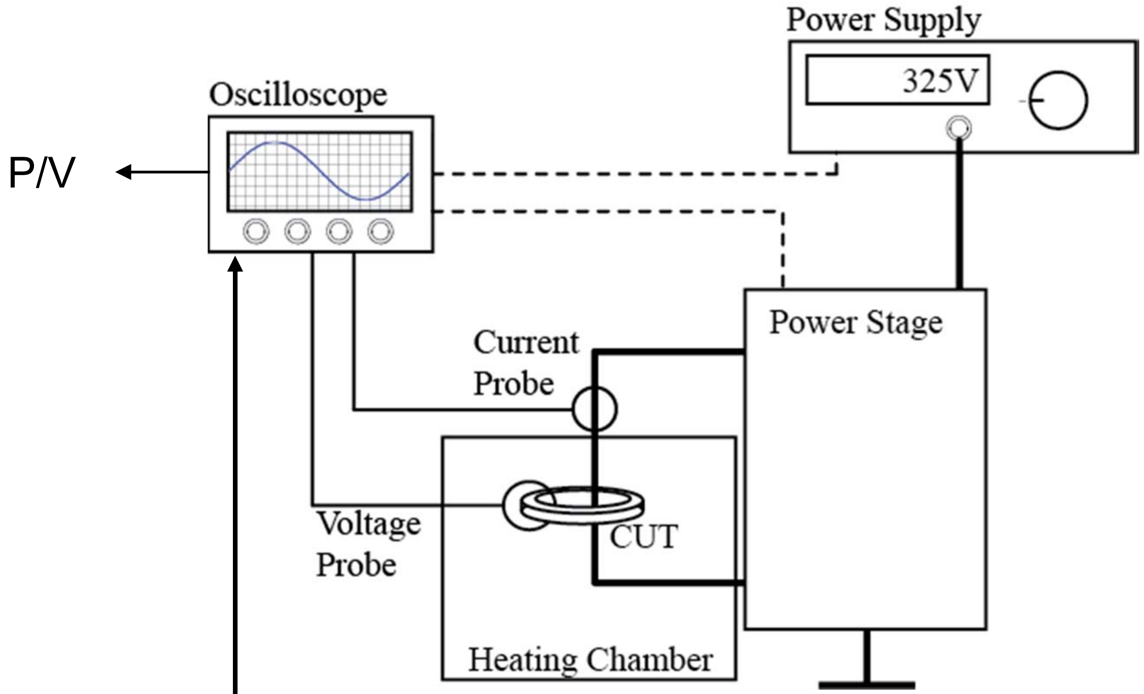

$$\frac{P}{V}=\frac{f\int_0^T i_1(t)\frac{N_1}{N_2}v_2(t)\,\mathrm{d}t}{A_e l_e}=\frac{f\int_0^T \frac{H(t)l_e}{N_1}\frac{N_1}{N_2}N_2A_e\frac{\mathrm{d}B(t)}{\mathrm{d}t}\mathrm{d}t}{A_e l_e}=f\int_{B(0)}^{B(T)}H(B)\mathrm{d}B=f\oint H\mathrm{d}B$$

Core Loss Modeling

Overview of Hybrid Modeling Approach

"The best of both worlds" (Steinmetz & Loss Map approach)

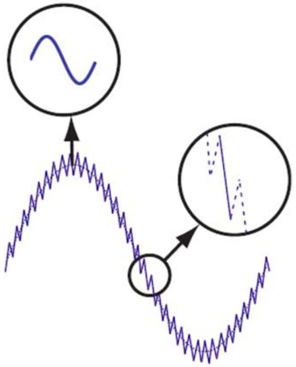

Loss Map
(Loss Material Database) **(2)/(3)**

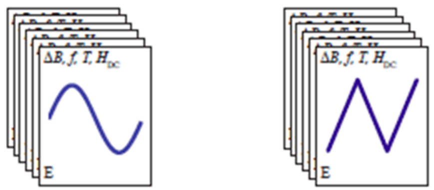

$$k, k_i, \alpha, \beta, \alpha_r, \beta_r, q_r, \tau$$

$$P_v = \frac{1}{T}\int_0^T k_i \left|\frac{\mathrm{d}B}{\mathrm{d}t}\right|^{\alpha} (\Delta B)^{\beta-\alpha}\,\mathrm{d}t + \sum_{l=1}^{n} Q_{rl} P_{rl}$$ **(1)**

$$\frac{P}{V}$$ **(4)**

Outline of Discussion

- Derivation of the i[2]GSE. **(1)**
- How to measure core losses in order to build loss map. **(2)**
- Use of loss map. **(3)**
- How to calculate core losses for cores of different shapes? **(4)**

Core Loss Modeling
Needed Loss Map Structure

Typical flux waveform

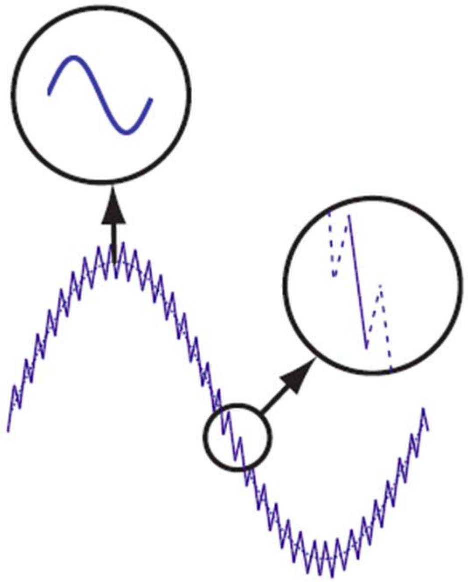

Content of Loss Map

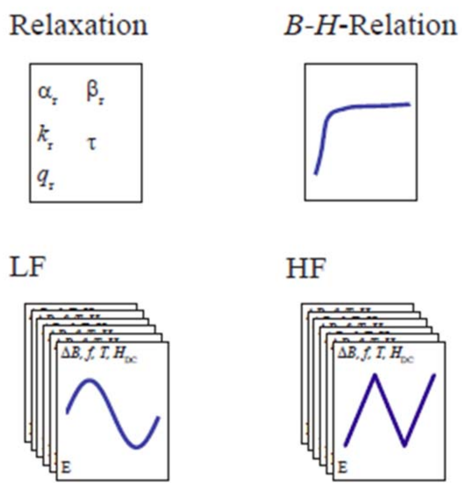

Core Loss Modeling
Minor and Major Loops

Idea

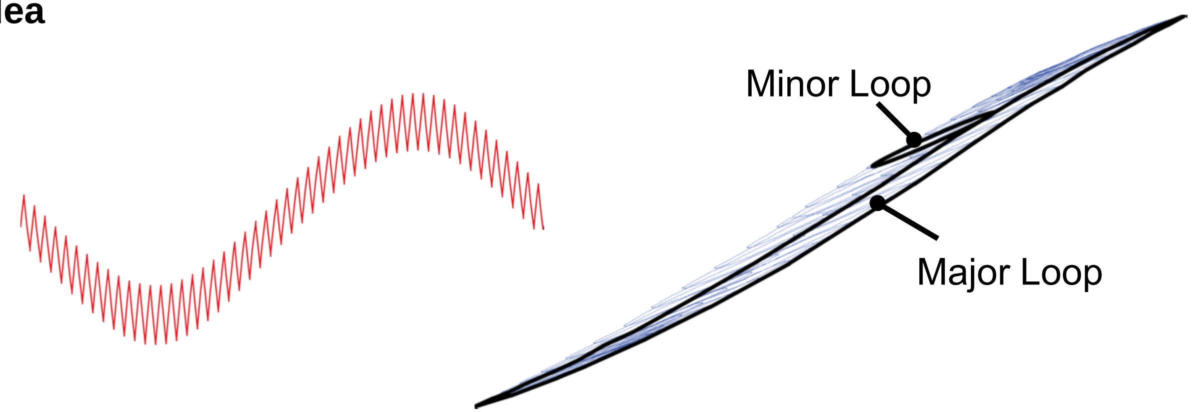

Losses due to Minor and Major Loops are calculated independent of each other and summed up.

Implementation

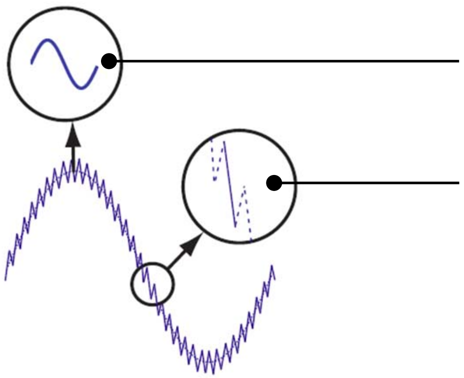

$$\left(\frac{P}{V}\right)_{\text{Major}}$$

$$\left(\frac{P}{V}\right)_{\text{Piecewise Linear Segment (+ Turning Point)}}$$

Actually, it is not considered how the minor loop closes: each piecewise linear segment is modeled as having half the losses of its corresponding closed loop (cf. next slides).

$$\Rightarrow \frac{P}{V} = \left(\frac{P}{V}\right)_{\text{Major}} + \sum \left(\frac{P}{V}\right)_{\text{Piecewise Linear Segment (+ Turning Point)}}$$

Core Loss Modeling

Hybrid Loss Modeling Approach (1)

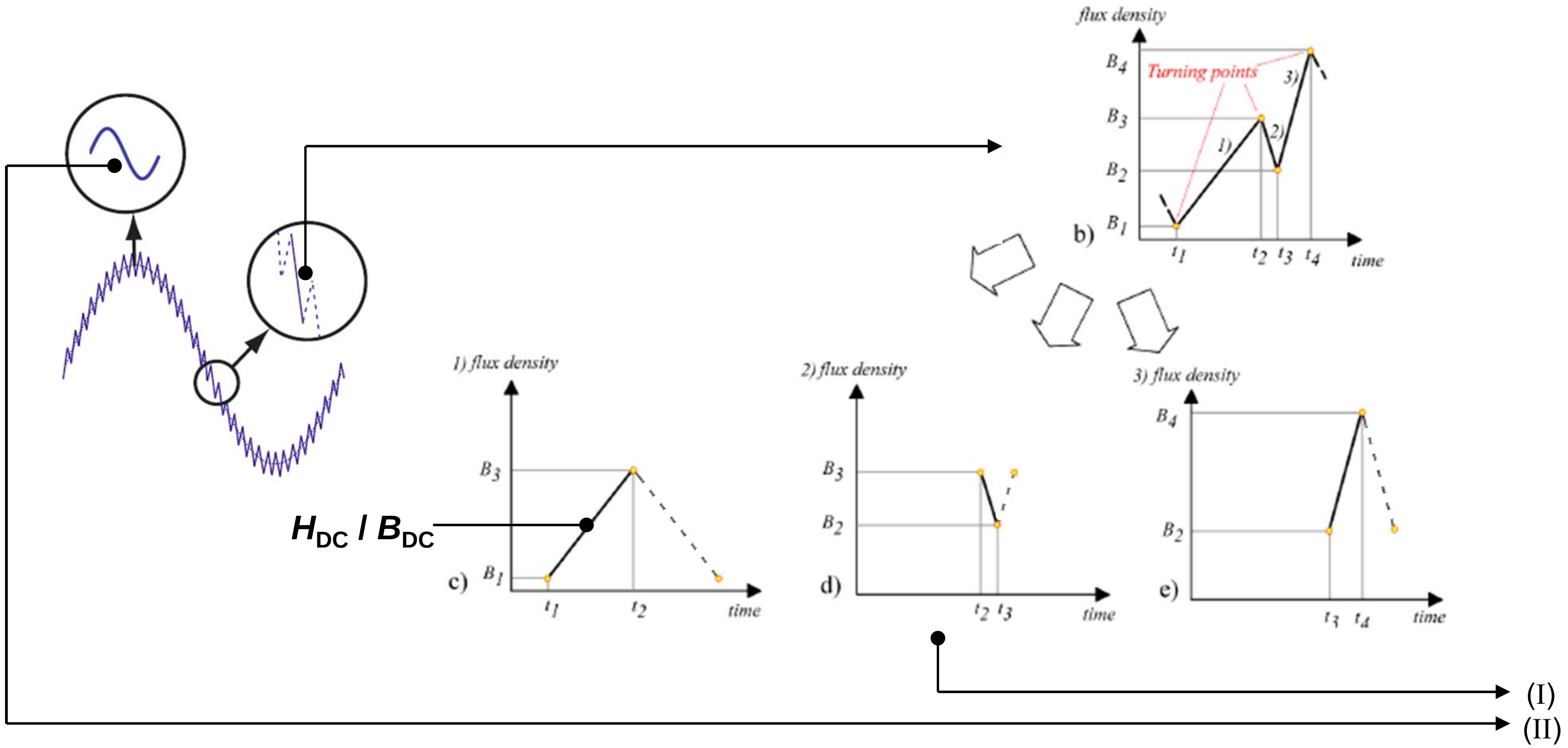

Core Loss Modeling

Hybrid Loss Modeling Approach (2)

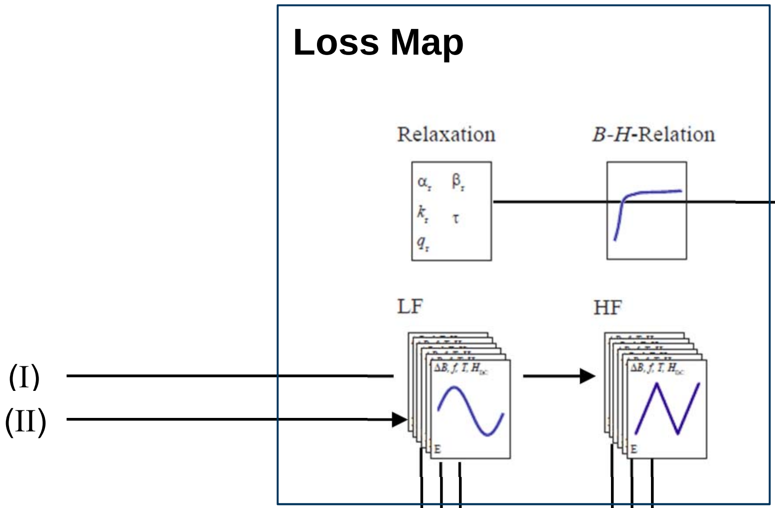

Evaluated for the according corner point in a piecewise-linear flux waveform.

Evaluated for the according piecewise-linear flux segment

$$P_{\mathrm{v}} = \frac{1}{T}\int_0^T k_i \left|\frac{\mathrm{d}B}{\mathrm{d}t}\right|^{\alpha} (\Delta B)^{\beta-\alpha}\,\mathrm{d}t + \sum_{l=1}^{n} Q_{\mathrm{r}l} P_{\mathrm{r}l}$$

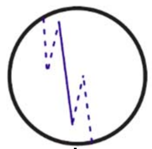

$$\frac{P}{V}$$

$$P_{\mathrm{v}1} = k_i\,(2 f_1)^{\alpha}\,(\Delta B_1)^{\beta}$$

$$P_{\mathrm{v}2} = k_i\,(2 f_2)^{\alpha}\,(\Delta B_2)^{\beta}$$

$$P_{\mathrm{v}3} = k_i\,(2 f_3)^{\alpha}\,(\Delta B_3)^{\beta}$$

Three loss map operating points are required in order to extract the parameters α, β, and k (or k_i).

These equations arise when one evaluates the i²GSE for symmetric triangular waveforms.

Core Loss Modeling

Hybrid Loss Modeling Approach (3)

Interpolation and Extrapolation

(H_{DC}*, T*, ΔB*, f*)

H*$_{DC}$ and *T

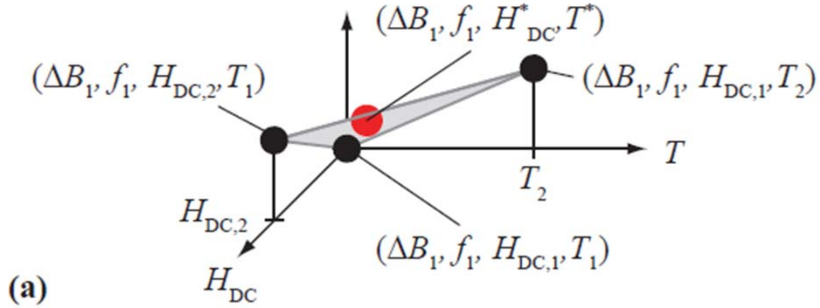

ΔB and *f*

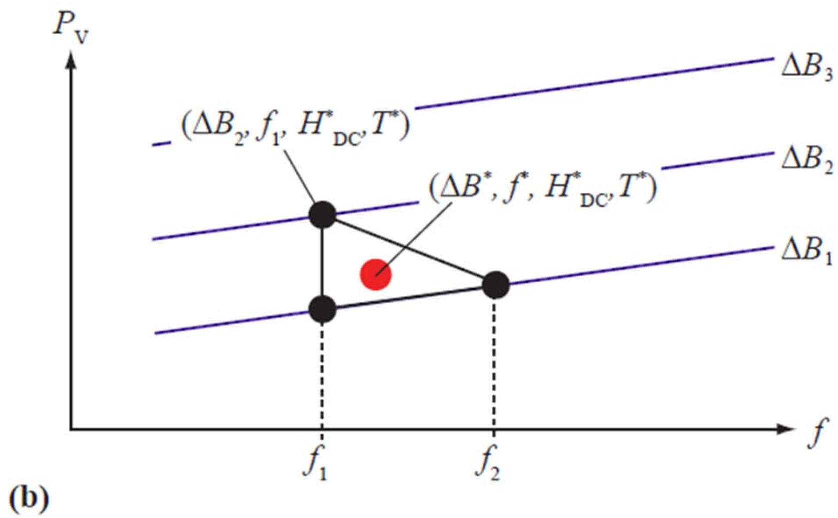

Core Loss Modeling

Hybrid Loss Modeling Approach (4)

Advantages of Hybrid Approach (Loss Map and i²GSE):

Relaxation effects are considered (i²GSE).

A good interpolation and extrapolation between premeasured operating points is achieved.

Loss map provides accurate i²GSE parameters for a wide frequency and flux density range.

A DC bias is considered as the loss map stores premeasured operating points at different DC bias levels.

Core Losses

Summary of Loss Density Calculation

Sinusoidal

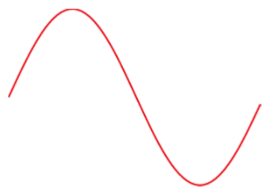

$$P = k\, f^{\,\alpha} B^{\beta}$$

Triangular

$$P_{\mathrm{v}} = \frac{1}{T}\int_0^T k_i \left|\frac{\mathrm{d}B}{\mathrm{d}t}\right|^{\alpha} (\Delta B)^{\beta-\alpha}\,\mathrm{d}t + \sum_{l=1}^{n} Q_{\mathrm{r}l} P_{\mathrm{r}l}$$

with $Q \geq 0$, $n = 1$

Trapezoidal

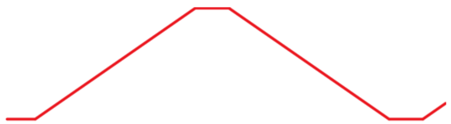

$$P_{\mathrm{v}} = \frac{1}{T}\int_0^T k_i \left|\frac{\mathrm{d}B}{\mathrm{d}t}\right|^{\alpha} (\Delta B)^{\beta-\alpha}\,\mathrm{d}t + \sum_{l=1}^{n} Q_{\mathrm{r}l} P_{\mathrm{r}l}$$

with $Q = 1$, $n = 2$

Combination

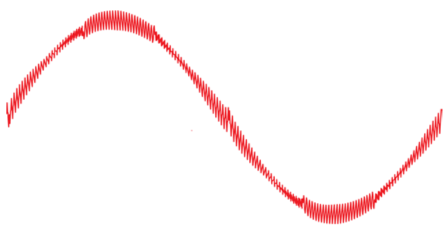

$$P_{\mathrm{v}} = \frac{1}{T}\int_0^T k_i \left|\frac{\mathrm{d}B}{\mathrm{d}t}\right|^{\alpha} (\Delta B)^{\beta-\alpha}\,\mathrm{d}t + \sum_{l=1}^{n} Q_{\mathrm{r}l} P_{\mathrm{r}l}$$

with different Q's and $n >> 0$.

Core Loss Modeling

Overview of Hybrid Modeling Approach

“The best of both worlds” (Steinmetz & Loss Map approach)

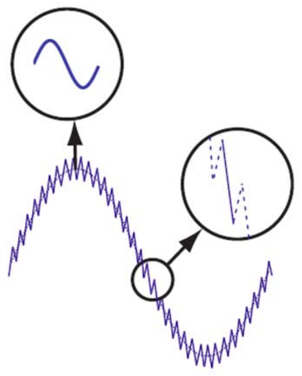

Loss Map
(Loss Material Database) **(2)/(3)**

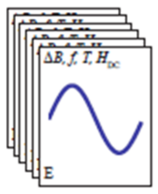

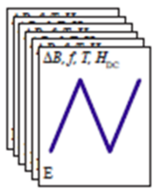

$$k, k_i, \alpha, \beta, \alpha_r, \beta_r, q_r, \tau$$

$$P_v = \frac{1}{T}\int_0^T k_i \left|\frac{dB}{dt}\right|^{\alpha} (\Delta B)^{\beta-\alpha}\, dt + \sum_{l=1}^{n} Q_{rl} P_{rl} \quad \textbf{(1)}$$

$$\frac{P}{V} \quad \textbf{(4)}$$

Outline of Discussion

- Derivation of the i²GSE. **(1)**
- How to measure core losses in order to build loss map. **(2)**
- Use of loss map. **(3)**
- How to calculate core losses for cores of different shapes? **(4)**

Core Loss Modeling
Effect of Core Shape

Procedure

1) The flux density in every core section of (approximately) homogenous flux density is calculated.

2) The losses of each section are calculated.

3) The core losses of each section are then summed-up to obtain the total core losses.

Reluctance Model

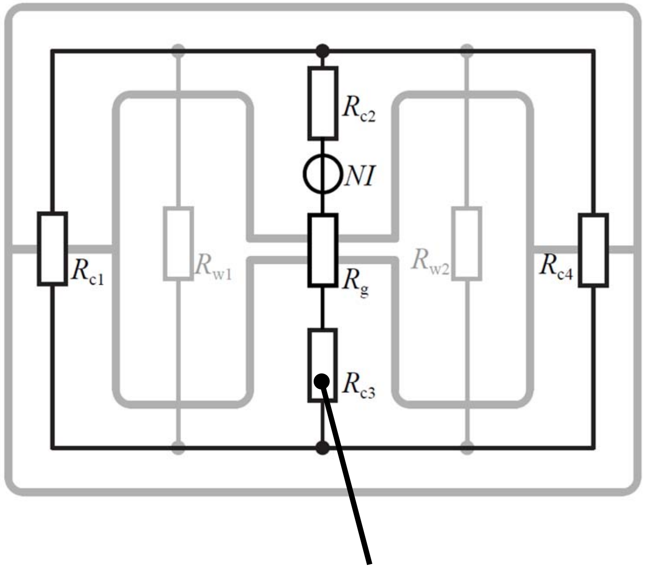

$$\emptyset = f(R_m(\emptyset), I) = f(\emptyset, I)$$

Core Loss Modeling

Effective Core Dimensions of Toroid

Motivation for Effective Core Dimensions

Core loss *densities* are needed to model core losses. It is difficult to determine these loss densities from a toroid, since the flux density is not distributed homogeneously in a toroid.

Definition: Ideal Toroid

A toroid is ideal when he has a homogenous flux density distribution over the radius ($r_1 \cong r_2$).

Idea for Real Toroid

Find effective core magnetic length and cross section, so one can calculate as if it were an ideal toroid, i.e. as if the flux density distribution were homogenous.

Effective magnetic length

$$l_e = \frac{2\pi \ln r_2 / r_1}{1/r_1 - 1/r_2}$$

Effective magnetic cross-section

$$A_e = \frac{h \ln^2 r_2 / r_1}{1/r_1 - 1/r_2}$$

Illustration

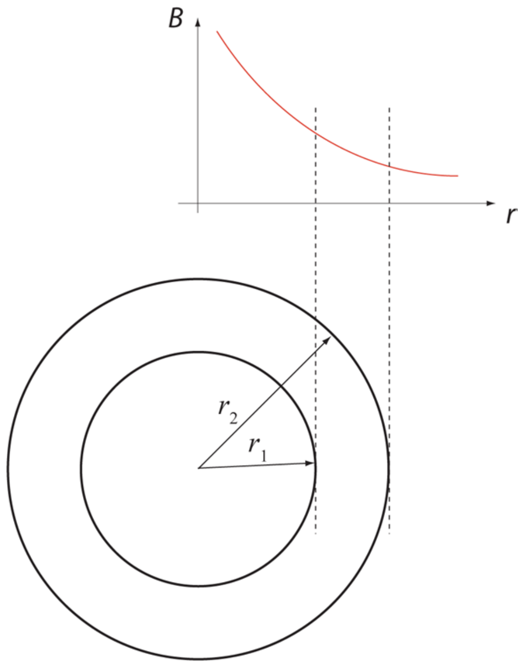

Core Loss Modeling
Impact of Core Shape on Eddy Current Losses

Eddy current loss density can be determined as [5]

$$P_{\mathrm{eddy}} = \frac{(\pi \hat{B} f d)^2}{k_{\mathrm{ec}} \rho}$$

Geometry	k_{ec}
laminations of thickness d	6
cylinder of diameter d	16
sphere of diameter d	20

For a laminated core it is

$$P_{\mathrm{eddy}} = \frac{(\pi \hat{B} f d)^2}{6 \rho}$$

→ The eddy current losses per unit volume depend not on the shape of the bulk material, but on the size and geometry of the insulated regions.

→ In case of laminated iron cores, it is still appropriate to calculate with core loss densities that have been measured on a sample core with a geometrically different bulk material, but with the same lamination or tape thickness.

[5] E. C. Snelling, "Soft Ferrites - Properties and Applications", 2nd edition, Butterworths, 1988

Core Loss Modeling
Effect in Tape Wound Cores

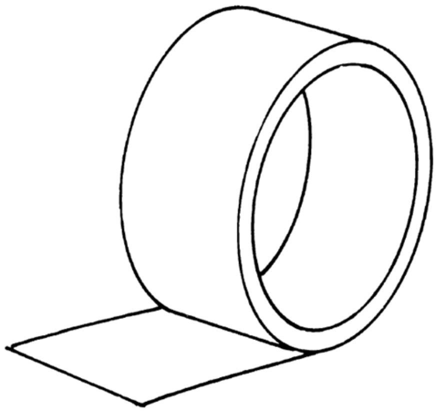

www.vacuumschmelze.de

Thin ribbons (approx. 20 μm)

Wound as toroid or as double C core.

Amorphous or nanocrystalline materials.

Losses in gapped tape wound cores higher than expected!

Core Loss Modeling

Effect in Tape Wound Cores - Cause 1 : Interlamination Short Circuits

Machining process

Surface short circuits introduced by machining
(particular a problem in in-house production).

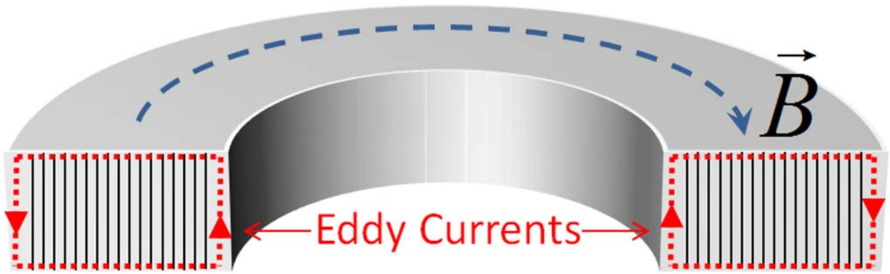

After treatment may reduce this effect. At ETH, a core was put in an 40% ferric chloride $FeCl_3$ solution after cutting, which substantially (more than 50%) decreased the core losses.

Core Loss Modeling

Effect in Tape Wound Cores - Cause 2 : Orthogonal Flux Lines (1)

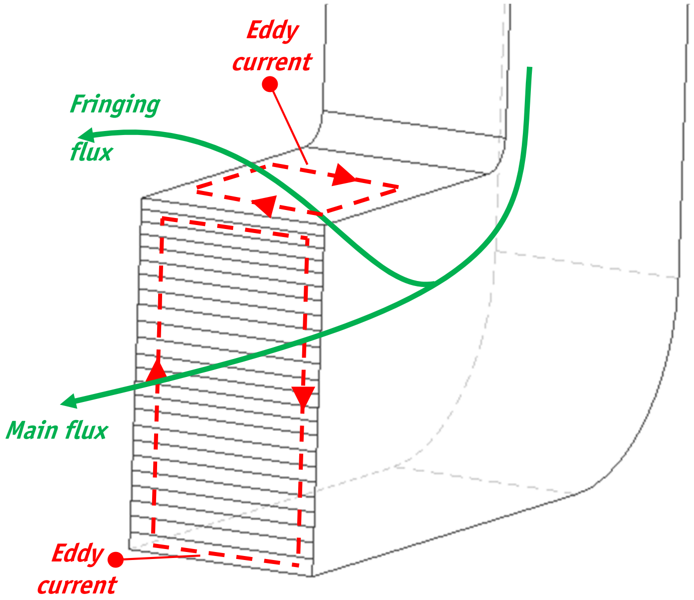

A flux orthogonal to the ribbons leads to very high eddy current losses!

Core Loss Modeling

Effect in Tape Wound Cores - Cause 2 : Orthogonal Flux Lines (2)

An experiment that illustrates well the loss increase due to an orthogonal flux is given here.

Displacements

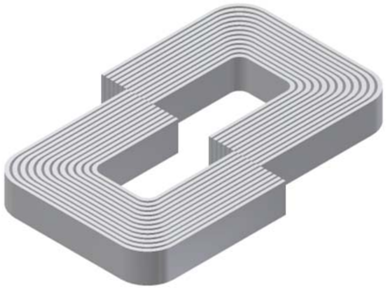

Horizontal Displacement

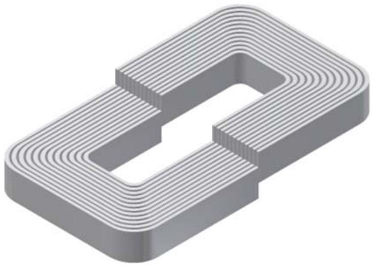

Vertical Displacement

Core Loss Results

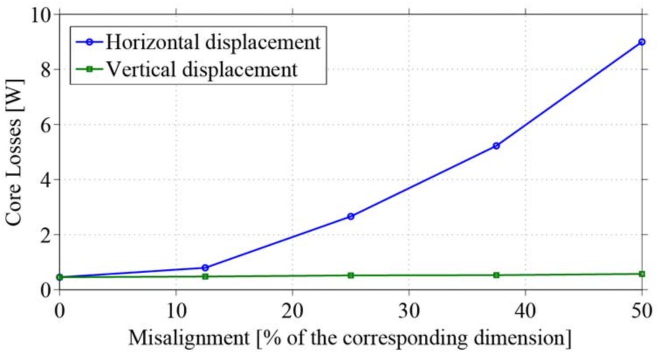

Core Loss Modeling

Effect in Tape Wound Cores - Cause 2 : Orthogonal Flux Lines (3)

Core loss increase due to leakage flux in transformers.

Measurement Set Up

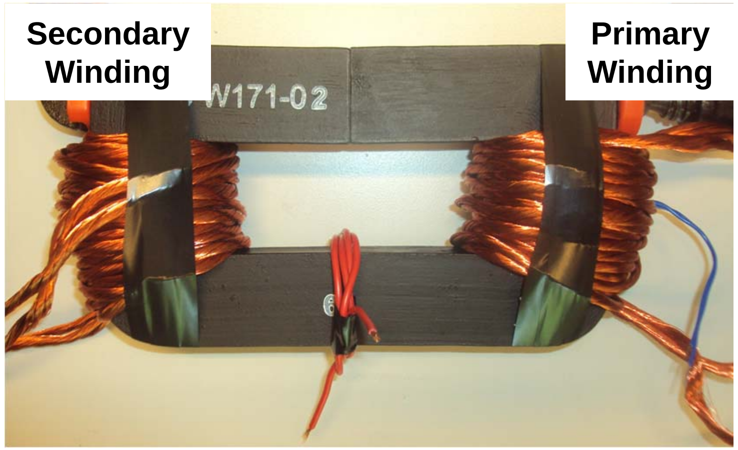

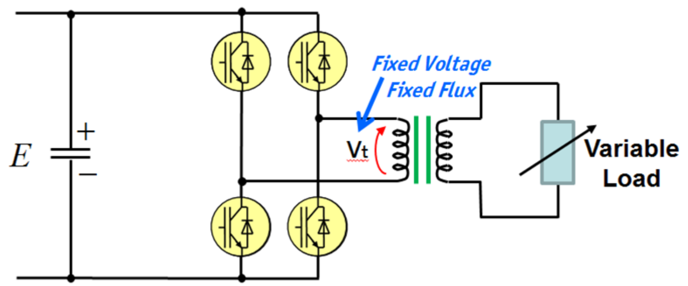

Results

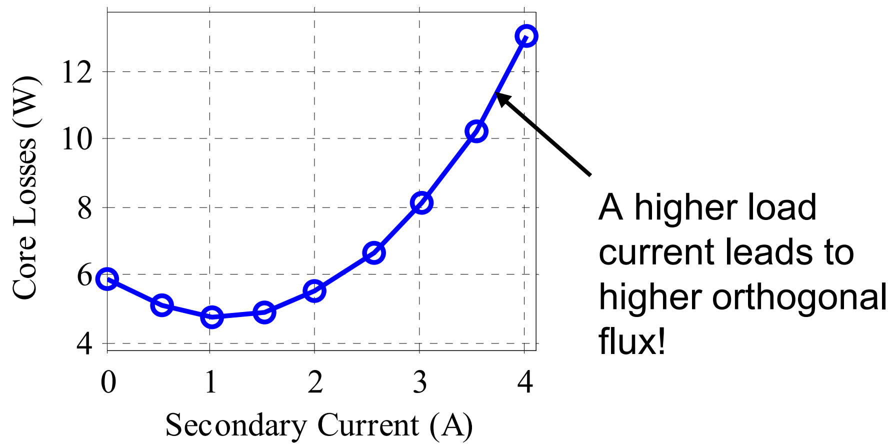

FEM

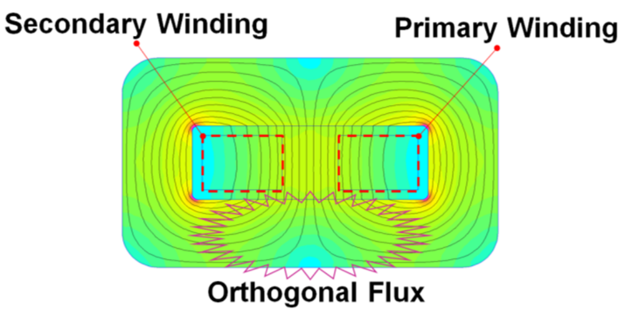

Core Loss Modeling

Effect in Tape Wound Cores - Cause 2 : Orthogonal Flux Lines (4)

In [10] a core loss increase with increasing air gap length has been observed.

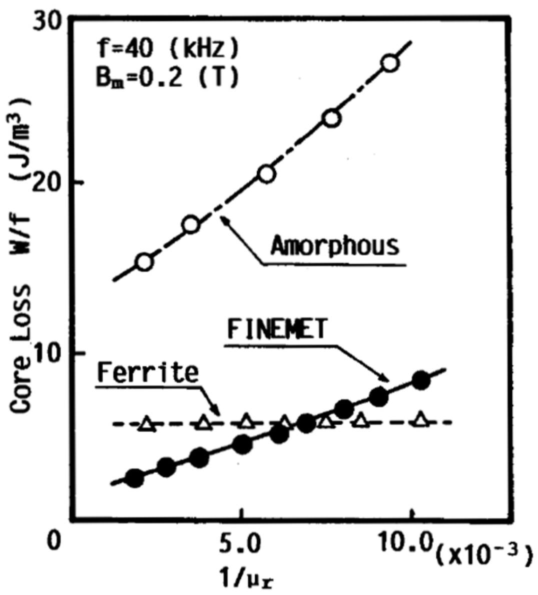

Fig.1 Core loss per cycle W/f in FINEMET, Fe-based amorphous, and ferrite cut cores as a function of inverse of the effective permeability μ_r.

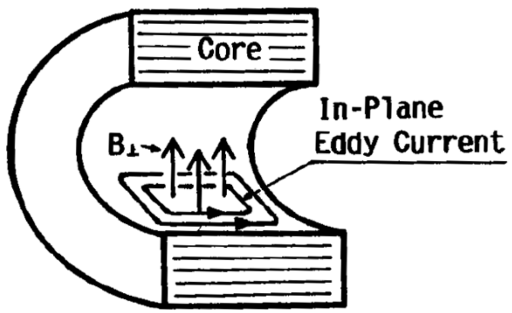

Fig.2 Schematic representation of in-plane eddy current generated by leakage flux normal to ribbon surfaces.

Figures from [10]

[10] H. Fukunaga, T. Eguchi, K. Koga, Y. Ohta, and H. Kakehashi, “High Performance Cut Cores Prepared From Crystallized Fe-Based Amorphous Ribbon”, in IEEE Transactions on Magnetics, vol. 26, no. 5, 1990.

Example
Core Loss Modeling

Photo & Dimensions

Dimensions

l_g	1.95 mm
do	60 mm
b	60 mm
a	20 mm
t	28 mm
ww	56.9 mm
d	2.24 mm

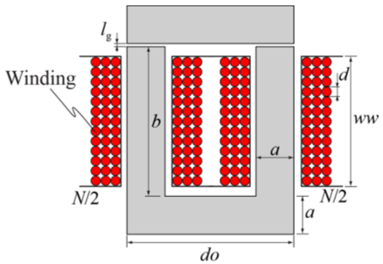

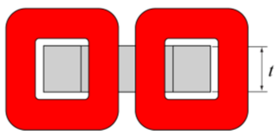

Material

Grain-oriented steel (M165-35S)

Flux Density Distribution

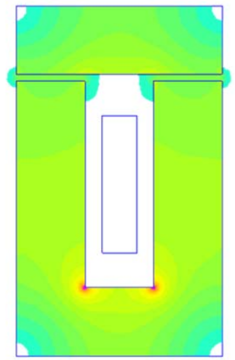

An approximately homogeneous flux density distribution inside the core.

Reluctance Model

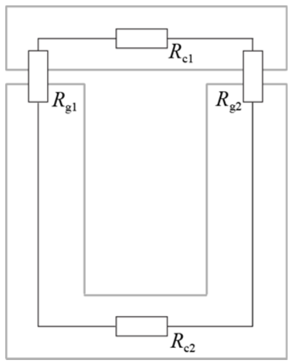

Flux Density Waveform

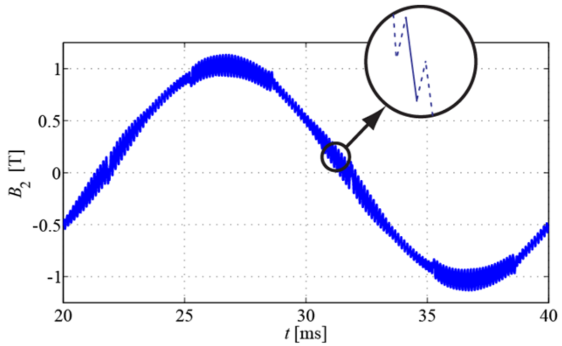

MATLAB Presentation

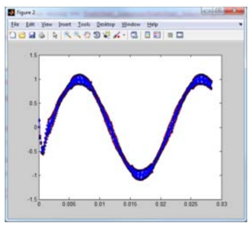

Outline

- Magnetic Circuit Modeling
- Core Loss Modeling
- **Winding Loss Modeling**
- Thermal Modeling
- Multi-Objective Optimization
- Summary & Conclusion

Winding Loss Modeling

Skin Effect (1)

H-field in conductor

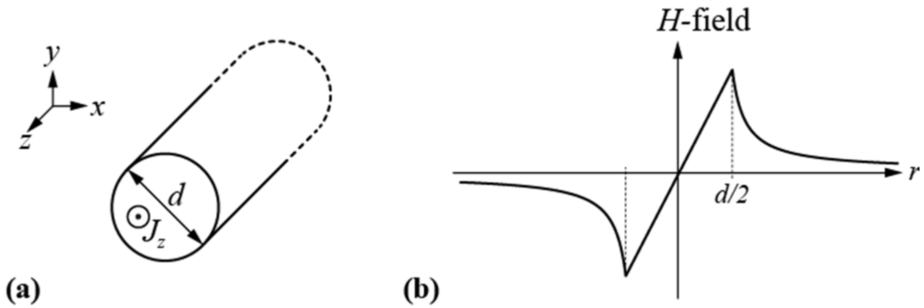

Ampere's Law

$$\oint \mathbf{H}\,\mathrm{d}\mathbf{l} = \iint \mathbf{J}\,\mathrm{d}\mathbf{A}$$

Induced Eddy Currents

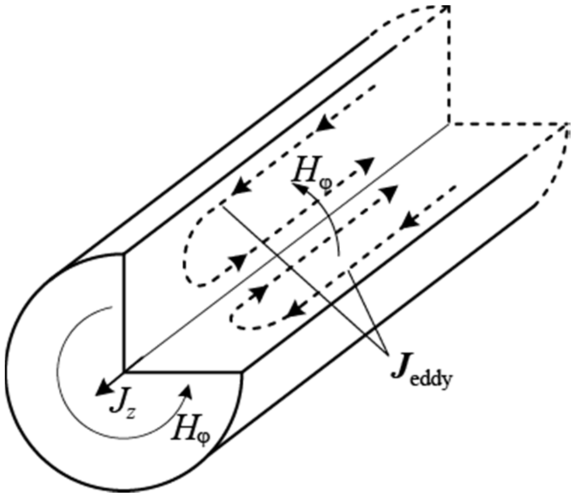

Faraday's Law

$$\oint \mathbf{E}\,\mathrm{d}\mathbf{l} = -\frac{\mathrm{d}}{\mathrm{d}t}\iint \mathbf{B}\,\mathrm{d}\mathbf{A}$$

Winding Loss Modeling
Skin Effect (2)

FEM Simulation

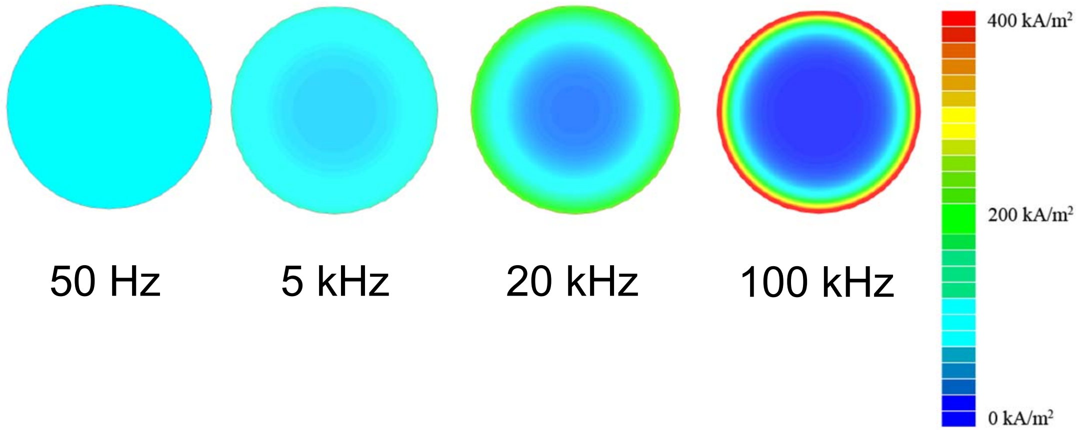

50 Hz 5 kHz 20 kHz 100 kHz

Current Distribution

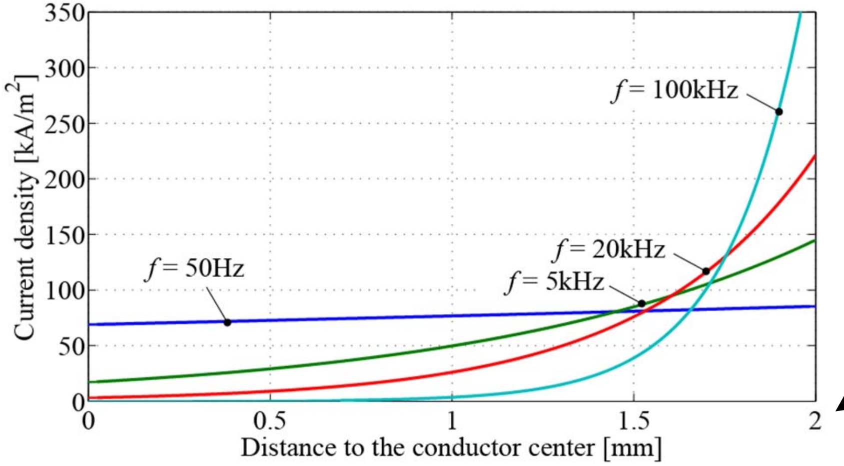

Outer radius of conductor

Winding Loss Modeling

Skin Effect (3)

Skin Depth (, where the current density has 1/e of surface value)

$$\delta = \frac{1}{\sqrt{\pi \mu_0 \sigma f}}$$

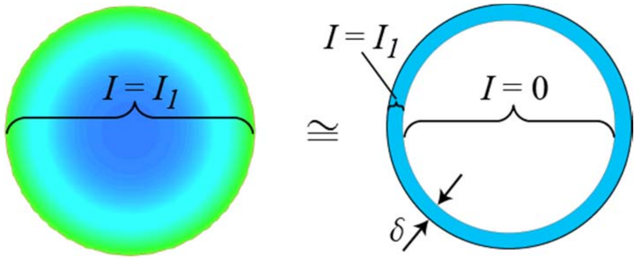

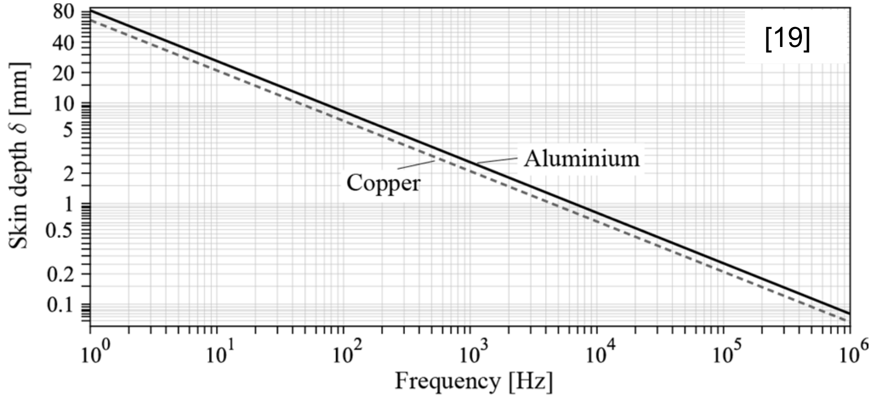

Power Loss Increase with Frequency

$$P_S = F_R(f) \cdot R_{DC} \cdot \hat{I}^2$$

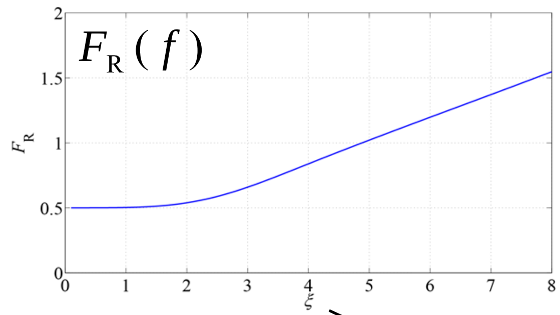

$$\xi = \frac{d}{\sqrt{2}\delta}$$

Winding Loss Modeling
Skin Effect (4)

Current Distributions

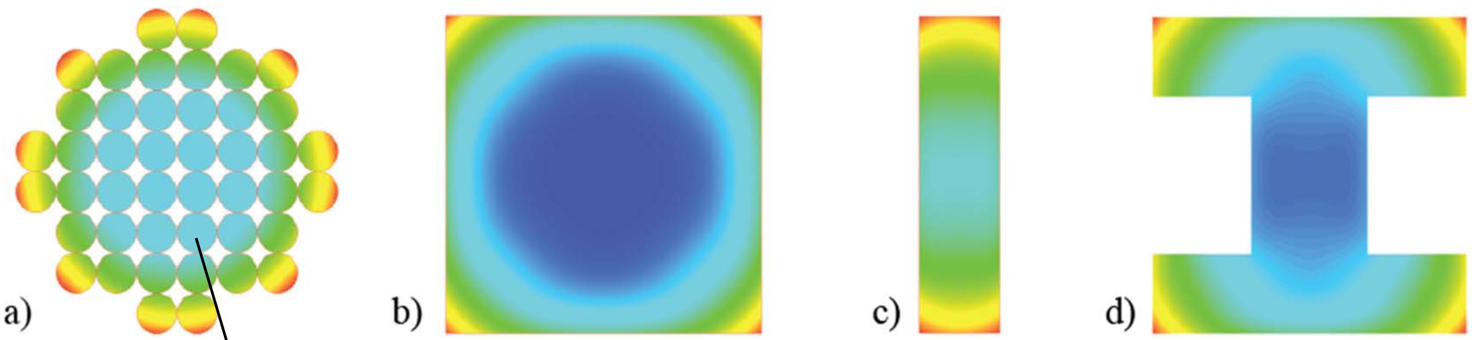

Parallel-connected (not
twisted) conductors!

Figure from [19]

Winding Loss Modeling
Proximity Effect (1)

H-field of neighboring conductor induces eddy currents

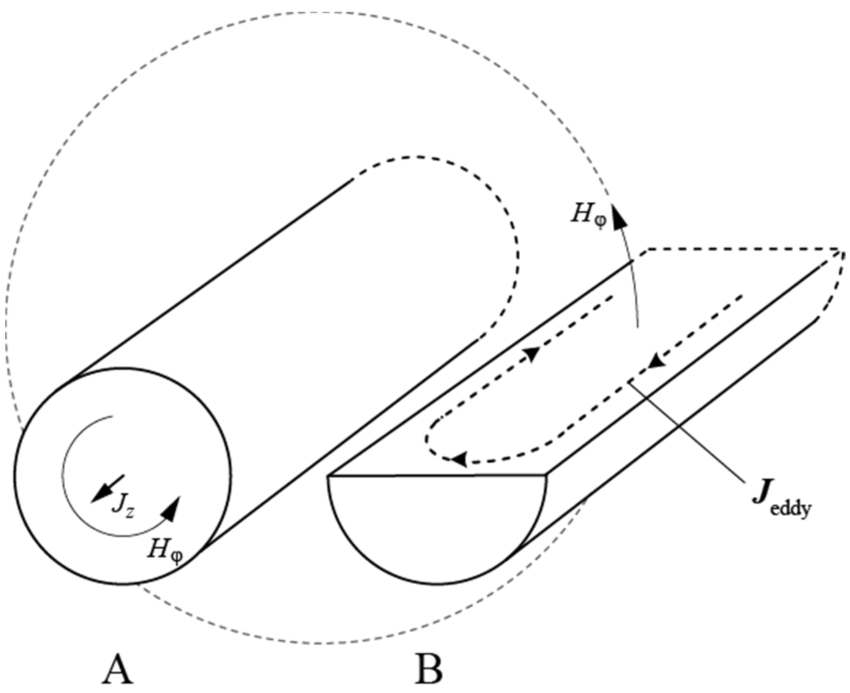

Ampere's Law

$$\oint \mathbf{H}\,\mathrm{d}\mathbf{l} = \iint \mathbf{J}\,\mathrm{d}\mathbf{A}$$

Faraday's Law

$$\oint \mathbf{E}\,\mathrm{d}\mathbf{l} = -\frac{\mathrm{d}}{\mathrm{d}t}\iint \mathbf{B}\,\mathrm{d}\mathbf{A}$$

Winding Loss Modeling
Proximity Effect (2)

Eddy Currents in Conductor

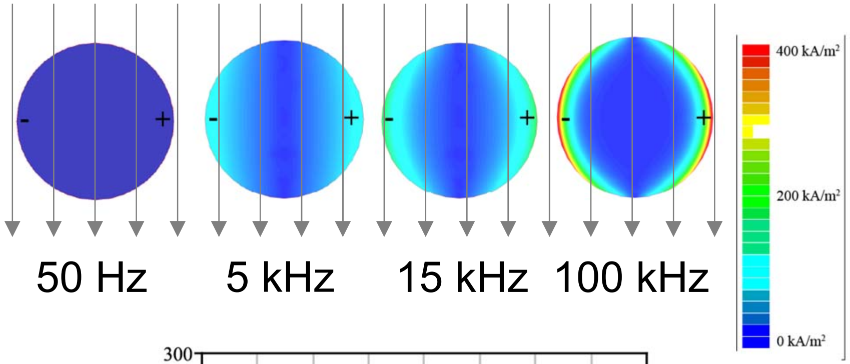

Induced Eddy Currents

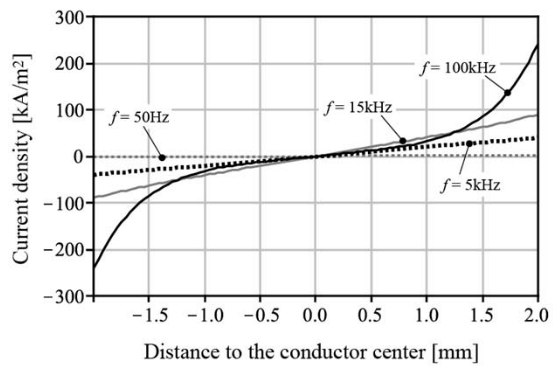

($H_{e,rms}$ = 35 A/m parallel to conductor)

Current Concentration

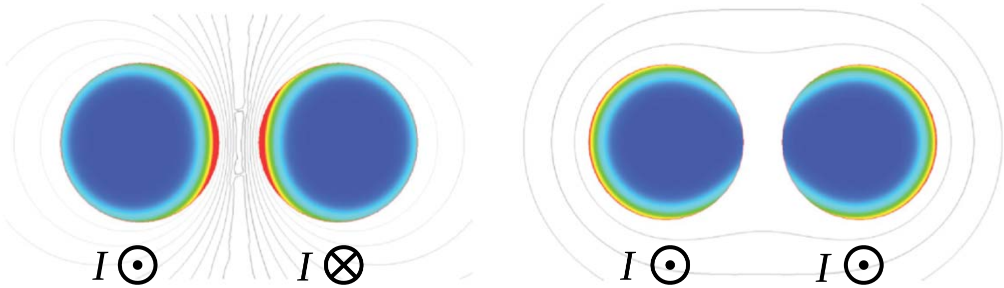

Figures from [19]

Winding Loss Modeling

Skin vs. Proximity Effect

Situation

(f = 100 kHz, I_{peak} = 1 A, $H_{e,peak}$ = 1000 A/m)

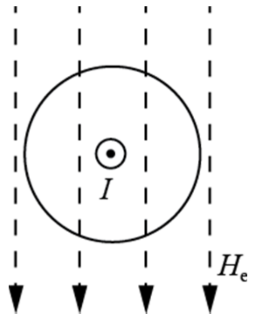

Results

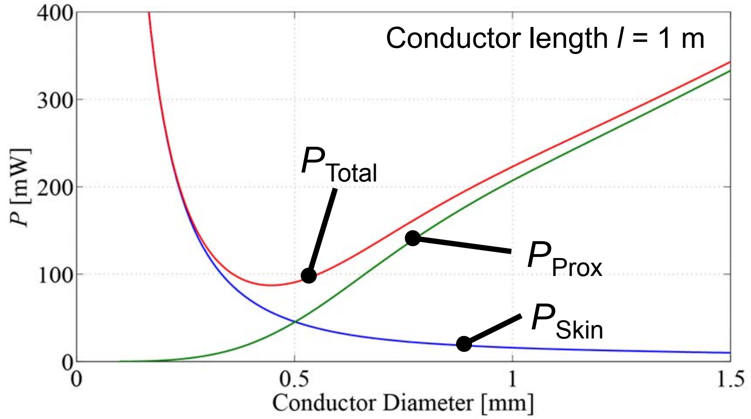

Definition

Skin Effect Losses P_{Skin}

Losses due to current I, including loss increase due to self-induced eddy currents.

Proximity Effect Losses P_{Prox}

Losses due to eddy currents induced by external magnetic field H_e.

Winding Loss Modeling

Litz Wire (1) - What are Litz wires?

Idea

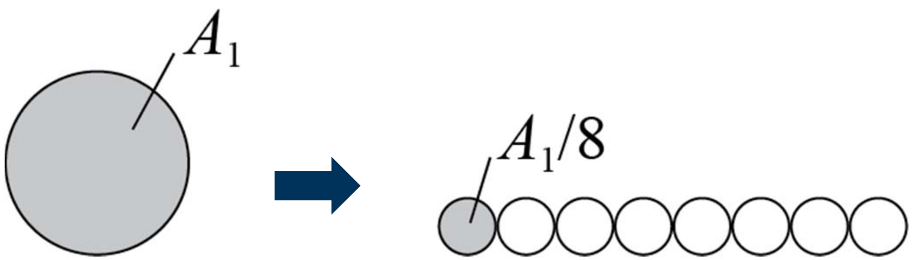

Advantages of Litz wires

HF losses can be reduced substantially

Disadvantages of Litz wires

High price

Heat dissipation difficult

Implementation

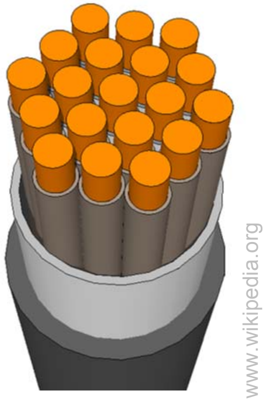

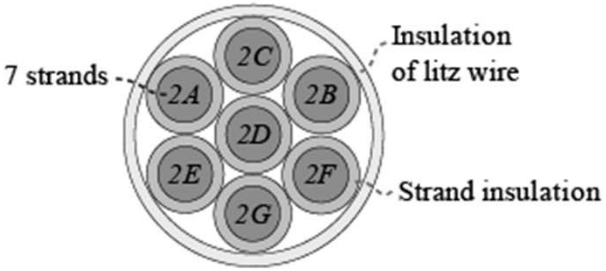

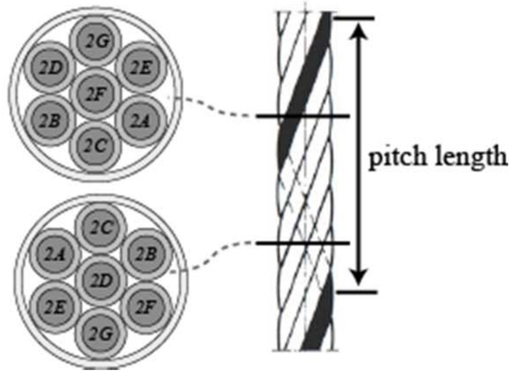

Winding Loss Modeling

Litz Wire (2) - Why Litz Wires Have to be Twisted? (1)

Bundle-Level Skin Effect

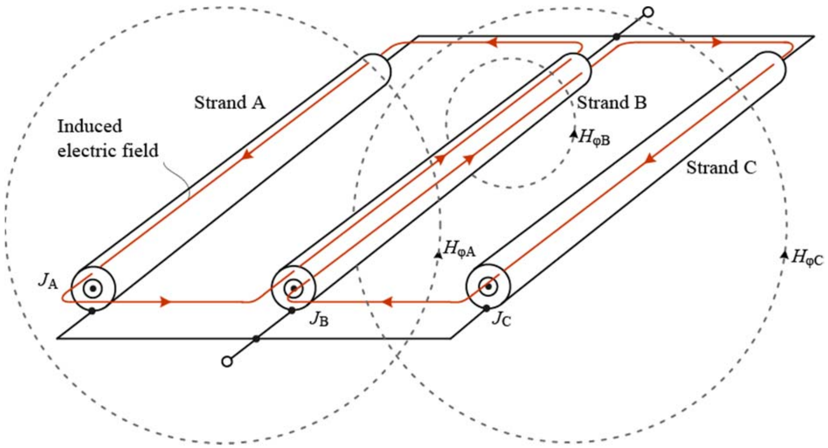

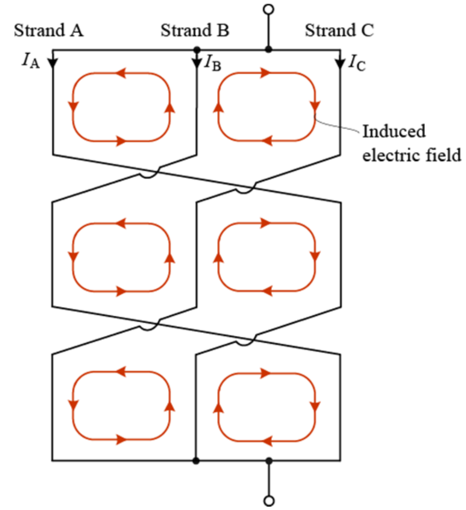

Current Distributions

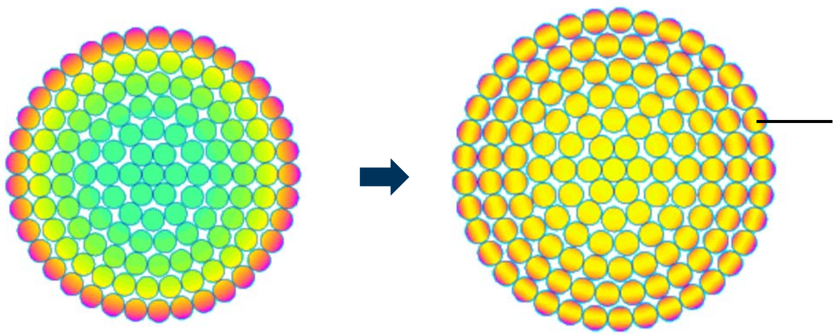

$$\oint \mathbf{H}\,\mathrm{d}\mathbf{l} = \iint \mathbf{J}\,\mathrm{d}\mathbf{A}$$ (Ampere's Law)

$$\oint \mathbf{E}\,\mathrm{d}\mathbf{l} = -\frac{\mathrm{d}}{\mathrm{d}t}\iint \mathbf{B}\,\mathrm{d}\mathbf{A}$$ (Faraday's Law)

Winding Loss Modeling

Litz Wire (3) - Why Litz Wires Have to be Twisted? (2)

Bundle-Level Proximity Effect

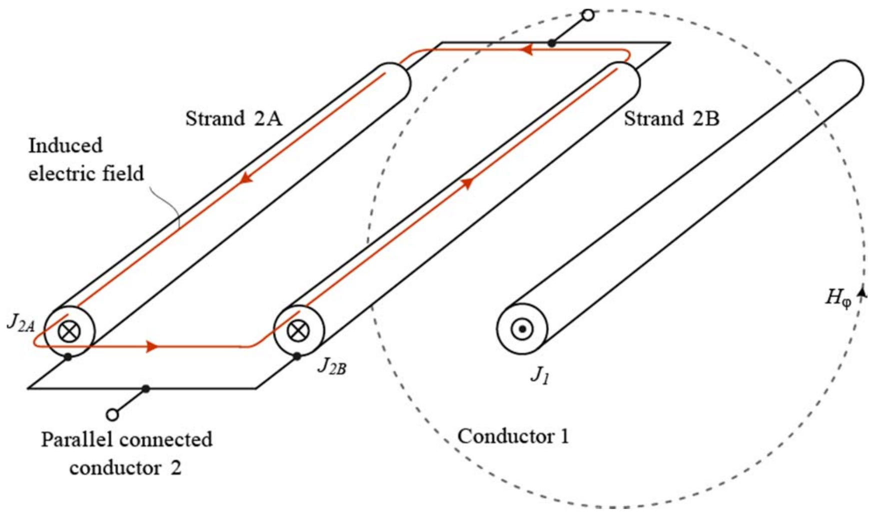

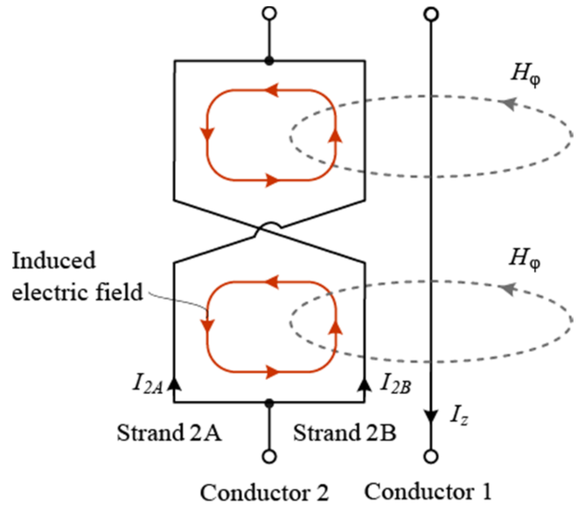

$$\oint \mathbf{H}\,\mathrm{d}\mathbf{l} = \iint \mathbf{J}\,\mathrm{d}\mathbf{A}$$ (Ampere's Law)

$$\oint \mathbf{E}\,\mathrm{d}\mathbf{l} = -\frac{\mathrm{d}}{\mathrm{d}t}\iint \mathbf{B}\,\mathrm{d}\mathbf{A}$$ (Faraday's Law)

Figures from [19]

Winding Loss Modeling

Litz Wire (4) – Strand-Level Effects

Internal and External Fields lead to Internal and External Proximity Effects

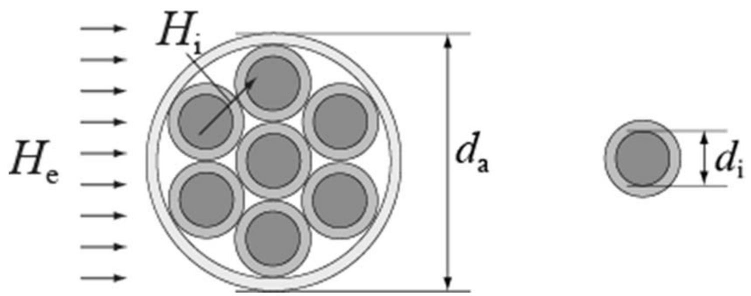

Losses in Litz Wires

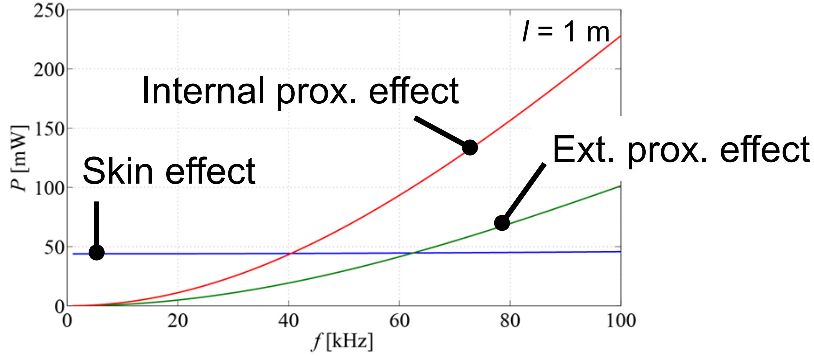

(25 x d_i = 0.5 mm, I_{peak} = 5 A, $H_{e,peak}$ = 300 A/m)

Losses in Solid Wires

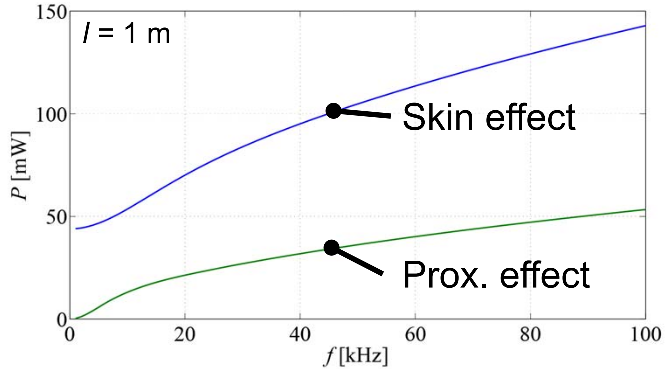

(d = 2.5 mm, I_{peak} = 5 A, $H_{e,peak}$ = 300 A/m)

Winding Loss Modeling

Litz Wire (5) – Types of Eddy-Current Effects in Litz Wire

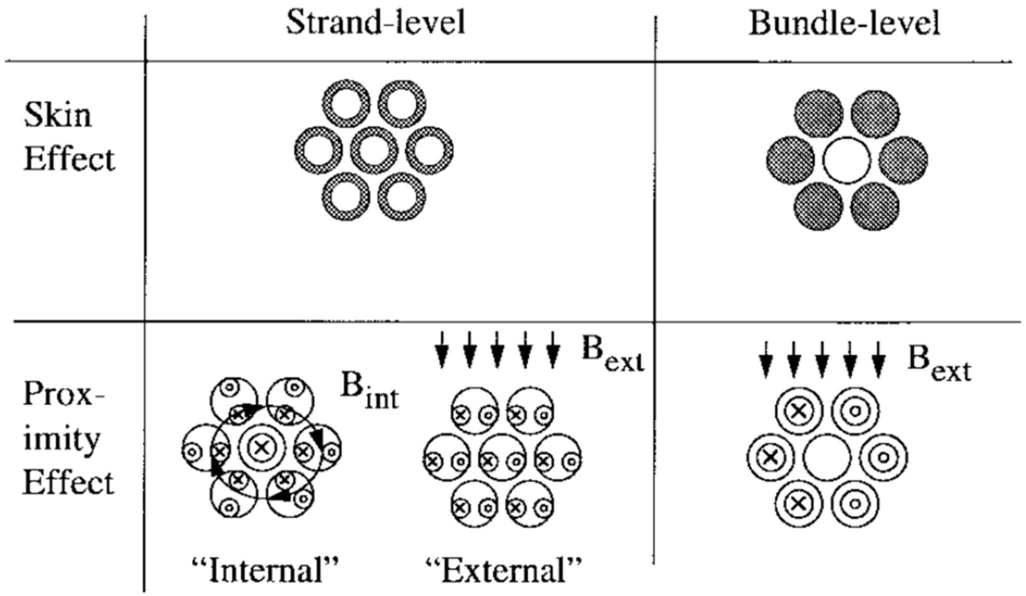

Figure from [11] Ch. R. Sullivan, "Optimal Choice for Number of Strands in a Litz-Wire Transformer Winding", in IEEE Transactions on Power Electronics, vol. 14, no. 2, 1999.

Winding Loss Modeling

Litz Wire (6) – Real Litz Wire

Ideal Litz Wire

(ideally twisted strands)

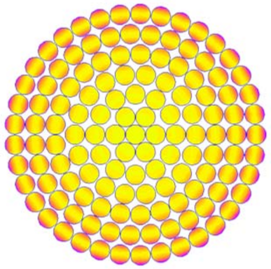

Worst Case Litz Wire

(parallel connected strands, no twisting)

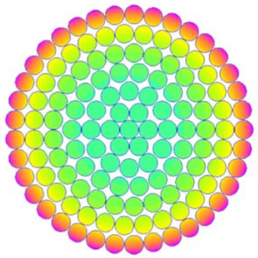

Operating Point

f = 20 kHz / n = 130 /

d_i = 0.4 mm

How do "real" Litz wires behave? [12]

Skin Effect / Internal Proximity Effect $$R_{\text{skin},\lambda} = \lambda_{\text{skin}} R_{\text{skin,ideal}} + (1 - \lambda_{\text{skin}}) R_{\text{skin,parallel}}$$

External Proximity Effect $$R_{\text{prox},\lambda} = \lambda_{\text{prox}} R_{\text{prox,ideal}} + (1 - \lambda_{\text{prox}}) R_{\text{prox,parallel}}$$

Litz Wire Type 1: 7 bundles with 35 strands each[1)]: $\lambda_{\text{skin}} \approx 0.5$ / $\lambda_{\text{prox}} \approx 0.99$

Litz Wire Type 2: 4 bundles with 61/62 strands each[1)]: $\lambda_{\text{skin}} \approx 0.9$ / $\lambda_{\text{prox}} \approx 0.99$

[12] H. Rossmanith, M. Doebroenti, M. Albach, and D. Exner, "Measurement and Characterization of High Frequency Losses in Nonideal Litz Wires", IEEE Transactions on Power Electronics, vol. 26, no. 11, November 2011

Winding Loss Modeling

Litz Wire (7) - Are Litz Wires Better than Solid Conductors?

Skin and Internal Proximity Effect

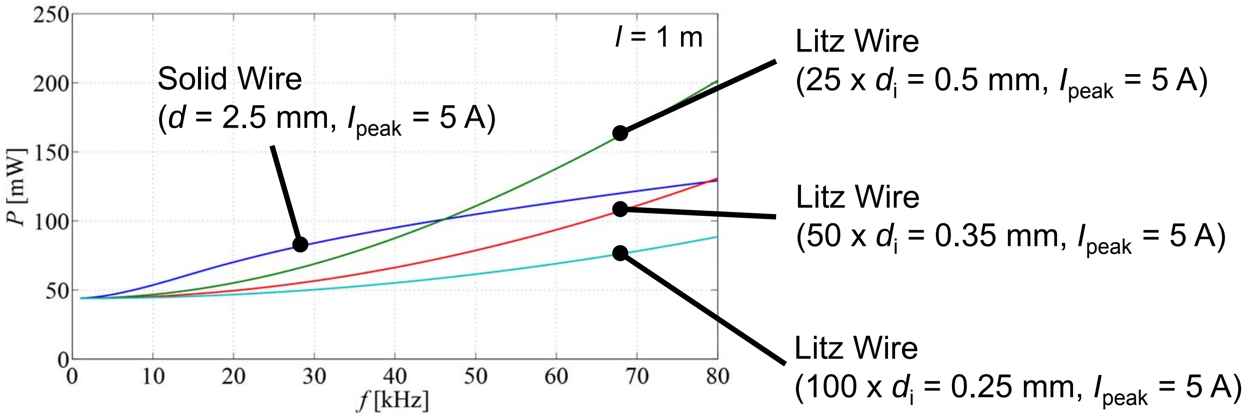

External Proximity Effect

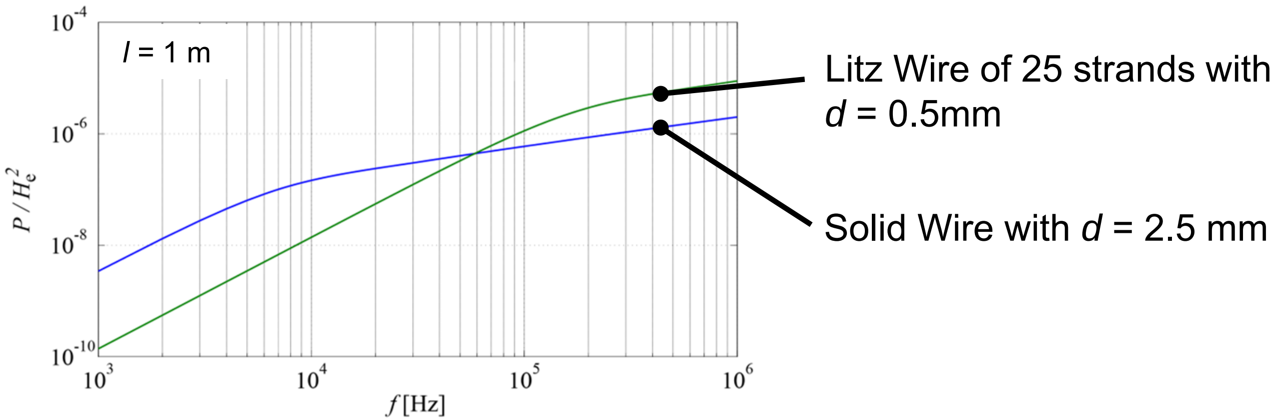

Winding Loss Modeling

Foil Windings Enclosed by Magnetic Material

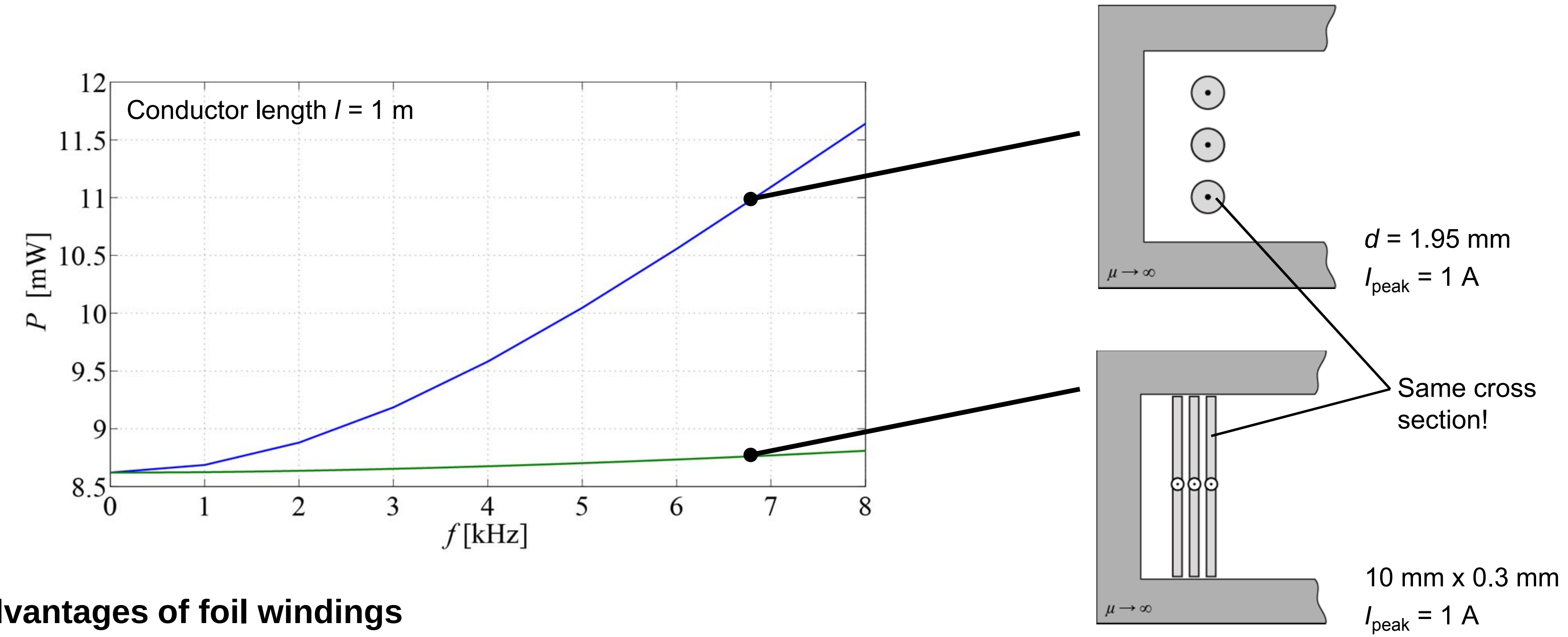

Advantages of foil windings

HF losses can be reduced

Lower price compared to Litz wire

High filling factor

Disadvantages of foil windings

Increased winding capacitance

Risk of orthogonal flux

➡ “Skin” of foil conductor larger than of round conductor with same cross section; hence, skin effect losses lower in foil conductor.

Winding Loss Modeling

Foil Windings Not Enclosed by Magnetic Material (1)

Single Conductor

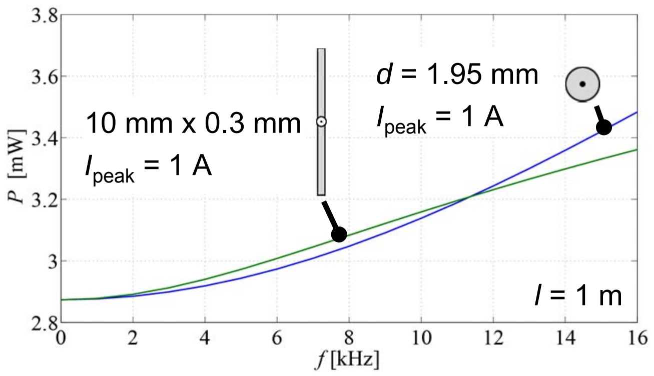

Three Conductors

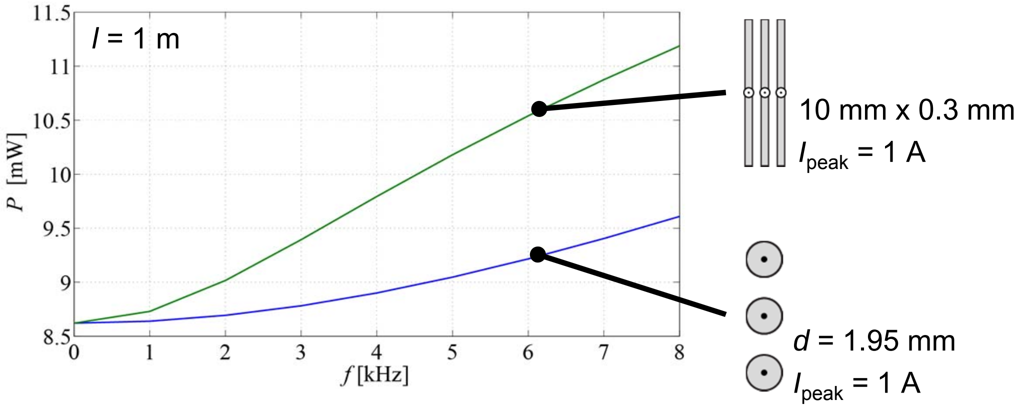

Orthogonal flux leads to increased skin and proximity effect.

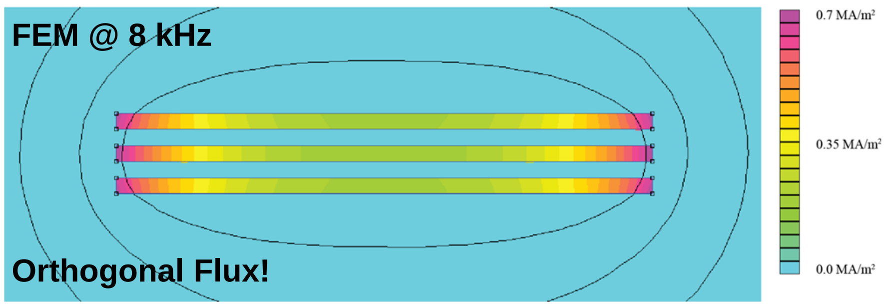

Winding Loss Modeling
Foil Windings Not Enclosed by Magnetic Material (2)

(Foil) Windings with Return Conductors

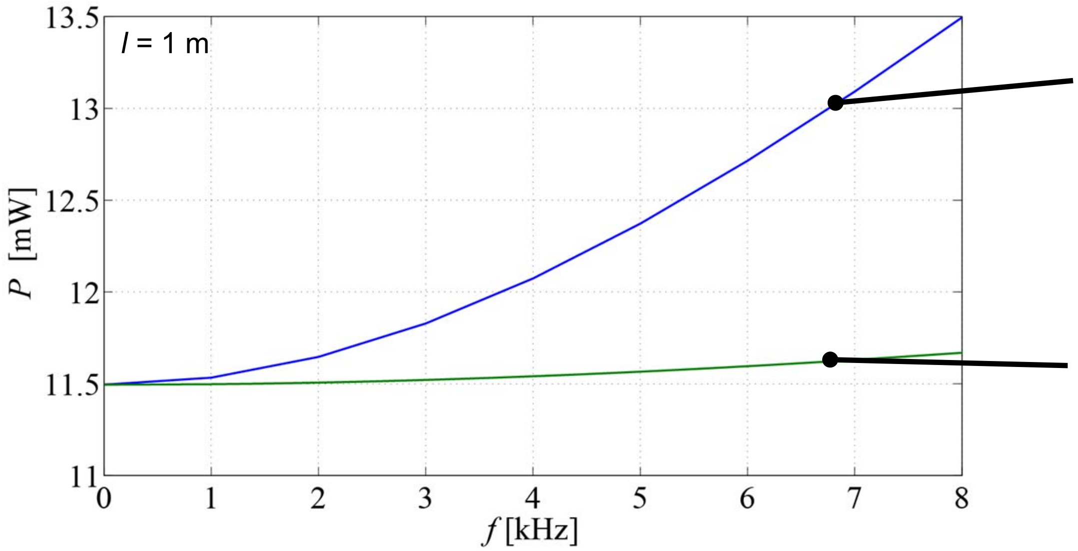

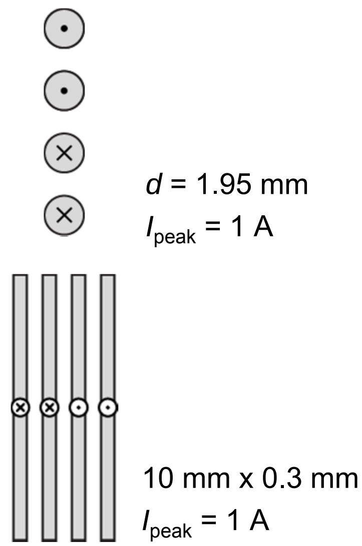

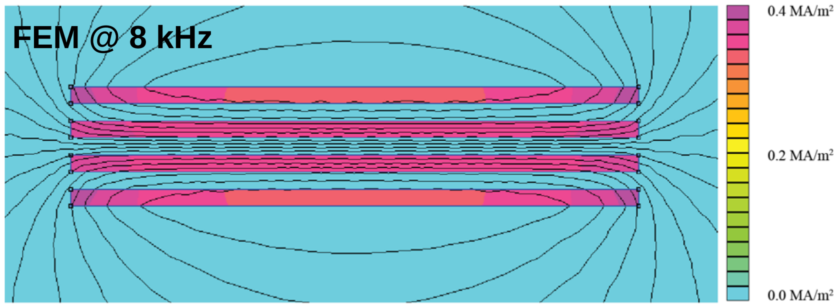

Winding Loss Modeling

Overview About Different Winding Types

Type	Price	Skin & Proximity	Filling Factor	Heat Dissipation
Round Solid Wire	++	--	+	+
Litz Wire	--	++	-	--
Foil Winding	+	+	++	+
Rectangular Wire	++	-	++	+

Rectangular Wire

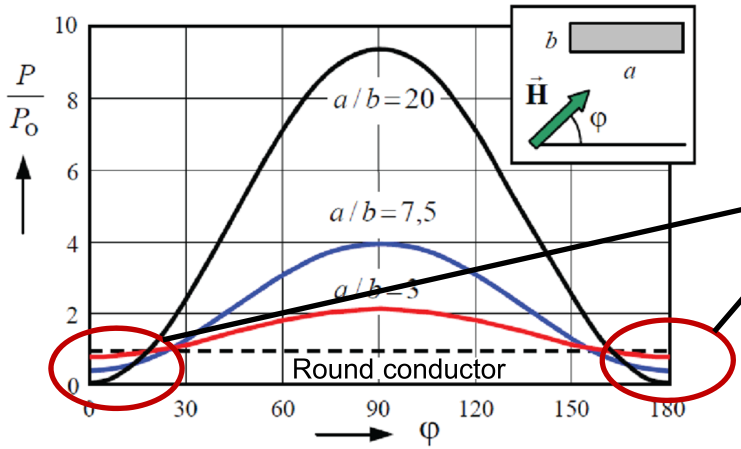

Foil windings are better only in this region!

P_0 … round conductor

Table and Figure from [13] M. Albach, "Induktive Komponenten in der Leistungselektronik", VDE Fachtagung - ETG Fachbereich Q1 "Leistungselektronik und Systemintegration", Bad Nauheim, 14.04.2011

Winding Loss Modeling
Skin Effect of Foil Conductor

Geometry Considered

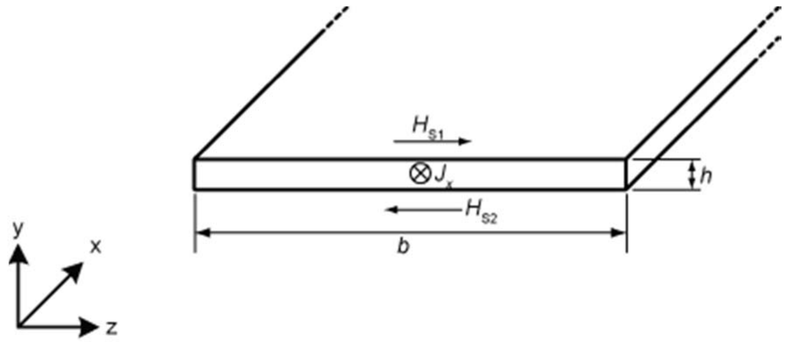

$$P_S = F_F(f) \cdot R_{DC} \cdot \hat{I}^2$$

(Loss per unit length)

with

$$F_F = \frac{v}{4} \frac{\sinh v + \sin v}{\cosh v - \cos v}$$

$$R_{DC} = \frac{1}{\sigma b h}$$

$$v = \frac{h}{\delta}$$

$$\delta = \frac{1}{\sqrt{\pi \mu_0 \sigma f}}$$

Current Distribution

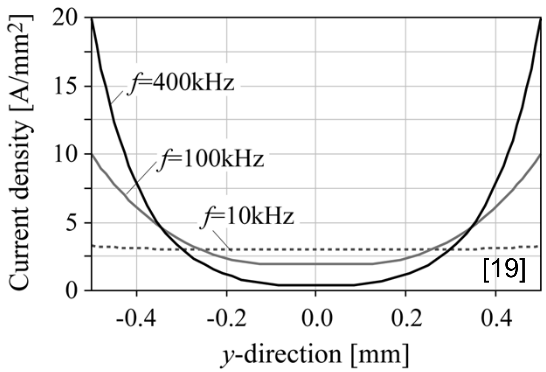

F_F evaluated

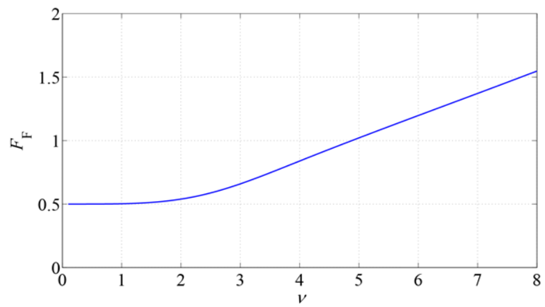

Winding Loss Modeling

Proximity Effect of Foil Conductor

Geometry Considered

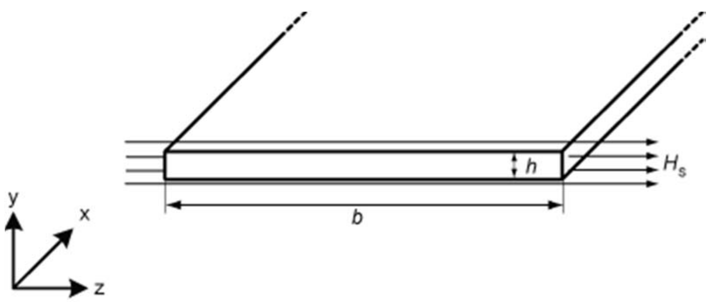

$$P_{\mathrm{P}} = G_{\mathrm{F}}(f) \cdot R_{\mathrm{DC}} \cdot \hat{H}_{\mathrm{S}}^{2}$$

(Loss per unit length)

with

$$G_{\mathrm{F}} = b^2 v \frac{\sinh v - \sin v}{\cosh v + \cos v}$$

$$R_{\mathrm{DC}} = \frac{1}{\sigma b h}$$

$$v = \frac{h}{\delta}$$

$$\delta = \frac{1}{\sqrt{\pi \mu_0 \sigma f}}$$

Current Distribution

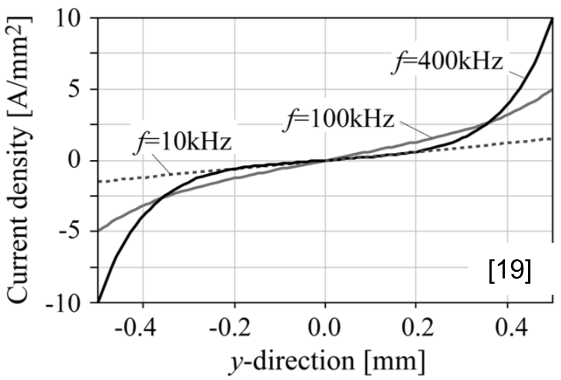

G_F evaluated

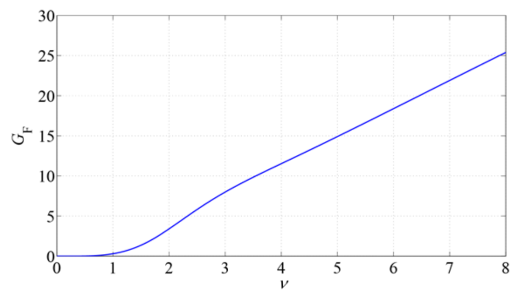

(b = 1 m)

Winding Loss Modeling
Skin Effect of Solid Round Conductor

Geometry Considered

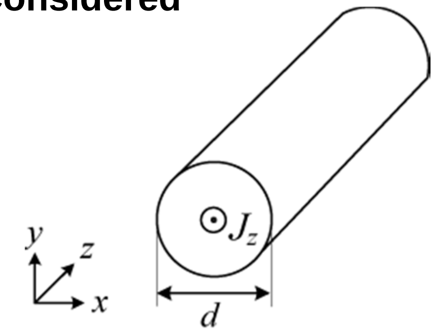

$$P_S = F_R(f) \cdot R_{DC} \cdot \hat{I}^2$$

(Loss per unit length)

with

$$R_{DC} = \frac{4}{\sigma \pi d^2}$$

$$\xi = \frac{d}{\sqrt{2}\delta}$$

$$\delta = \frac{1}{\sqrt{\pi \mu_0 \sigma f}}$$

F_R evaluated

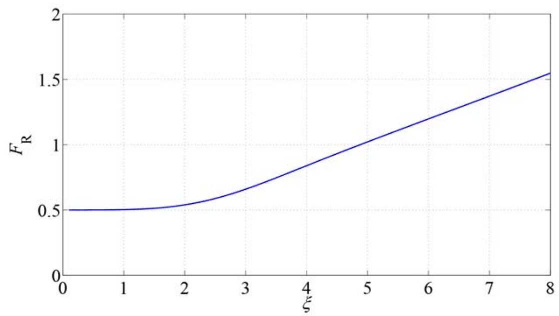

$$F_R = \frac{\xi}{4\sqrt{2}} \left[\frac{\mathrm{ber}_0(\xi)\mathrm{bei}_1(\xi) - \mathrm{ber}_0(\xi)\mathrm{ber}_1(\xi)}{\mathrm{ber}_1(\xi)^2 + \mathrm{bei}_1(\xi)^2} - \frac{\mathrm{bei}_0(\xi)\mathrm{ber}_1(\xi) - \mathrm{bei}_0(\xi)\mathrm{bei}_1(\xi)}{\mathrm{ber}_1(\xi)^2 + \mathrm{bei}_1(\xi)^2} \right]$$

Winding Loss Modeling

Proximity Effect of Solid Round Conductor

$$P_{\mathrm{P}} = G_{\mathrm{R}}(f) \cdot R_{\mathrm{DC}} \cdot \hat{H}_{\mathrm{S}}^{2}$$

(Loss per unit length)

with

$$R_{\mathrm{DC}} = \frac{4}{\sigma \pi d^{2}}$$

$$\xi = \frac{d}{\sqrt{2}\delta}$$

$$\delta = \frac{1}{\sqrt{\pi \mu_0 \sigma f}}$$

$$G_{\mathrm{R}} = -\frac{\xi \pi^{2} d^{2}}{2\sqrt{2}} \left[\frac{\mathrm{ber}_2(\xi)\mathrm{ber}_1(\xi) + \mathrm{ber}_2(\xi)\mathrm{bei}_1(\xi)}{\mathrm{ber}_0(\xi)^2 + \mathrm{bei}_0(\xi)^2} + \frac{\mathrm{bei}_2(\xi)\mathrm{bei}_1(\xi) - \mathrm{bei}_2(\xi)\mathrm{ber}_1(\xi)}{\mathrm{ber}_0(\xi)^2 + \mathrm{bei}_0(\xi)^2} \right]$$

Geometry Considered

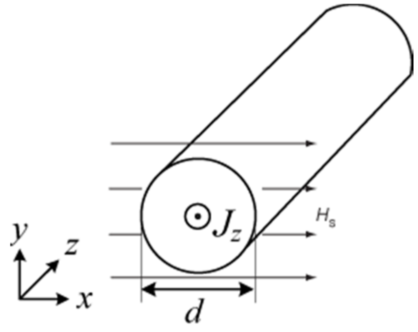

G_{R} evaluated

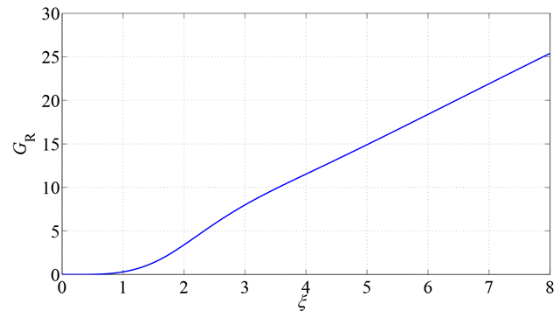

(*d* = 1 m)

Winding Loss Modeling

Skin and Proximity Effect of Litz Wire

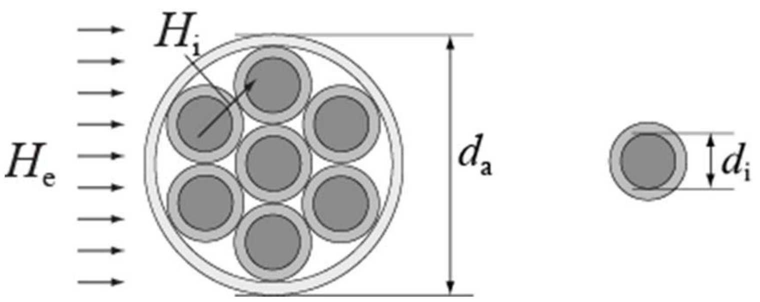

Skin Effect

$$P_S = n \cdot R_{DC} \cdot F_R(f) \cdot \left(\frac{\hat{I}}{n}\right)^2$$

(Loss per unit length)

Proximity Effect

$$P_P = P_{P,e} + P_{P,i}$$

$$= n \cdot R_{DC} \cdot G_R(f) \cdot \left(H_e^2 + \frac{\hat{I}^2}{2\pi^2 d_a^2}\right)$$

(Loss per unit length)

Average internal field H_i under the assumption of a homogeneous current distribution inside the Litz wire.

Losses in Litz Wires

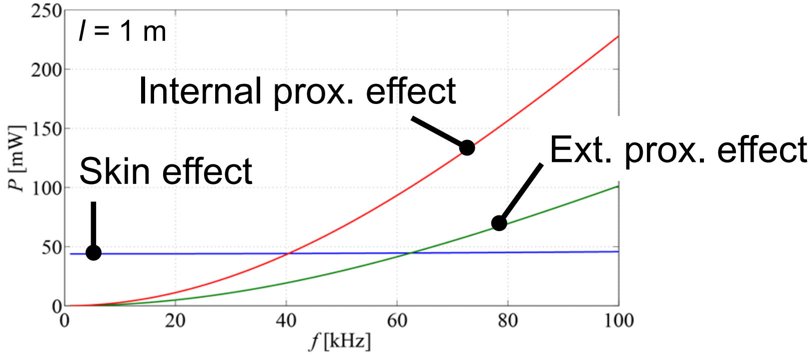

(25 x d_i = 0.5 mm, I_{peak} = 5 A, $H_{e,peak}$ = 300 A/m)

Winding Loss Modeling

Orthogonality of Winding Losses

It is valid to calculate the losses for each frequency component independently and total them up.

$$P = \sum_{i=0}^{\infty} \left(P_{\mathrm{S},\mathrm{i}} + P_{\mathrm{P},\mathrm{i}} \right)$$

It is valid to calculate the skin and proximity losses independently and total them up.

[14] J. A. Ferreira, “Improved analytical modeling of conductive losses in magnetic components”, in IEEE Transactions on Power Electronics, vol. 9, no. 1, 1994.

Winding Loss Modeling

Calculation of External Field H_e (1D - Approach)

Un-Gapped Transformer Cores

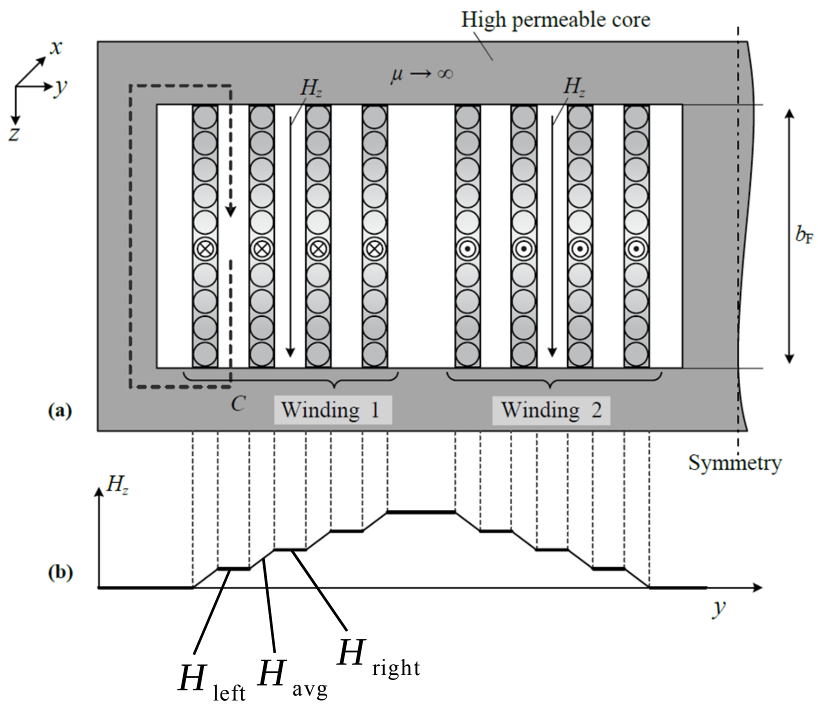

$$\oint \mathbf{H}\,d\mathbf{l} = \iint \mathbf{J}\,d\mathbf{A}$$ (Ampere's Law)

$$P = R_{DC}\left(F_{R/F}\hat{I}^2 NM + NG_{R/F}\sum_{m=1}^{M}\hat{H}^2_{avg,m}\right) l_m$$

with

$$H_{avg} = \frac{1}{2}\left(H_{left} + H_{right}\right)$$

it is

$$P = R_{DC}\hat{I}^2\left(F_{R/F}NM + N^3 MG_{R/F}\frac{4M^2-1}{12b_F^2}\right) l_m$$

where

N … the number of conductors per layer
(i.e. N = 1 for foil windings)

M … the number of layers.

Figure from [19]

Winding Loss Modeling
Short Foil Conductors

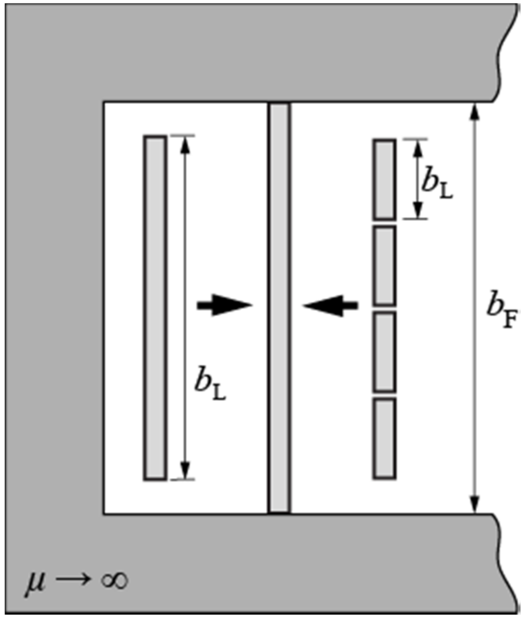

“Porosity Factor”

$$\eta = \frac{N b_L}{b_F}$$

Redefinition of Parameters

$$\sigma' = \eta \sigma$$

$$\delta' = \frac{1}{\sqrt{\pi f \sigma' \mu_0}}$$

$$\nu' = \frac{h}{\delta'}$$

Winding Loss Modeling

FEM Simulations : Foil Windings

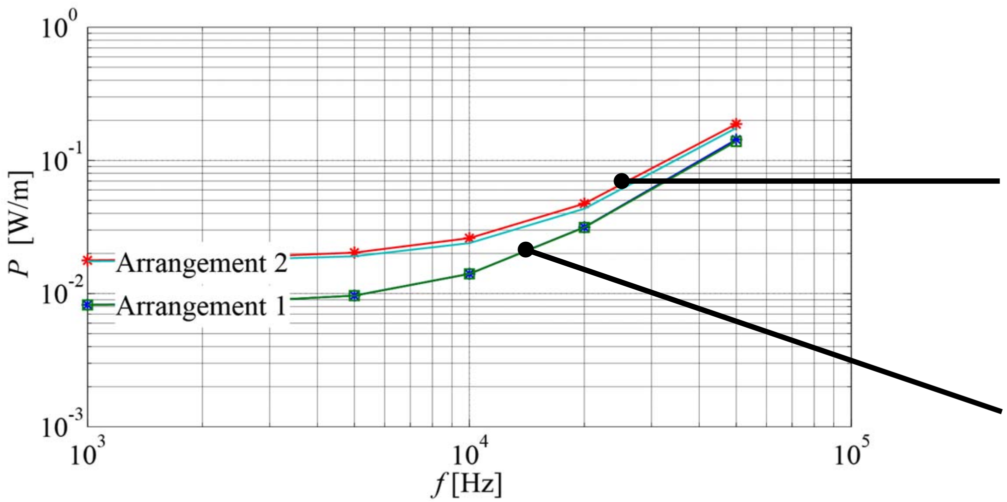

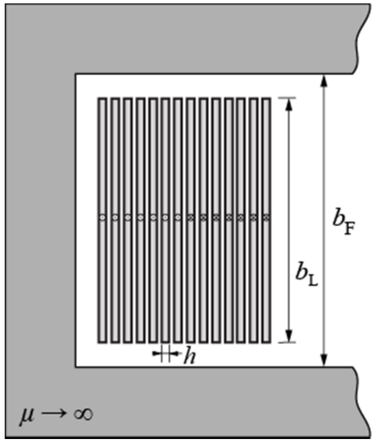

N = 2 x 10
h = 0.3 mm
b_L = 33 mm
b_F = 37 mm
I_{peak} = 1 A

Error < 6.5%

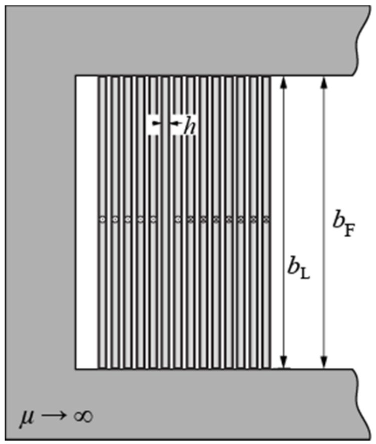

N = 2 x 7
h = 0.4 mm
b_L = 37 mm
b_F = 37 mm
I_{peak} = 1 A

Winding Loss Modeling

Calculation of External Field H_e (2D - Approach)

Gapped cores: 2D approach is necessary !

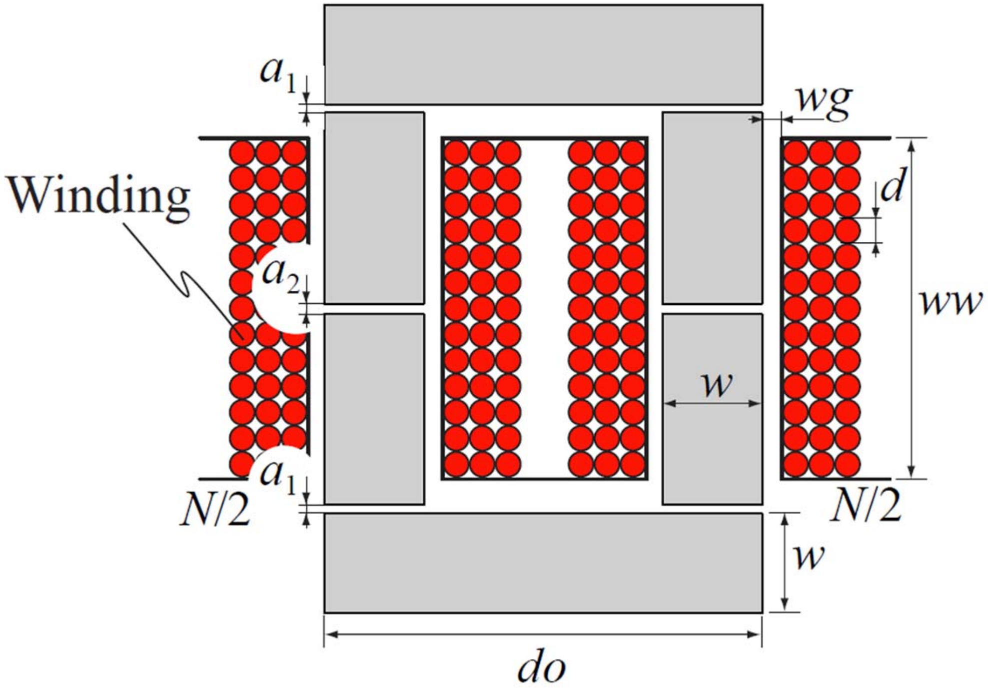

Winding Loss Modeling

Effect of the Air Gap Fringing Field

The air gap is replaced by a fictitious current, which …

… has the value equal to the magneto-motive force (mmf) across the air gap.

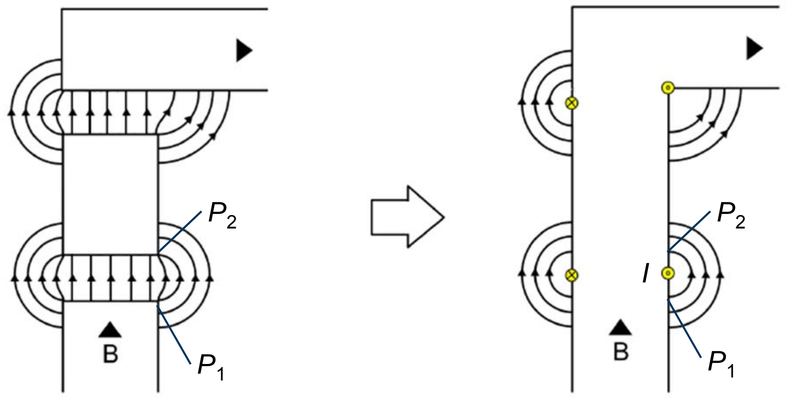

$$V_{\mathrm{m,air}} = \int_{P_1}^{P_2} \mathbf{H}\,\mathrm{d}\mathbf{l} = \phi \cdot R_{\mathrm{air}}$$

$$V_{\mathrm{m,air}} = \int_{P_1}^{P_2} \mathbf{H}\,\mathrm{d}\mathbf{l} = I$$

→ An accurate air gap reluctance model is needed!

Winding Loss Modeling

Effect of the Core Material

The method of images (mirroring)

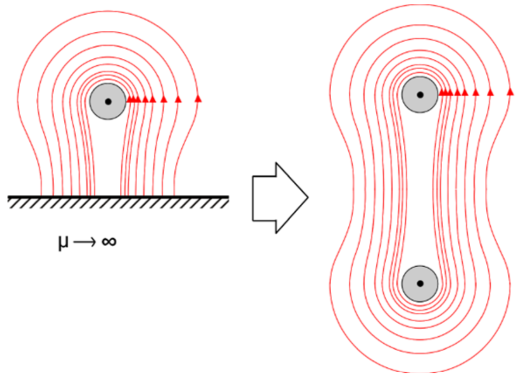

"Pushing the walls away"

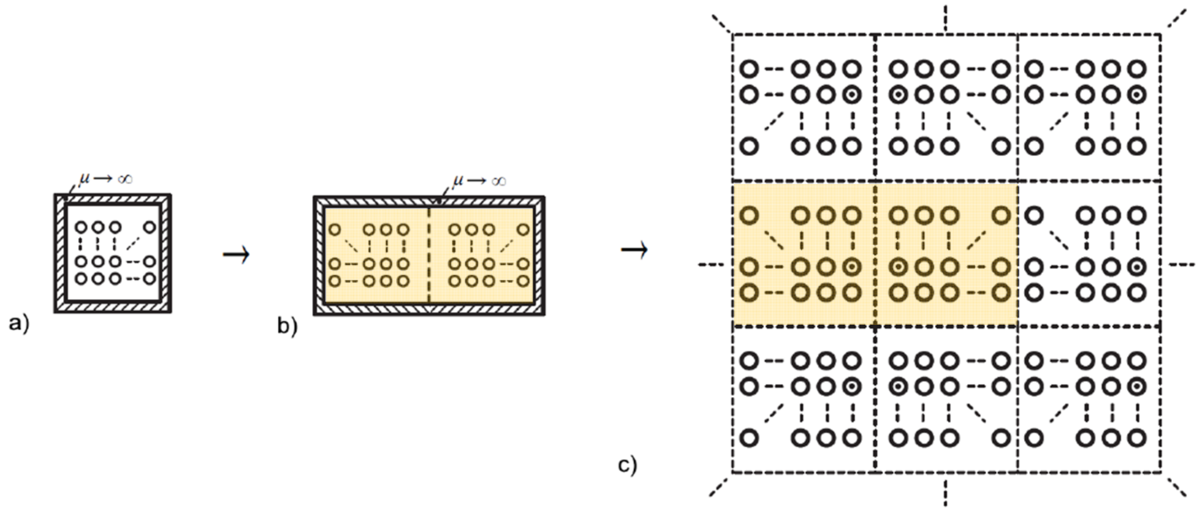

Winding Loss Modeling

Calculation of External Field H_e (2D - Approach)

Gapped cores: 2D approach

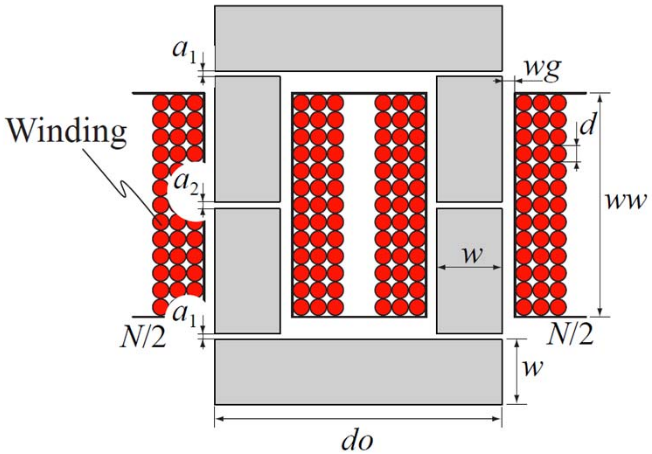

Winding Arrangement

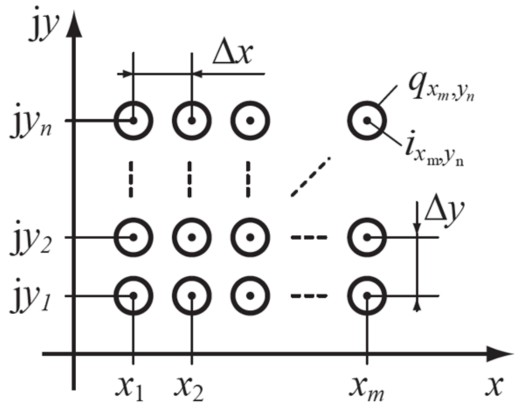

External field vector across conductor $q_{xi;yk}$

$$\hat{H}_e = \left| \sum_{u=1}^{m} \sum_{l=1}^{n} \epsilon(u,l) \frac{\hat{i}_{x_u,y_l}\left((y_l - y_k) - \mathrm{j}(x_u - x_i)\right)}{2\pi\left((x_u - x_i)^2 + (y_l - y_k)^2\right)} \right|$$

Winding Loss Modeling
Different Winding Sections

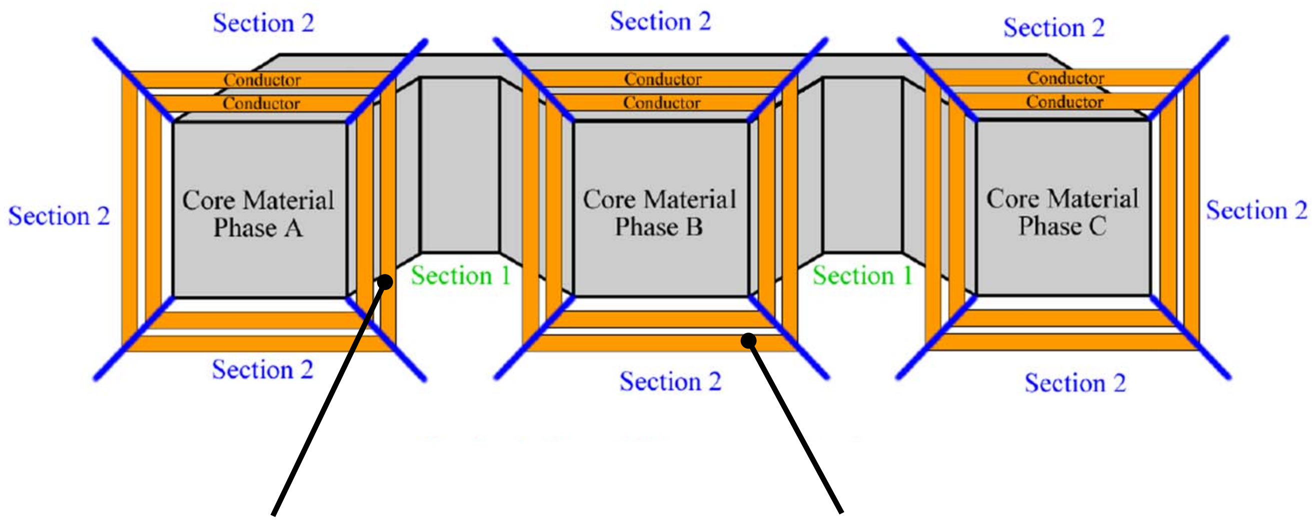

Section 1
Many mirroring steps necessary in order to push the walls away.

Section 2
Only one mirroring step necessary (only one wall).

➡ Normally, higher proximity losses in Section 1.

Winding Loss Modeling

FEM Simulations : Round Windings (Including Litz Wire Windings) (1)

Major Simplification

- magnetic field of the induced eddy currents neglected.
- This can be problematic at frequencies above (rule-of-thumb) [15]

$$f_{\max} = \frac{2.56}{\pi \mu_0 \sigma d^2}$$

Results of considered winding arrangements

f-range	$f < f_{\max}$	$f > f_{\max}$
Error	< 5%	> 5% (always < 25%)

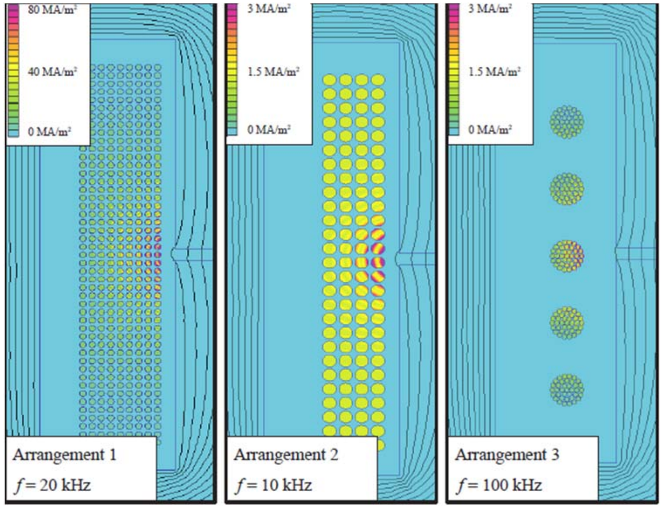

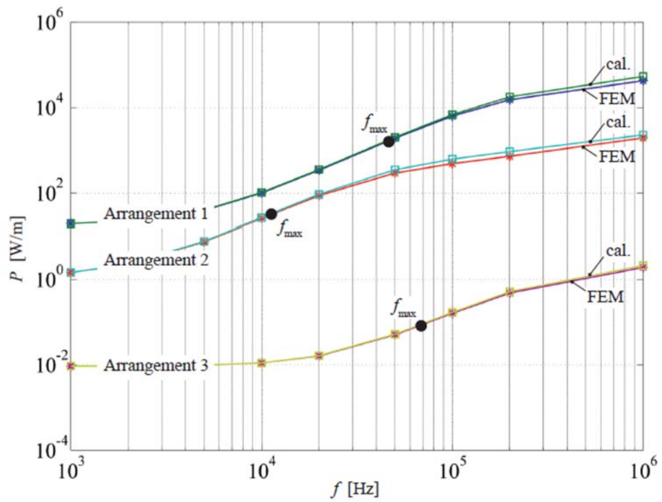

[15] A. Van den Bossche, V. C. Valchev, "Inductors and Transformers for Power Electronics", CRC Press. Taylor & Francis Group, 2005

Winding Loss Modeling

FEM Simulations : Round Windings (Including Litz Wire Windings) (2)

FEM Simulation

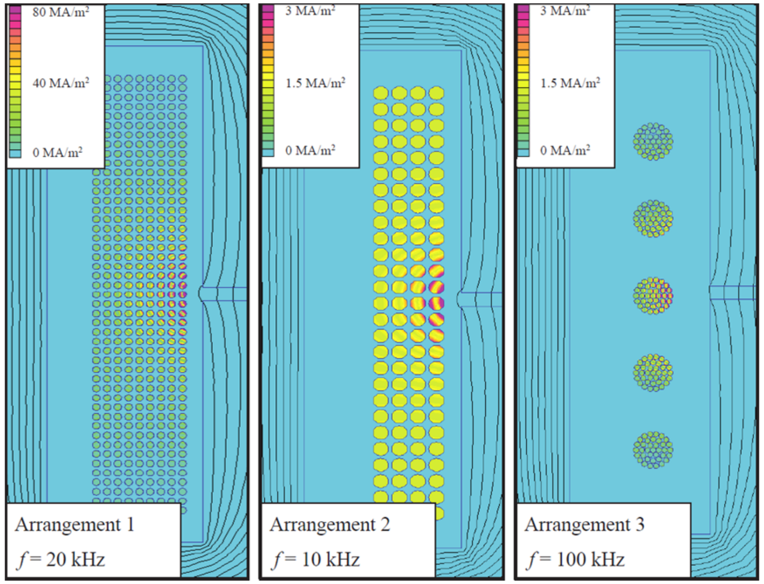

Results

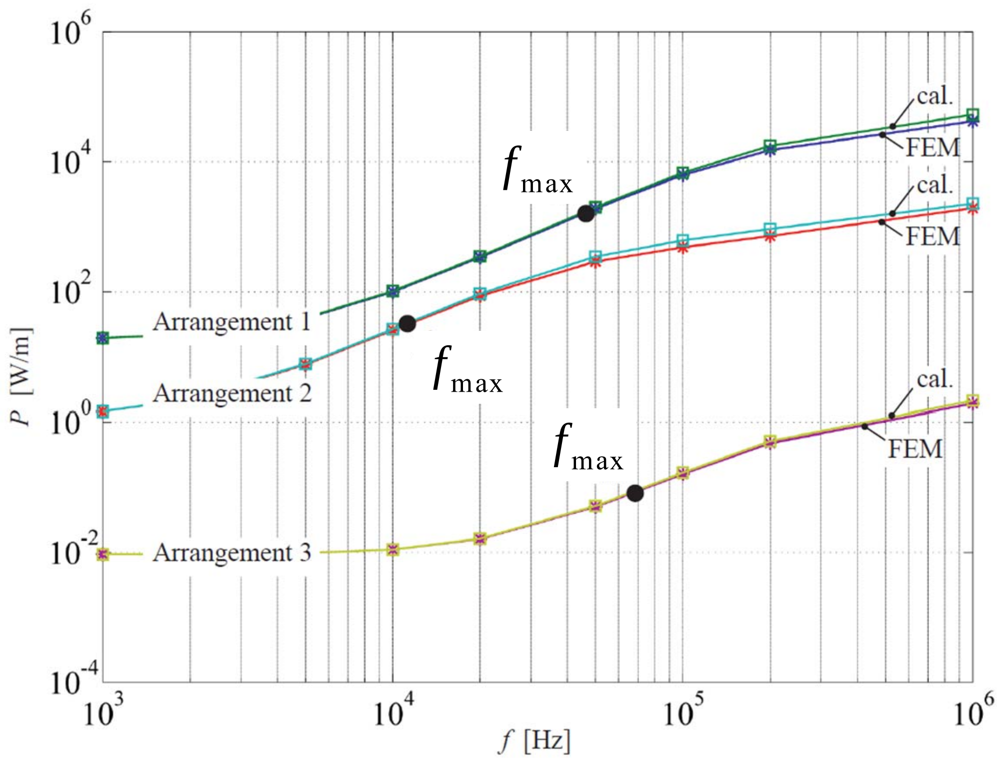

Winding Loss Modeling

Methods to Decrease Winding Losses (1)

Interleaving

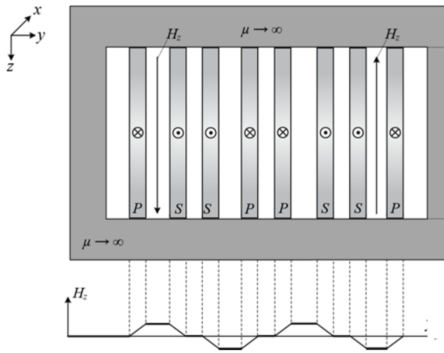

Optimal Foil Thickness

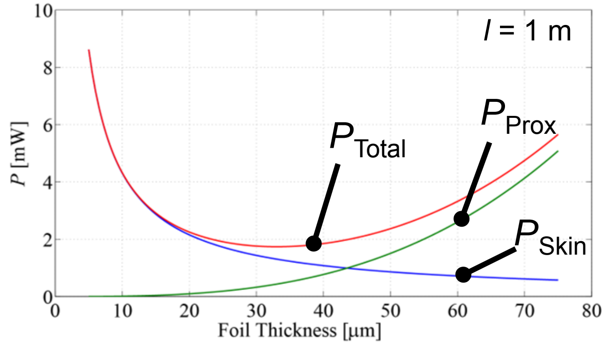

(f = 20 kHz, I_{peak} = 1 A, b = 20 cm, $H_{e,peak}$ = 1000 A/m)

Avoid Orthogonal Flux in Foil Windings

Optimal Solid Wire Thickness

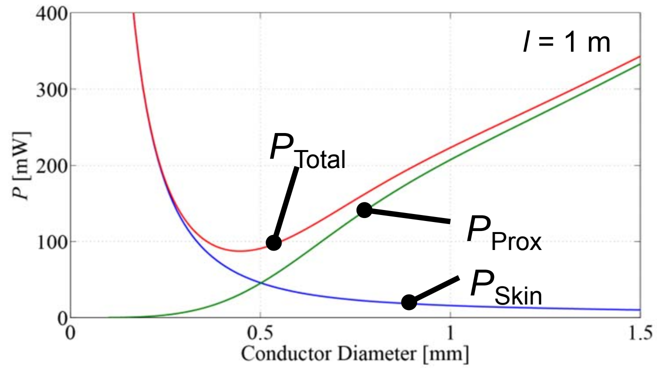

(f = 100 kHz, I_{peak} = 1 A, $H_{e,peak}$ = 1000 A/m)

Litz Wire

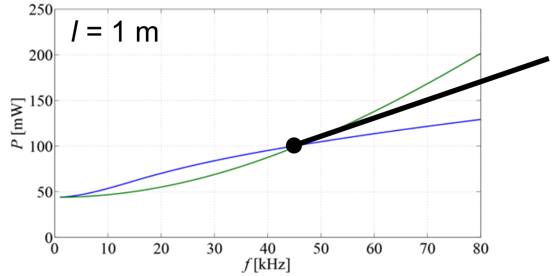

Push this point to higher frequencies!

→ Increase number of strands.

Winding Loss Modeling
Methods to Decrease Winding Losses (2)

Arrangement of Windings

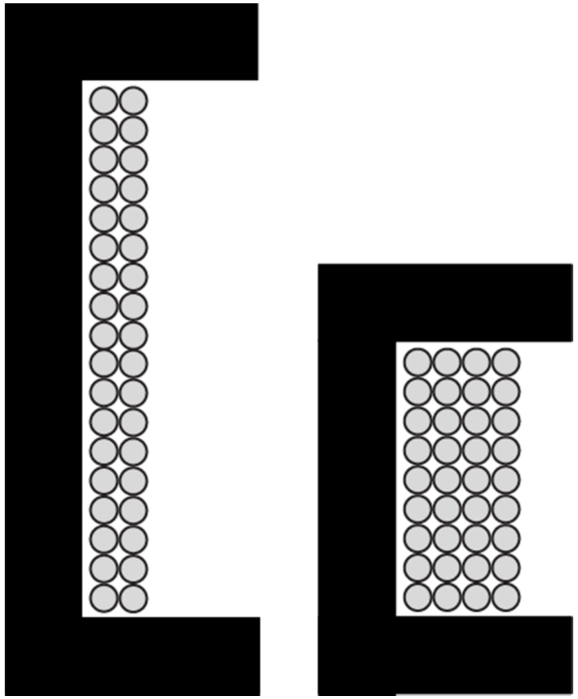

Proximity losses increase in more compact winding arrangements.

Winding Loss Modeling

Methods to Decrease Winding Losses (3)

Aluminum vs. Copper [13]

Aluminum (vs. Copper):
- Lighter
- Lower costs
- Lower Conductivity $\sigma = 38 \cdot 10^6$ 1/(Ωm)
  (Copper: $\sigma = 58 \cdot 10^6$ 1/(Ωm))

→ Lower Skin Depth!

Skin- and DC losses higher than in copper conductors.

Proximity losses are lower in aluminum conductors over a wide frequency range. Figure shows a comparison of single round solid conductors in external field.

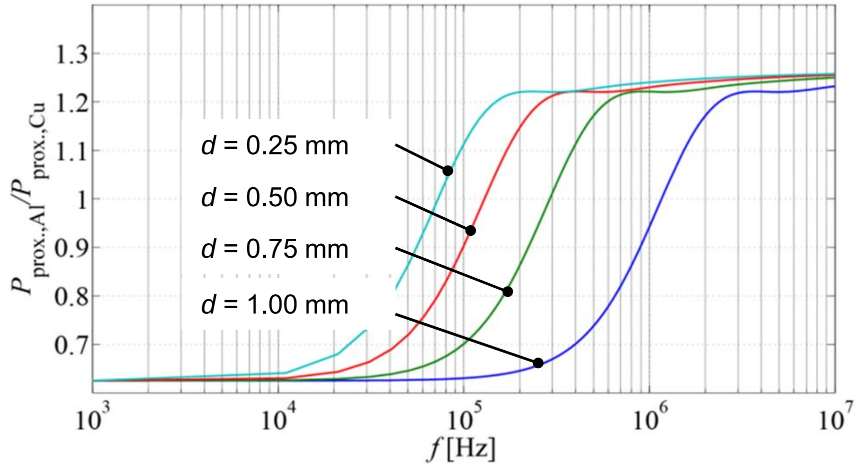

[13] M. Albach, “Induktive Komponenten in der Leistungselektronik”, VDE Fachtagung - ETG Fachbereich Q1 "Leistungselektronik und Systemintegration", Bad Nauheim, 14.04.2011

Example
Winding Loss Modeling

Photo & Dimensions

Dimensions

l_g	1.95 mm
do	60 mm
b	60 mm
a	20 mm
t	28 mm
ww	56.9 mm
d	2.24 mm

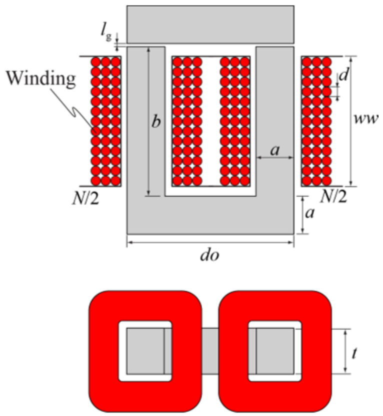

Material
Grain-oriented steel (M165-35S)

Current Waveform

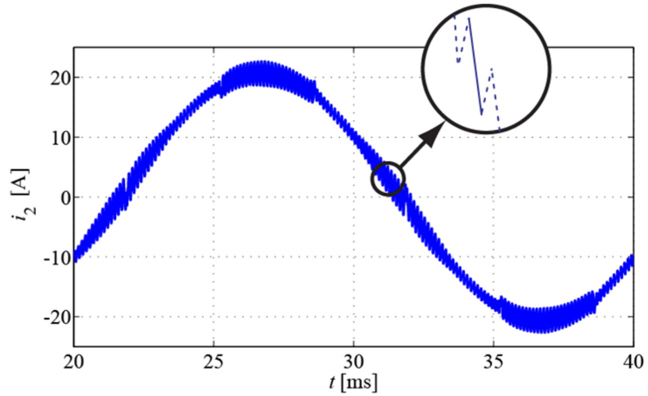

Demonstration in MATLAB

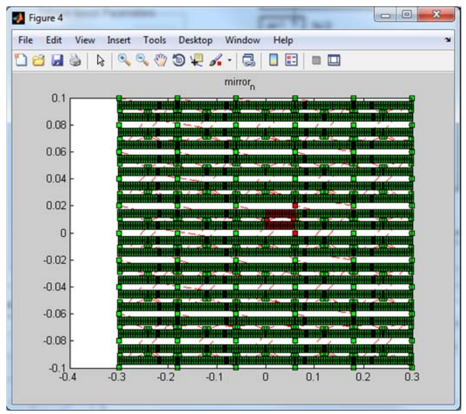

Outline

- Magnetic Circuit Modeling
- Core Loss Modeling
- Winding Loss Modeling
- **Thermal Modeling**
- Multi-Objective Optimization
- Summary & Conclusion

Thermal Modeling
Motivation & Model (1)

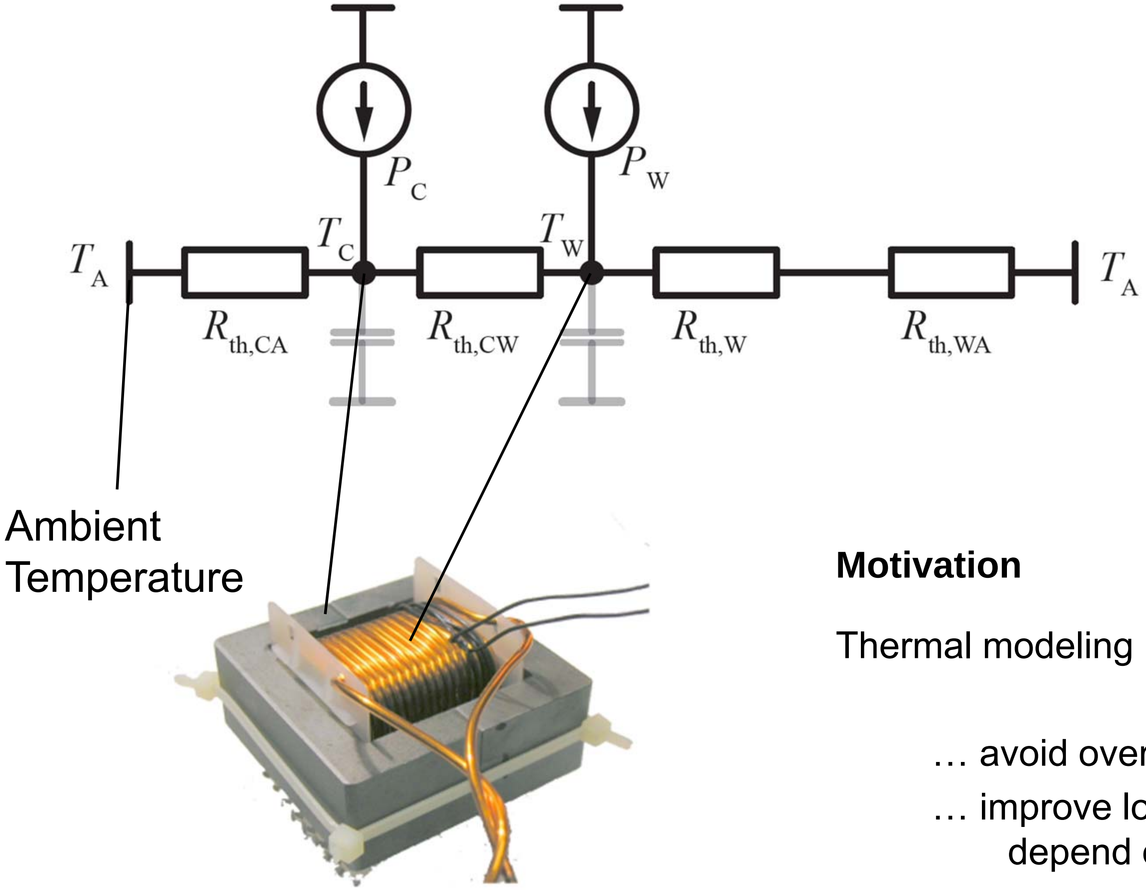

Motivation

Thermal modeling is important to …

… avoid overheating.

… improve loss calculation (since the losses depend on temperature).

Thermal Modeling
Motivation & Model (2)

Model

Inductor

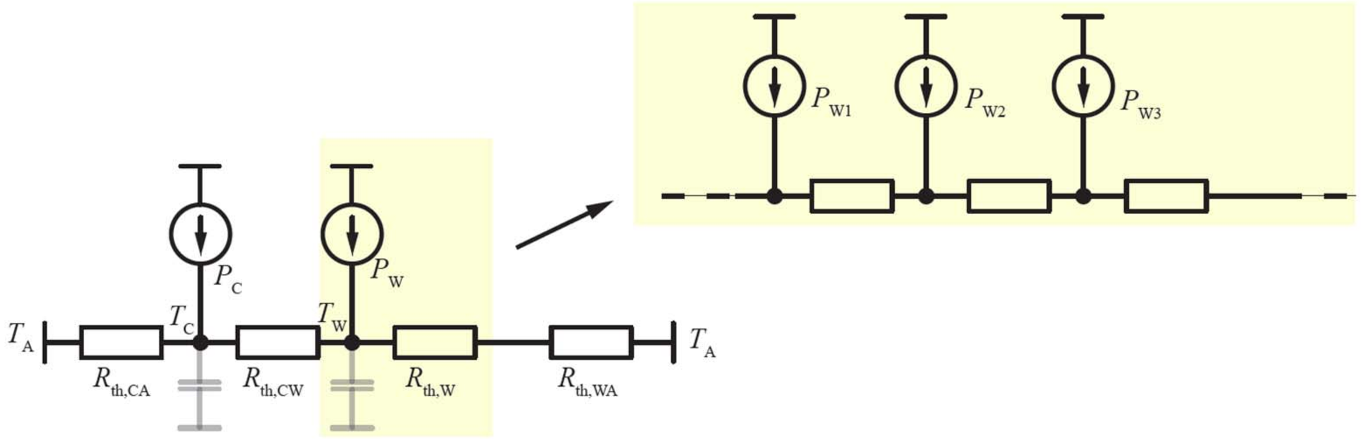

Transformer

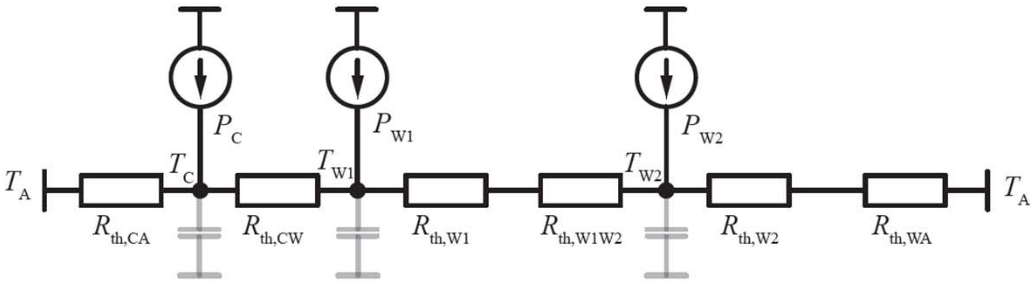

→ Determination of thermal resistors is challenging!

Thermal Modeling

Heat Transfer Mechanisms

$$R_{\mathrm{th}} = \frac{\Delta T}{P} = f(T)$$

Conduction

Independent of temperature *T* for most materials
Difficult to determine interfaces between materials

$$R_{\mathrm{th}} = \frac{\Delta T}{P} = \frac{l}{A\lambda}$$

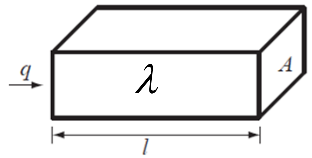

Convection

Combined effect of conduction and fluid flow
Changes with changing absolute temperature (nonlinear)
Good empirical calculation approach available

$$R_{\mathrm{th}} = \frac{\Delta T}{P} = \frac{1}{\alpha A}$$

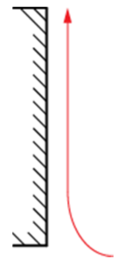

Radiation

Small compared to other mechanisms
Modeling the system is demanding
(nonlinear eq. / to describe which components "sees" the other component).

$$P = \varepsilon_{eff} A_1 \sigma (T_b^4 - T_a^4)$$

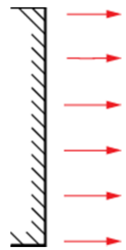

Thermal Modeling

Thermal Resistance Calculation : (Natural) Convection (1)

$$R_{\mathrm{th}} = \frac{\Delta T}{P} = \frac{1}{\alpha A}$$

α is a coefficient that is influenced by …

… the absolute temperature,
… the fluid property,
… the flow rate of the fluid,
… the dimensions of the considered surface,
… orientation of the considered surface,
… and the surface texture.

Thermal Modeling

Thermal Resistance Calculation : (Natural) Convection (2)

Empirical solutions known for …

vertical plane

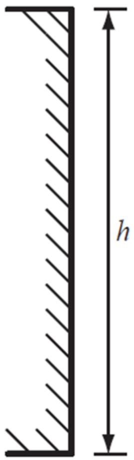

horizontal plane

-top:

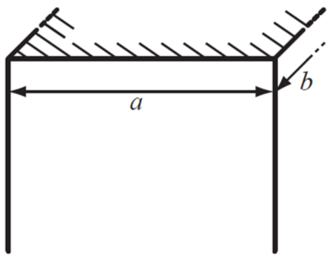

- bottom :

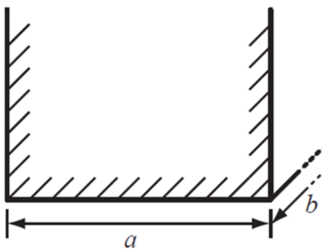

gap

- horizontal:

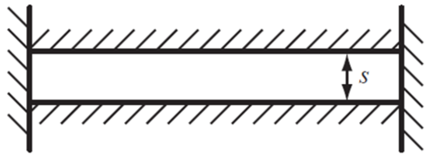

- vertical:

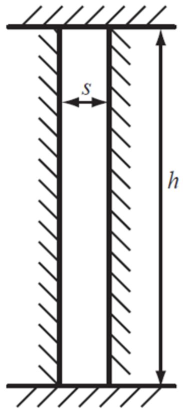

and more …

Thermal Modeling
Thermal Resistance Calculation : (Natural) Convection (3)

Structure of Empirical Solutions - Theory

g	gravity of earth: 9.81 m/s^2
l	characteristic length
β	volumetric thermal expansion coefficient : 1/T (air)
v	kinematic viscosity: 162.6 $\cdot 10^{-7}$ m^2/s (air)

Name	Measure of …	
Nusselt number *Nu*	… improvement of heat transfer compared to the case with hypothetical static fluid.	$Nu = \frac{l}{A\lambda} \Big/ \frac{1}{\alpha A} = \frac{\alpha l}{\lambda} = f(Gr, Pr)$
Grashof number *Gr*	… ration between buoyancy and frictional force of fluid.	$Gr = \frac{g l^3}{v^3} \beta \Delta T$
Prandtl number *Pr*	… ratio between viscosity and heat conductivity of fluid.	$Pr = 0.7 \quad \text{(for air)}$
Rayleigh number *Ra*	… flow condition (laminar or turbulent) of fluid.	$Ra = Pr \cdot Gr$

Procedure

λ is the heat conductivity of the fluid
λ_{air} = 25.873 mW/(m K) @ 20°C [16]

$$Nu(Gr, Pr) \;\Rightarrow\; \alpha = \frac{Nu(Gr, Pr)\lambda}{l} \;\Rightarrow\; R_{\mathrm{th}} = \frac{1}{\alpha A}$$

[16] VDI Heat Atlas, Springer-Verlag, Berlin, 2010

Thermal Modeling

Thermal Resistance Calculation : (Natural) Convection (4)

Structure of Empirical Solutions - Example

Vertical Plane

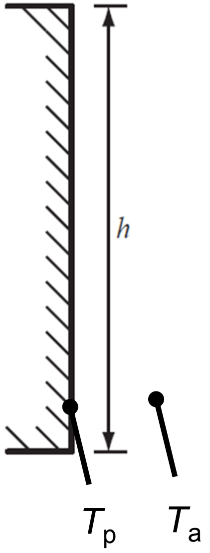

$$Nu = \left(0.825 + 0.387\left(Ra \cdot f_1(Pr)\right)^{1/6}\right)^2$$

$$f_1 = \left(1 + \left(\frac{0.492}{Pr}\right)^{9/16}\right)^{-16/9}$$

$$\alpha = \frac{Nu(Gr, Pr)\lambda}{l}$$

(l = h)

$$R_{th} = \frac{\Delta T}{P} = \frac{1}{\alpha A}$$

Reference:

[16] VDI Heat Atlas, Springer-Verlag, Berlin, 2010

Example

(h = 10 cm, T_p = 60 °C, T_a = 20 °C, $A = h \cdot h$)

→ R_{th} = 16.6 K/W

Increase of Winding Surface

Thermal Modeling

Thermal Resistance Calculation : Conduction

Overview

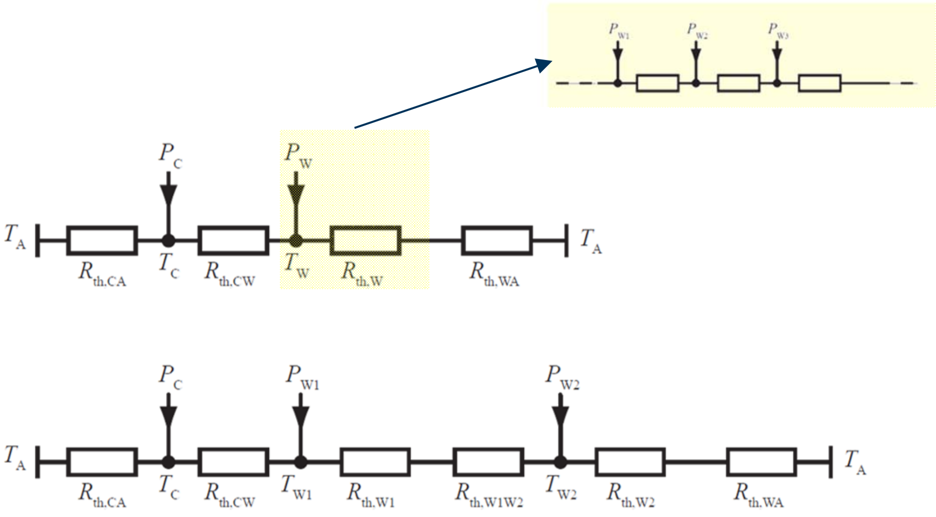

Normally, with natural convection it is

$$R_{th,W} << R_{th,WA}$$

Round Conductor

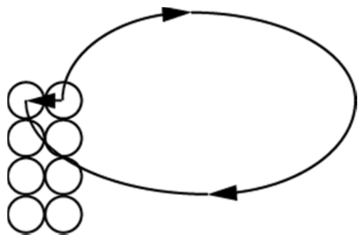

$R_{th,W}$ is difficult to determine. One difficulty is, e.g., to model the influence of pressure on the thermal resistance.

Litz wire shows low thermal conductivity.

Foil Conductor

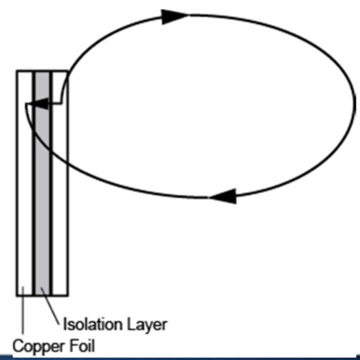

Example
Thermal Modeling (1)

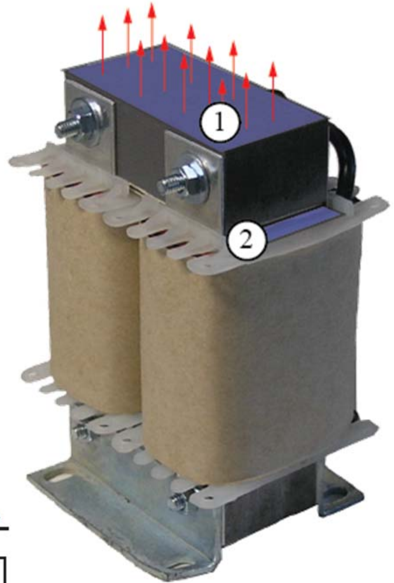

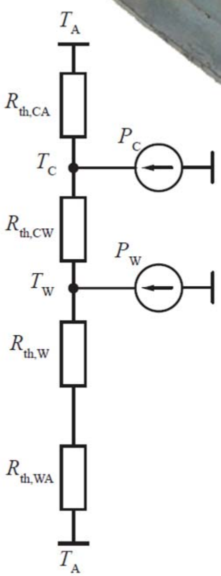

(1) Horizontal Plane - Top

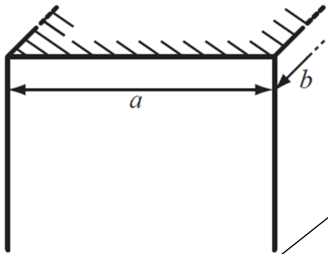

g	gravity of earth: 9.81 m/s^2
l	characteristic length: $l = a*b / (2(a+b))$
β	volumetric thermal expansion coefficient : 1/T (air)
v	kinematic viscosity: 162.6 $\cdot 10^{-7}$ m^2/s (air)

$$Gr = \frac{gl^3}{v^3}\beta\Delta T$$

$$Pr = 0.7 \quad \text{(for air)}$$

$$Ra = Pr \cdot Gr$$

$$Nu = \begin{cases} 0.766\,(Ra \cdot f_2(Pr))^{1/5} & \text{for } Ra \cdot f_2(Pr) \le 7\cdot 10^4 \quad \text{(laminar)} \\ 0.15\,(Ra \cdot f_2(Pr))^{1/3} & \text{for } Ra \cdot f_2(Pr) > 7\cdot 10^4 \quad \text{(turbulent)} \end{cases}$$

with

$$f_2 = \left(1 + \left(\frac{0.322}{Pr}\right)^{11/20}\right)^{-20/11}$$

$$\alpha = \frac{Nu(Gr, Pr)\lambda}{l}$$

$$R_{th} = \frac{\Delta T}{P} = \frac{1}{\alpha A}$$

Resistor R_{th} is now calculated for one operating point!
(→ more iterations are necessary!)

Example

Thermal Modeling (2)

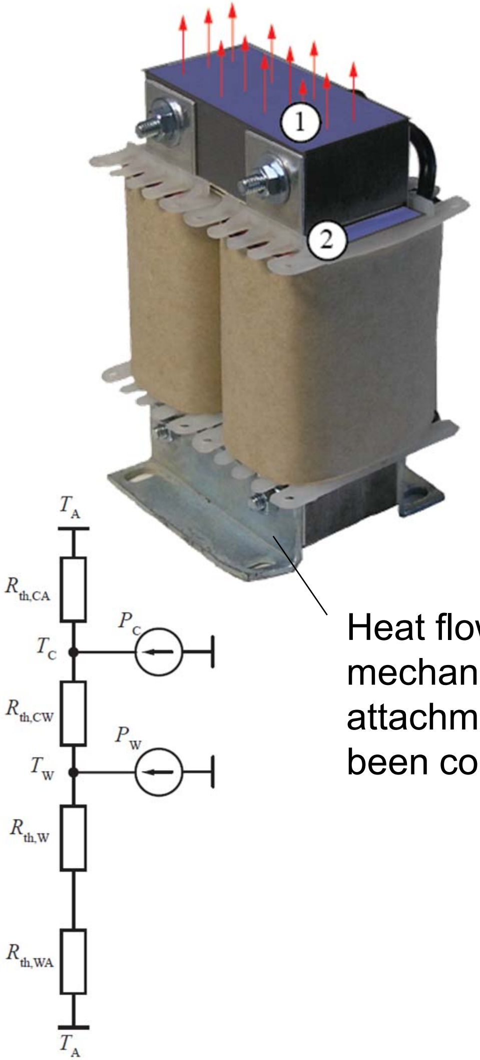

Heat flow via mechanical attachment has not been considered.

(2) Core to Winding

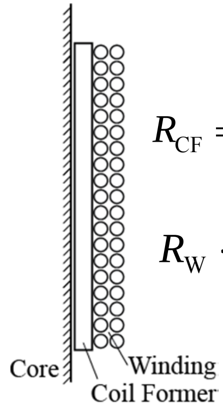

$$R_{CF} = \frac{l}{A\lambda} = 1.05\,\frac{\mathrm{K}}{\mathrm{W}}$$

$$R_W \ll R_{WA}$$

Drawing represents the cross-section of one coil former side (there are total 2 x 4 coil former sides).

Measurement Results

(ΔB=0.18 T, f = 10kHz, triangular)

	Calc.	Meas.
P_{core}	107 °C	112 °C
$P_{winding}$	100 °C	104 °C

Quantity Values

$R_{th,CA}$ = 3.6 K/W

$R_{th,WA}$ = 4.7 K/W

Outline

- Magnetic Circuit Modeling
- Core Loss Modeling
- Winding Loss Modeling
- Thermal Modeling
- **Multi-Objective Optimization**
- Summary & Conclusion

Multi-Objective Optimization – Volume vs. Losses

Introduction to the PFC Rectifier (1)

Simplified Schematic

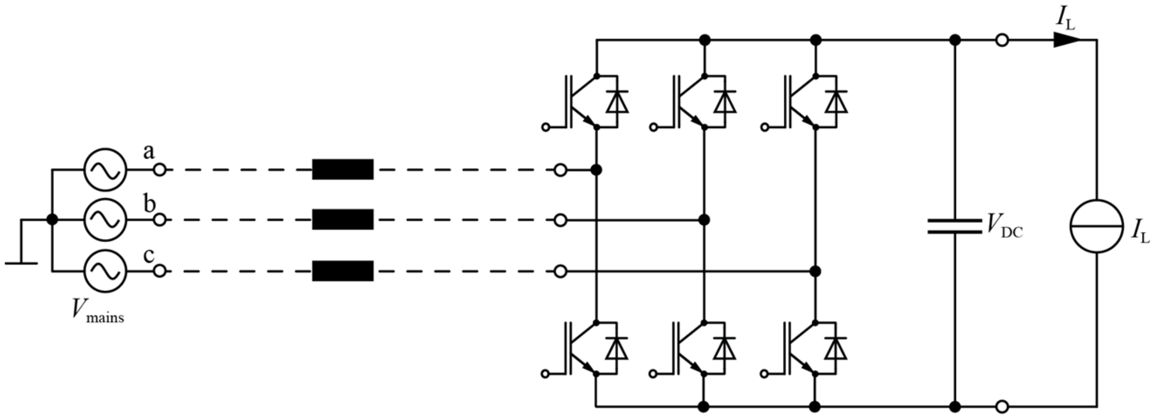

Converter Specifications

Parameter	Variable	Value	
Input Voltage AC	V_{mains}	230	V
Mains Frequency	f_{mains}	50	Hz
DC-Voltage	V_{DC}	650	V
Load Current	I_L (nominal)	15.4	A
Switching Frequency	f_{sw}	8	kHz

Photo of Converter

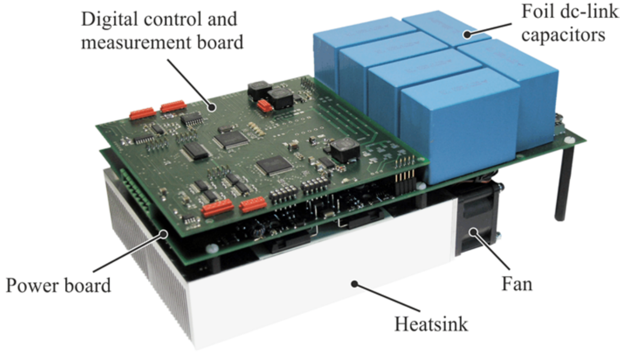

Multi-Objective Optimization – Volume vs. Losses

Introduction to the PFC Rectifier (2)

Simplified Schematic

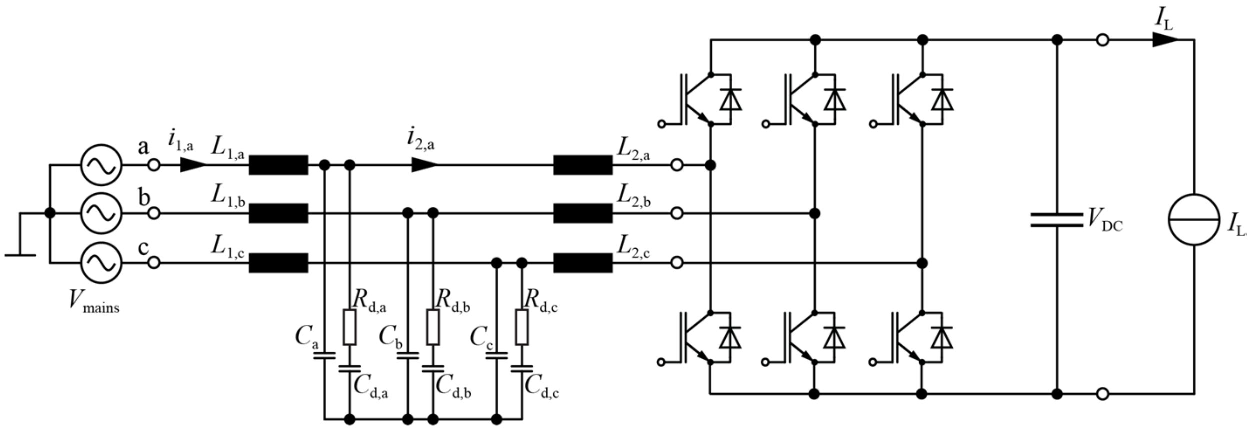

Filter Specifications

Input Current THD ≤ 4 %

Max. current ripple in boost inductors 4 A

LCL filter consists of

three boost inductors

and a damped three-phase *LC* filter.

Multi-Objective Optimization – Volume vs. Losses

Introduction to the PFC Rectifier (3)

Selected Inductor Shape

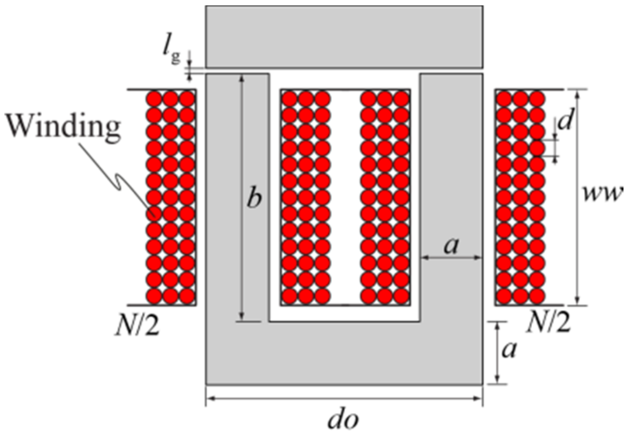

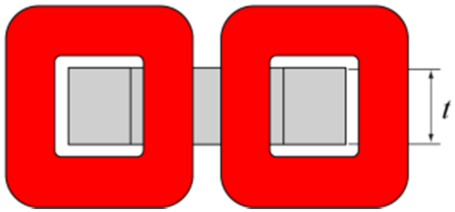

Photo of Inductor

Degrees of Freedom

$$\begin{pmatrix} l_g \\ a \\ N \\ do \\ b \\ t \\ ww \\ d \end{pmatrix}$$

Material

Grain-oriented steel
(M165-35S,
lam. thickness 0.35 mm)

Multi-Objective Optimization – Volume vs. Losses

Modeling LCL Filter (1)

Procedure

1) A reluctance model is introduced to describe the electric / magnetic interface, i.e. $L = f(i)$.

↓

2) Core losses are calculated.

↓

3) Winding losses are calculated.

↓

4) Inductor temperature is calculated.

↓

Considered effects

- Air gap stray field
- Non-linearity of core material

- DC Bias
- Different flux waveforms
- Wide range of flux densities and frequencies

- Skin and proximity effect
- Stray field proximity effect
- Effect of core to magnetic field distribution

Multi-Objective Optimization – Volume vs. Losses

Modeling LCL Filter (2)

EPCOS X2 MKP Film Capacitor

(Rated voltage 305 V)

www.epcos.com

Volume Calculation

$$0.18\ \mu\mathrm{F/cm^3}$$

Power Loss Calculation

$$P = 2\pi f C \tan\delta\, V^2$$

Multi-Objective Optimization – Volume vs. Losses

Modeling LCL Filter (3)

Simplified Schematic

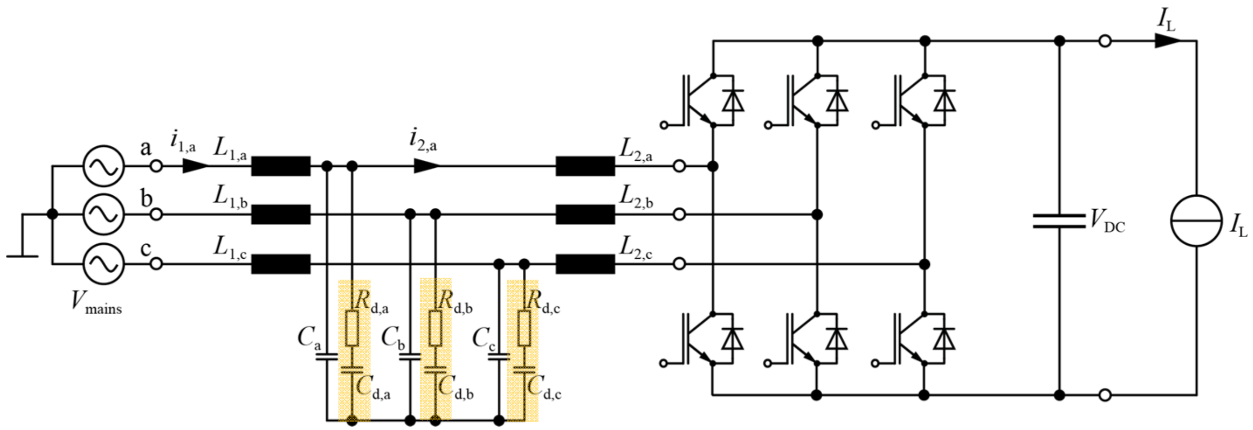

Trade-off between damping capacitor size and damping achieved

→ $C = C_d$

Optimal damping achieved with [17]

$$R_d = \sqrt{2.1 \frac{L_1}{C}}$$

[17] R. W. Erickson and D. Maksimovic, “Fundamentals of Power Electronics”, Springer Science+Business Media, LLC, 2004

Multi-Objective Optimization – Volume vs. Losses

Optimization of LCL Filter (1)

Simplified Schematic

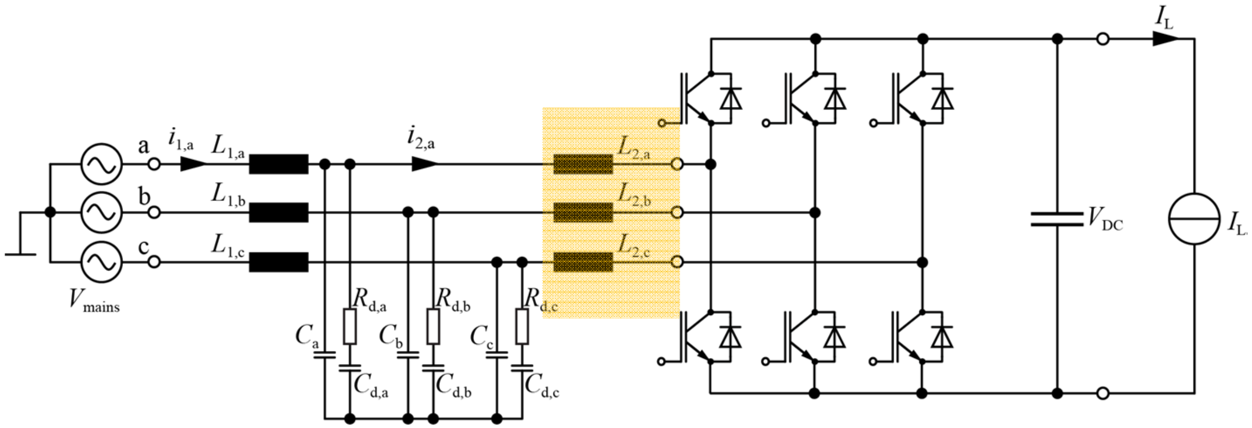

Constraints concerning boost inductors

max. current ripple $I_{HF,pp,max}$
max. temperature T_{max}
max. volume V_{max}

Multi-Objective Optimization – Volume vs. Losses

Optimization of LCL Filter (2)

Simplified Schematic

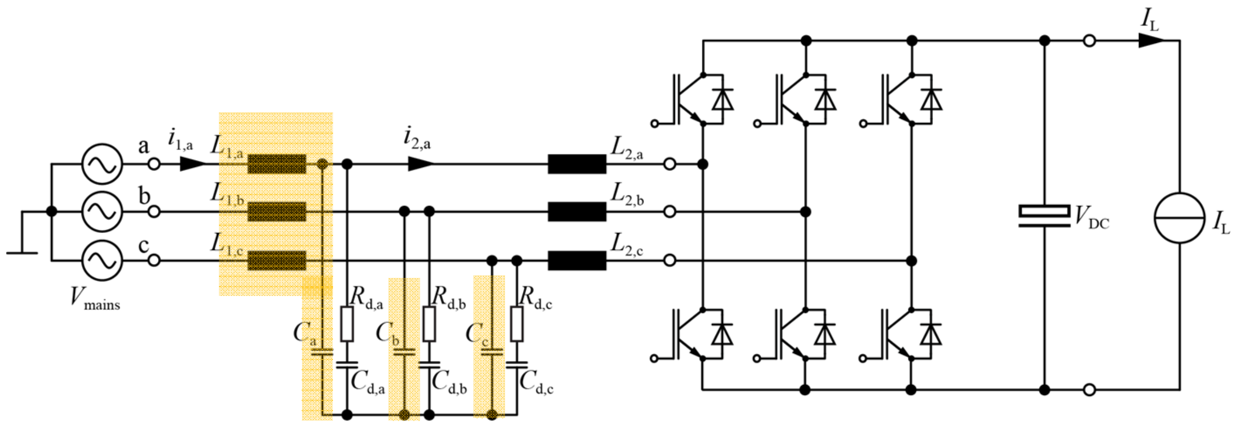

Constraints concerning *LC* filter

max. THD of mains current

max. temperature T_{max}

max. volume V_{max}

Multi-Objective Optimization – Volume vs. Losses

Optimization of LCL Filter (3)

Selected Inductor Shape

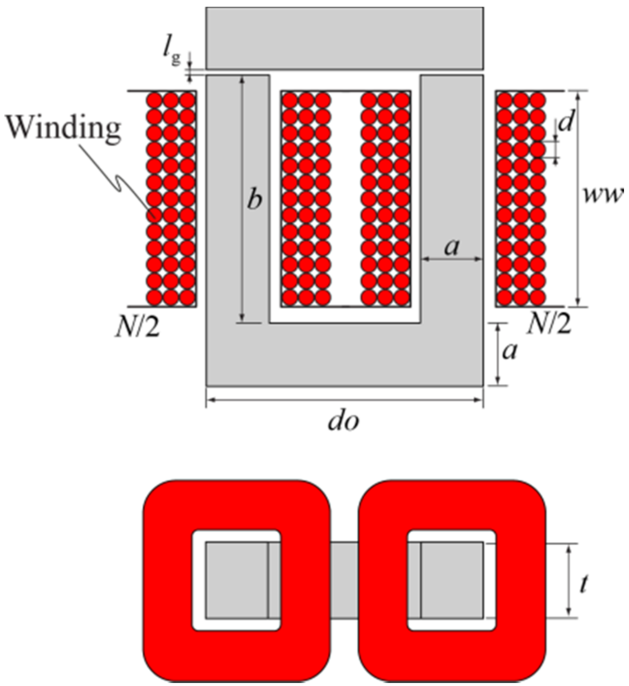

Filter Design Parameterization

$$X = \begin{pmatrix} l_{g,L1} & l_{g,L2} \\ a_{L1} & a_{L2} \\ N_{L1} & N_{L2} \\ do_{L1} & do_{L2} \\ b_{L1} & b_{L2} \\ t_{L1} & t_{L2} \\ ww_{L1} & ww_{L2} \\ d_{L1} & d_{L2} \end{pmatrix}$$

Filter *C* Calculation

$$C = \frac{1}{L_1 \omega_0^2} = \frac{1}{L_1 (2\pi f_{sw} \cdot 10^{\frac{A}{40\,dB}})^2}$$

→ The filter capacitance is calculated to meet the THD constraint.

Multi-Objective Optimization – Volume vs. Losses
Optimization of LCL Filter (4)

Simplified current / voltage waveforms for optimization procedure

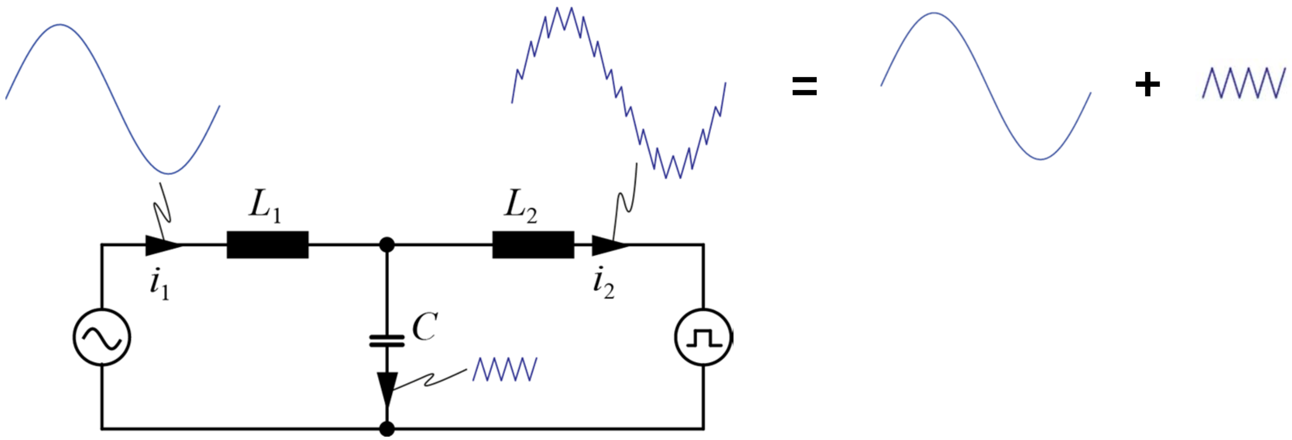

Expectations

Loss overestimation in L_2 expected.

Loss underestimation in L_1 expected.

Multi-Objective Optimization – Volume vs. Losses

Optimization of LCL Filter (5)

Optimization Flow Chart (1)

Optimization Constraints and Conditions

- max. $I_{HF,pp,max}$ in boost inductors L_2	4 A
- max. THD of mains current	4 %
- max. temperature T_{max}	125 °C
- max. volume V_{max}	10 dm^3
- switching frequency f_{sw}	8 kHz
- DC link voltage V_{DC}	650 V
- load current I_L	15.4 A

→ **Calculate L_2**

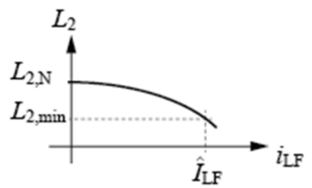

(I) Next slide

Boost Inductor

$$L_{2,\mathrm{min}} = \frac{\sqrt{2}|V_{\mathrm{mains}}|}{V_{\mathrm{DC}}/\sqrt{3}} \cos(\pi/6) \cdot \frac{\frac{2}{3}V_{\mathrm{DC}} - \sqrt{2}V_{\mathrm{mains}}}{I_{\mathrm{HF,pp,max}} \cdot f_{\mathrm{sw}}}$$

$L_{2,min}$ can be calculated based on the constraint $I_{HF,pp,max.}$. The maximum current ripple $I_{HF,pp,max}$ occurs when the fundamental current peaks.

Multi-Objective Optimization – Volume vs. Losses

Optimization of LCL Filter (6)

Optimization Flow Chart (2)

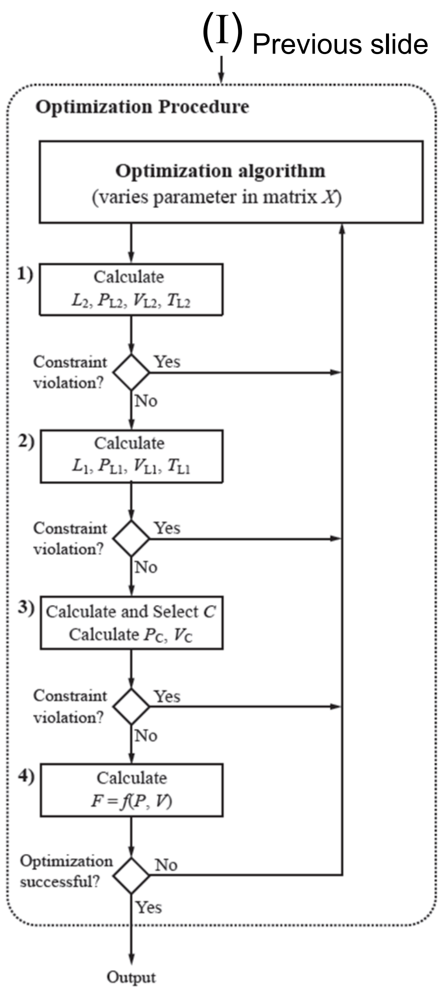

Cost Function

$$F = k_{\mathrm{Loss}} P + k_{\mathrm{Volume}} V$$

Filter *C* Calculation

$$C = \frac{1}{L_1 \omega_0^2} = \frac{1}{L_1 (2\pi f_{\mathrm{sw}} \cdot 10^{\frac{A}{40\,\mathrm{dB}}})^2}$$

Multi-Objective Optimization – Volume vs. Losses

Results – LCL Filter (1)

Filter Losses vs. Filter Volume

Pareto Front

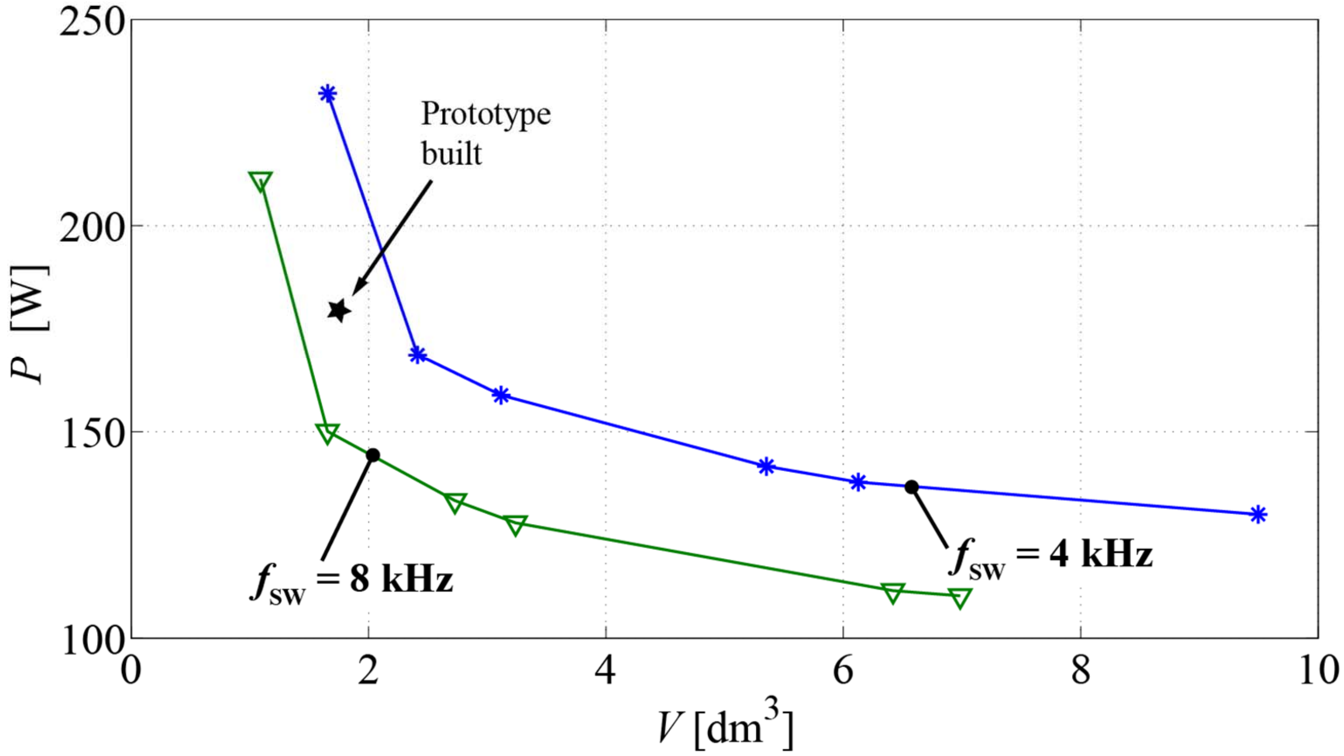

Multi-Objective Optimization – Volume vs. Losses

Results – LCL Filter (2)

Results L_1

Simulated Current Waveform

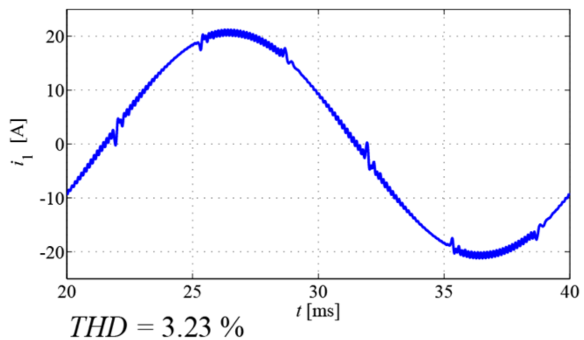

$THD = 3.23\ \%$

$P_{Loss} = 3.0$ W

(a)

Measured Current Waveform

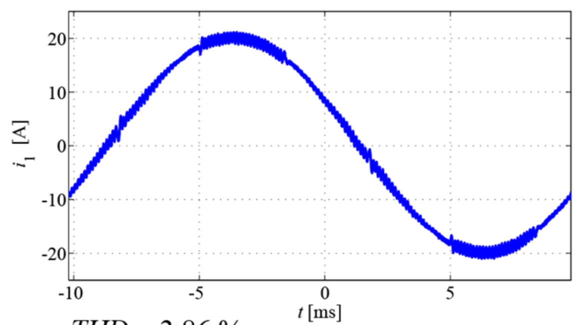

$THD = 3.86\ \%$

$P_{Loss} = 3.4$ W

(b)

Photo

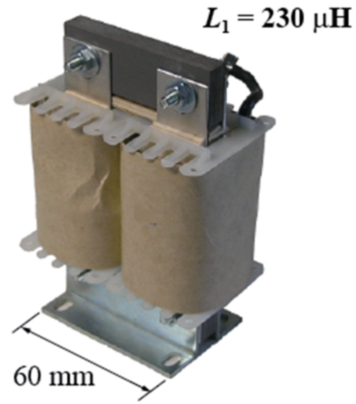

Dimensions
(cf. Fig. 1)

N	44
l_g	4.7 mm
do	60 mm
b	60 mm
a	20 mm
t	8.2 mm
ww	56.9 mm
d	3.15 mm

Conclusion

Loss modeling accurate.

THD underestimated
(frequency modeling necessary).

Multi-Objective Optimization – Volume vs. Losses

Results – LCL Filter (3)

Results L_2

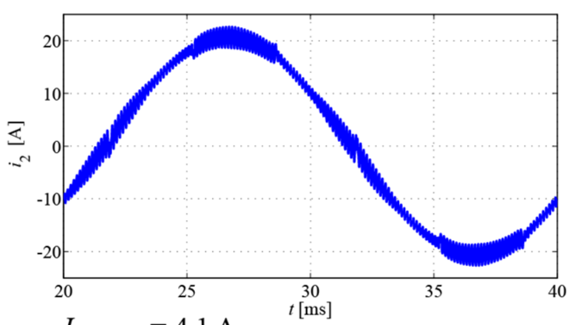

$I_{\mathrm{HF,pp,max}} = 4.1$ A

$P_{\mathrm{Loss}} = 44.9$ W

(a)

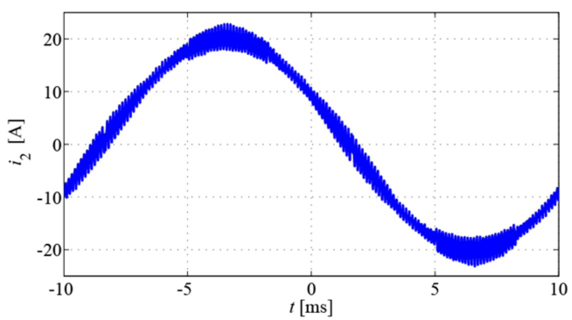

$I_{\mathrm{HF,pp,max}} = 4.7$ A

$P_{\mathrm{Loss}} = 46.8$ W

(b)

Photo

Dimensions

l_g	1.95 mm
do	60 mm
b	60 mm
a	20 mm
t	28 mm
ww	56.9 mm
d	2.24 mm

Conclusion

Loss modeling very accurate.

Current ripple underestimated (frequency modeling necessary).

Multi-Objective Optimization – Volume vs. Losses
Results – LCL Filter (4)

Photo of Capacitors

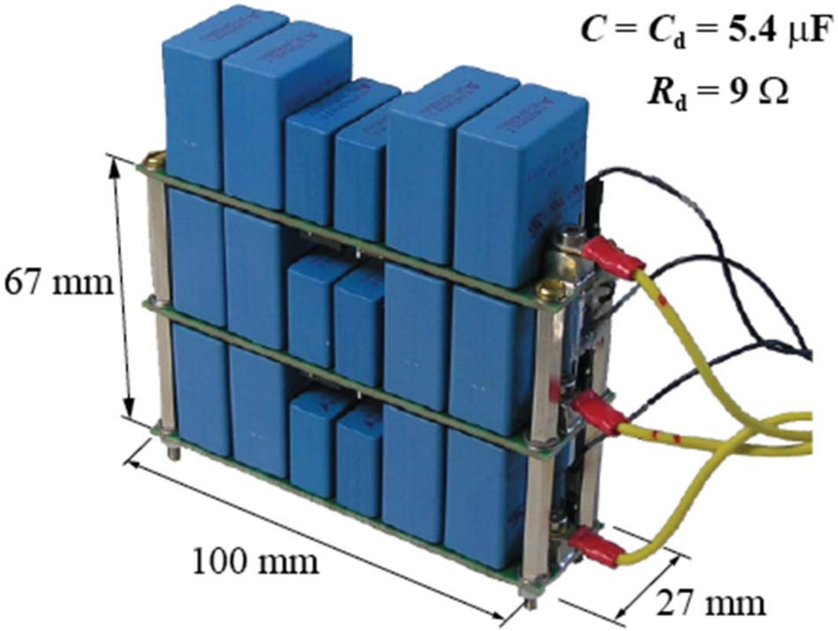

Multi-Objective Optimization – Volume vs. Losses

Overall System Optimization (1) – Converter Model

Converter Model

Transistor chip area
Diode chip area
Cooling system volume V_{CS}
Fundamental current
L_2
Switching frequency

→ Converter Model →

Transistor junction temperature
Diode junction temperature
Converter volume (incl. DC link cap.)
Converter losses

IGBT Infineon Trench and Field Stop 1200 V IGBT4 series

$$\left\{ \begin{array}{l} A_{T,D} = f(I_N) \\ P_{cond} = f(A_{T,D}, i) \\ P_{sw} \propto f_{sw} \end{array} \right.$$

(extracted from data sheet)

Cooling System Performance Index (CSPI) [18]

$$R_{th} = \frac{1}{CSPI \cdot V_{CS}}$$

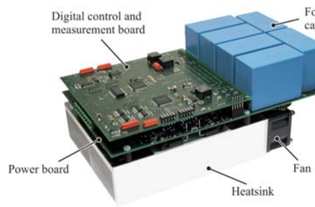

CSPI ≈ 15 W / (K liter)

[18] U. Drofenik, G. Laimer, J. W. Kolar, “Theoretical converter power density limits for forced convection cooling”, Proc. of. PCIM Europe, Nuremberg, 2005

Multi-Objective Optimization – Volume vs. Losses

Overall System Optimization (2) – Optimization Constraints

Optimization Constraints

Parameter	Variable	Value	
Max. junction temp.	$T_{\mathrm{j,max}}$	125	°C
Max. cooling system vol.	$V_{\mathrm{CS,max}}$	0.8	dm^3
Heatsink height		4	cm
Max. area per chip	$A_{\mathrm{T,max}}/A_{\mathrm{D,max}}$	1	cm^2
DC link voltage	V_{DC}	650	V
max. DC link voltage overshoot	ΔV_{DC}	50	V
Fund. peak-peak current	$I_{(1),\mathrm{pp}}$	20.5	A

Multi-Objective Optimization – Volume vs. Losses
Overall System Optimization (3) – Converter Pareto Front

Converter Losses vs. Converter Volume

Pareto Front

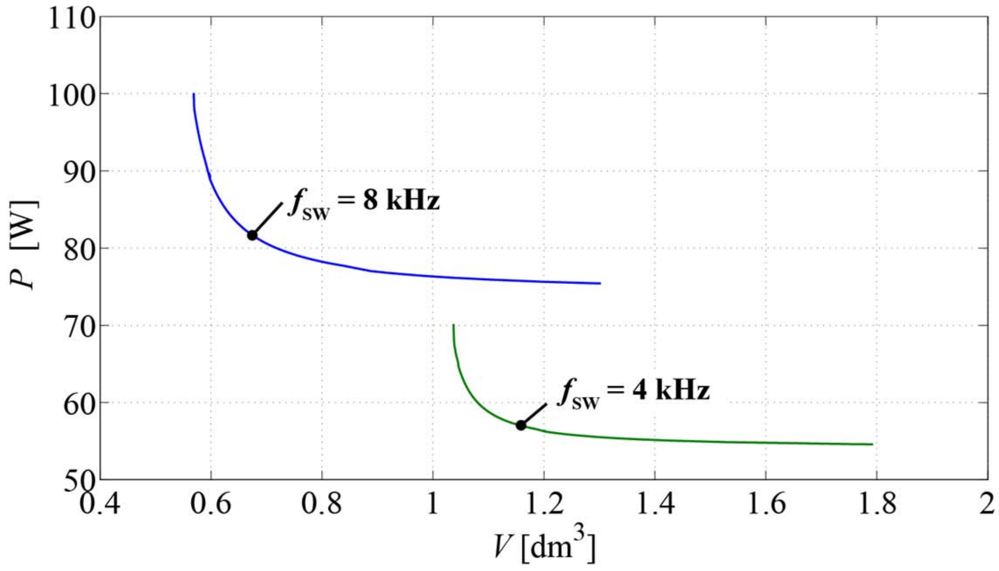

Converter volume (incl. DC link cap.)

A decreasing switching frequency leads to lower losses!

Multi-Objective Optimization – Volume vs. Losses

Overall System Optimization (3) – Optimal Designs

PFC Rectifier with Input LCL filter

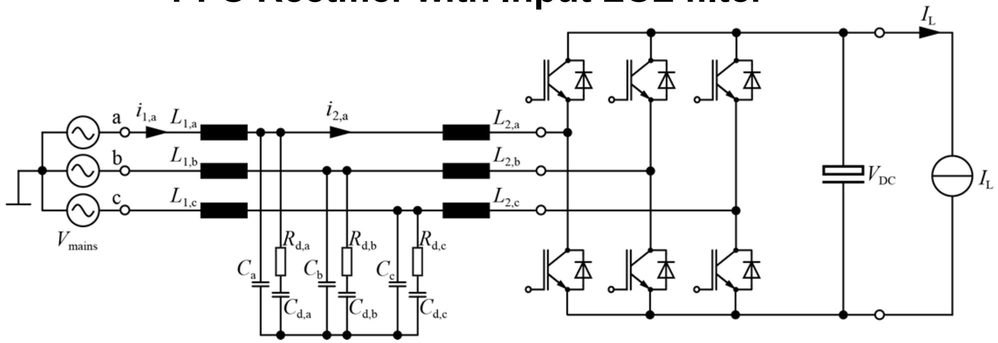

Losses of loss-optimized designs

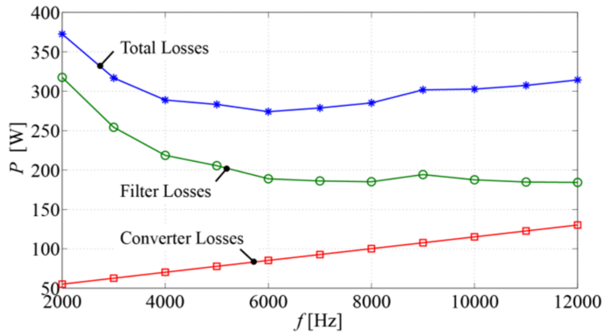

Volume of volumetric-optimized designs

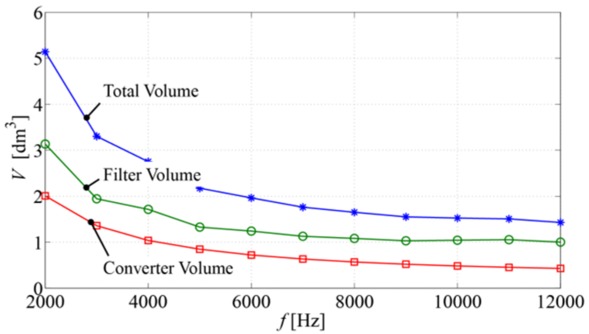

→ In order to get an optimal system design, an overall system optimization has to be performed.

→ It is (often) not enough to optimize subsystems independently of each other.

Outline

- Magnetic Circuit Modeling
- Core Loss Modeling
- Winding Loss Modeling
- Thermal Modeling
- Multi-Objective Optimization
- Summary & Conclusion

Summary & Conclusion

Magnetic Circuit Modeling

Air Gap Reluctance Calculation

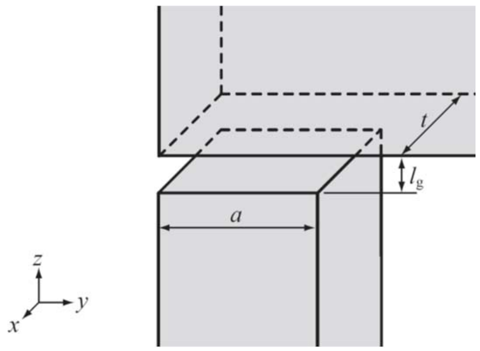

zy-plane

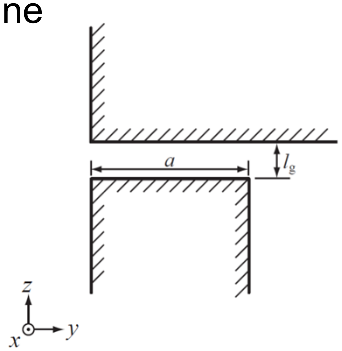

Air gap per unit length

$$\Rightarrow R'_{zy} \Rightarrow \sigma_y = \frac{R'_{zy}}{\frac{l_g}{\mu_0 a}}$$

zx-plane

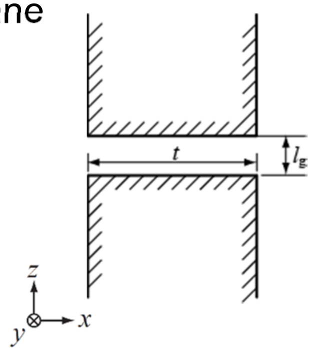

$$\Rightarrow R'_{zx} \Rightarrow \sigma_x = \frac{R'_{zx}}{\frac{l_g}{\mu_0 t}}$$

Results

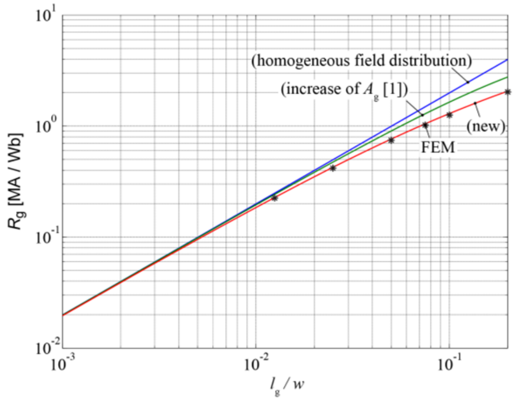

$$\Rightarrow R_g = \sigma_x \sigma_y \frac{l_g}{\mu_0 a t}$$

Summary & Conclusion
Core Loss Modeling

“The best of both worlds” (Steinmetz & Loss Map approach)

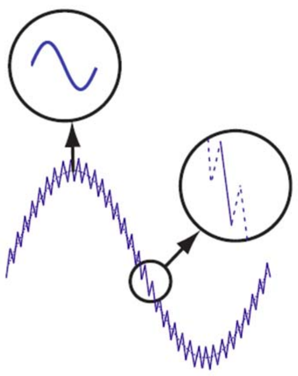

Loss Map
(Loss Material Database)

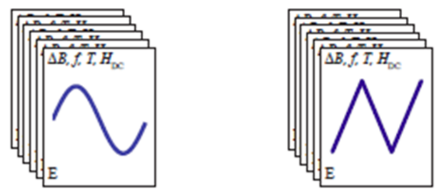

$$k, k_i, \alpha, \beta, \alpha_r, \beta_r, q_r, \tau$$

$$P_v = \frac{1}{T}\int_0^T k_i \left|\frac{dB}{dt}\right|^{\alpha} (\Delta B)^{\beta-\alpha}\, dt + \sum_{l=1}^{n} Q_{rl} P_{rl} \longrightarrow \frac{P}{V}$$

Summary & Conclusion
Winding Loss Modeling

Optimal Solid Wire Thickness

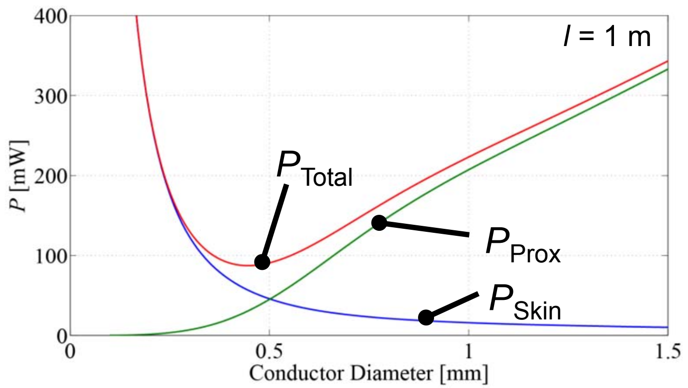

(f = 100 kHz, I_{peak} = 1 A, $H_{e,peak}$ = 1000 A/m)

Foil vs. Round Conductors

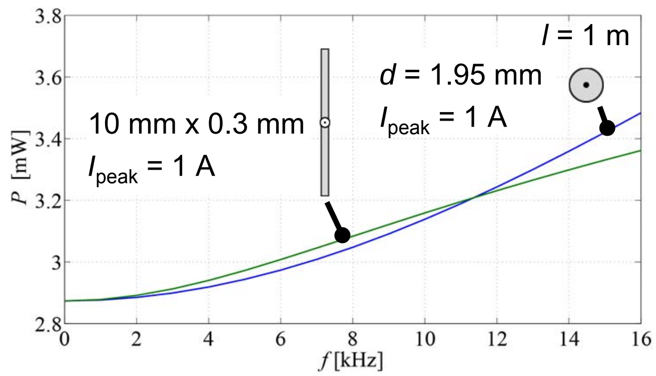

Losses in Litz Wires

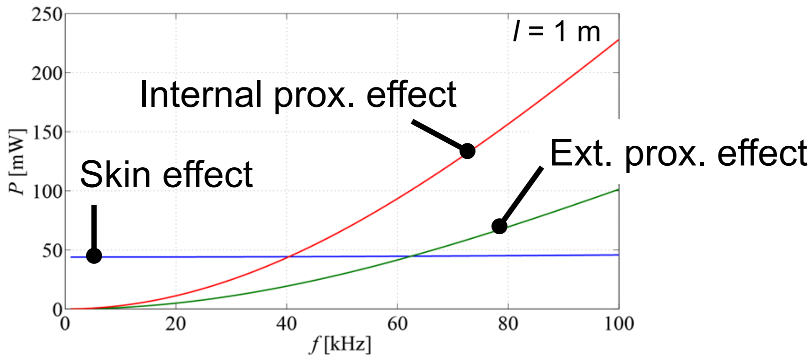

Gapped cores: 2D approach

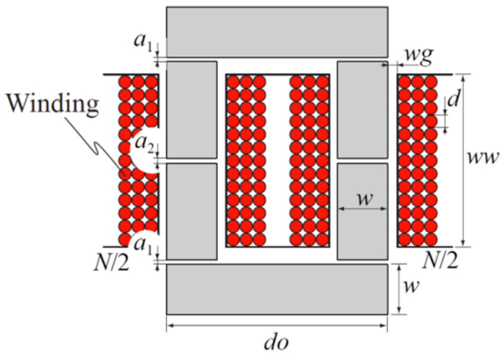

Summary & Conclusion

Magnetic Design Environment

Core Material Database

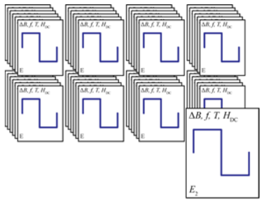

Magnetics Design Software

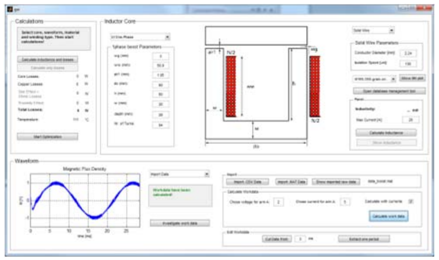

Circuit Simulator

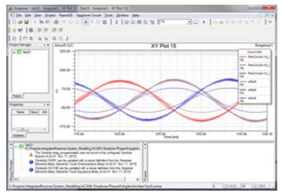

Automated Measurement System

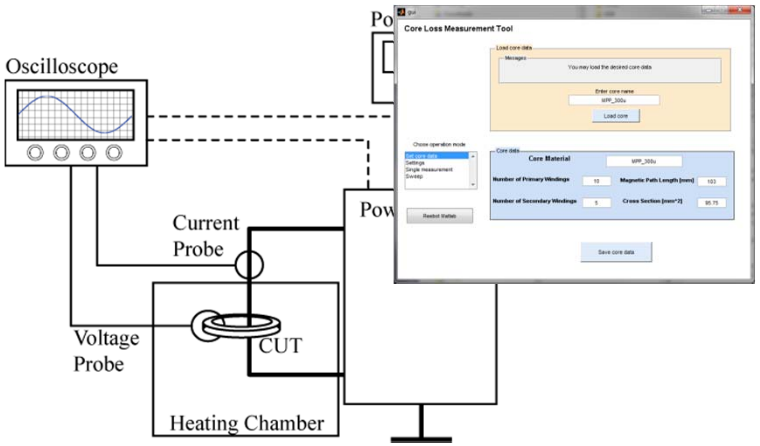

Prototype

Verification (e.g. with Calorimeter)

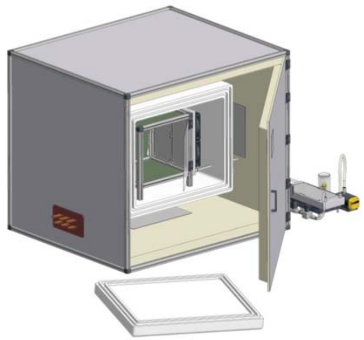

Summary & Conclusion

Multi-Objective Optimization - Next Steps

PFC Rectifier with Input LCL filter

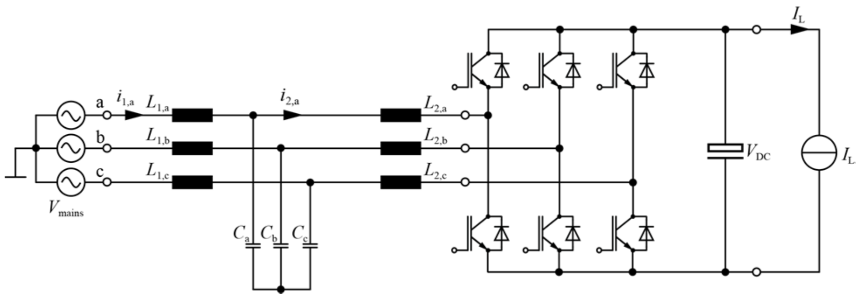

Losses of loss-optimized designs

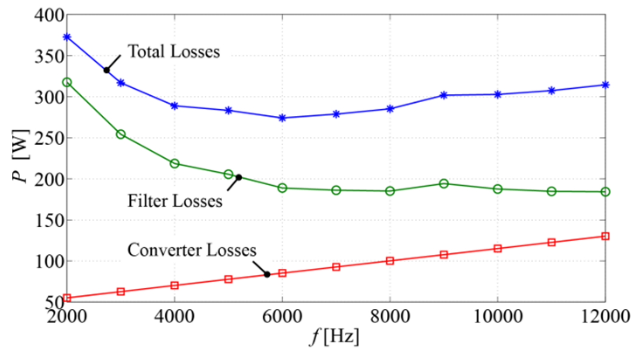

Filter Pareto Front

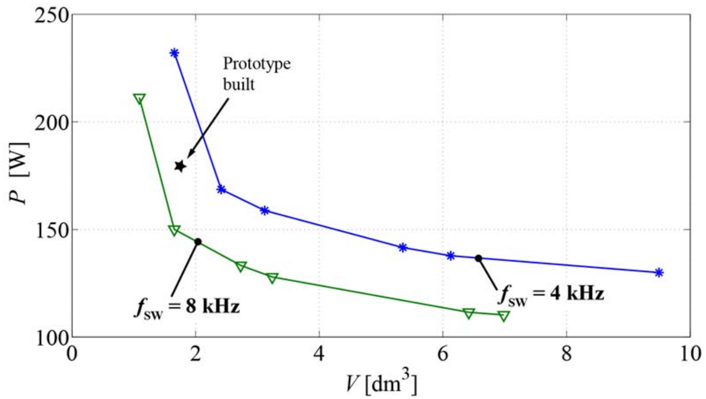

Next Steps

Comparison of different rectifier topologies (2-level, 3-level), modulation schemes, etc. on filter size, filter losses.

Thank you !

Additional References

[6] J. Mühlethaler, J.W. Kolar, and A. Ecklebe, "A Novel Approach for 3D Air Gap Reluctance Calculations", in Proc. of the ICPE - ECCE Asia, Jeju, Korea, 2011

[9] J. Mühlethaler, J. Biela, J.W. Kolar, and A. Ecklebe, "Improved Core Loss Calculation for Magnetic Components Employed in Power Electronic Systems", in Proc. of the APEC, Ft. Worth, TX, USA, 2011.

[19] Jürgen Biela, "Wirbelstromverluste in Wicklungen induktiver Bauelemente", Part of script to lecture Power Electronic Systems 1, ETH Zurich, 2007

[20] J. Mühlethaler, J.W. Kolar, and A. Ecklebe, "Loss Modeling of Inductive Components Employed in Power Electronic Systems", in Proc. of the ICPE - ECCE Asia, Jeju, Korea, 2011

[21] J. Mühlethaler, J. Biela, J.W. Kolar, and A. Ecklebe, "Core Losses under DC Bias Condition based on Steinmetz Parameters", in Proc. of the IPEC - ECCE Asia, Sapporo, Japan, 2010.

[22] B. Cougo, A. Tüysüz, J. Mühlethaler, J.W. Kolar, "Increase of Tape Wound Core Losses Due to Interlamination Short Circuits and Orthogonal Flux Components", in Proc. of the IECON, Melbourne, 2011.

[23] J. Mühlethaler, M. Schweizer, R. Blattmann, J.W. Kolar, and A. Ecklebe, "Optimal Design of LCL Harmonic Filters for Three-Phase PFC Rectifiers", in Proc. of the IECON, Melbourne, 2011

Contact

Jonas Mühlethaler
muehlethaler@lem.ee.ethz.ch
www.pes.ee.ethz.ch